

## Transition Metal Catalyzed Synthesis of Carboxylic Acids, Imines, and Biaryls

**Santilli, Carola; Madsen, Robert**

*Publication date:*  
2017

*Document Version*  
Publisher's PDF, also known as Version of record

[Link back to DTU Orbit](#)

*Citation (APA):*  
Santilli, C., & Madsen, R. (2017). Transition Metal Catalyzed Synthesis of Carboxylic Acids, Imines, and Biaryls. Kgs. Lyngby: DTU Chemistry.

### DTU Library Technical Information Center of Denmark

---

#### General rights

Copyright and moral rights for the publications made accessible in the public portal are retained by the authors and/or other copyright owners and it is a condition of accessing publications that users recognise and abide by the legal requirements associated with these rights.

- Users may download and print one copy of any publication from the public portal for the purpose of private study or research.
- You may not further distribute the material or use it for any profit-making activity or commercial gain
- You may freely distribute the URL identifying the publication in the public portal

If you believe that this document breaches copyright please contact us providing details, and we will remove access to the work immediately and investigate your claim.

---

# **Transition Metal Catalyzed Synthesis of Carboxylic Acids, Imines, and Biaryls**

---

Phd Thesis – August 2017  
Carola Santilli



---

Department of Chemistry  
Technical University of Denmark



# Acknowledgements

---

This dissertation describes the work conducted during my PhD studies. The work was performed at the Technical University of Denmark under the supervision of Professor Robert Madsen, from September 2013 to May 2017.

This period was particularly intense for me not just from an educational point of view but also and especially for a personal one thanks to all the people I had the chance to meet, and which towards I want to express all my gratitude for being always there.

First and foremost I would like to thank my supervisor Robert Madsen for giving me the opportunity to be part of his research group, for the guidance during these three years, for the trust and all the precious advices. Thanks to give me the opportunity to come here in Denmark with my before boyfriend and now husband and father of my little girls, Andrea.

I am very grateful to Ilya Makarov for being a great advisor during my first project, for all the patience, the motivation and for sharing his precious knowledge with me. Thanks to the entire Robert Madsen group, both present and former colleagues, for all the nice conversations and support you have given me right away. In particular Clotilde, Dominika and Gyrithe who have been my office mates for the first period of my PhD and with whom I shared beautiful moments. Thanks to Andreas, my first lab mate for all the fun moments, the music, South Park, and philosophical and historical documentaries you made me listen to during the laboratory work! Thanks to my present colleagues Emilie, Bo, Fabrizio, Fabrizio and Simone for all lunches, cafes and chocolates we had together! This last period was very enjoyable with you all, guys!

A special thank goes to my dear friends Enzo, Giuseppe, Fabrizio and Luca for being always present when I needed, for all the nice conversations and laughs. Thanks for supporting me constantly and for never making me feel alone. Vi voglio bene!

My sincere gratitude goes to the technical staff of the chemistry department. Thanks to the dear Anne Hector, to Lars Egede Bruhn, Brian Dideriksen, Brian Ekman-Gregersen, Charlie Johansen and Tina Gustafsson for their great help.

I am very grateful to Emilie! Thanks for all the time you spent proofreading this thesis! For the great support and valid advices you gave me during the writing, and all the nice talks and laughs we had! You are so sweet!

I am immensely grateful to my mom and dad, to my sisters, Federica and Vittoria, to my grandparents for your infinite love, for your constant presence, and your great motivation that always comforted me in difficult times.

Last but not least, my deepest gratitude goes to my colleague, friend, and lovely husband Andrea! Thanks for everything! For all the love, the patience, the help you constantly give me every day! For all the listening and the support, for all the great advices you gave me during these three years, for believing in me! Thanks for all the beautiful moments we shared, they are so many! Thanks for proofreading my thesis and for all the interesting discussions we had. Without you I would not be here. You are my life.

Thanks to my little daughter, Beatrice, your beautiful smile fills my everyday life! Thanks to the little babygirl I'm expecting. Your little taps have been keeping me company during the thesis writing! I look forward to meet you.

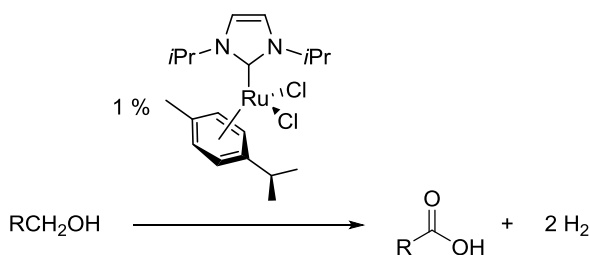
Carola Santilli  
August 2017

# Abstract

---

## Dehydrogenative synthesis of carboxylic acids catalyzed by a ruthenium *N*-heterocyclic carbene complex

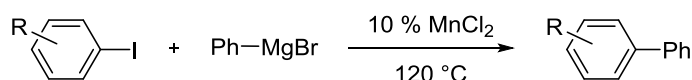
A new methodology for the synthesis of carboxylic acids from primary alcohols and hydroxide has been developed. The reaction is catalyzed by the ruthenium *N*-heterocyclic carbene complex  $[\text{RuCl}_2(\text{I}^{\text{Pr}})(p\text{-cymene})]$  where dihydrogen is generated as the only by-product (Scheme i). The dehydrogenative reaction is performed in toluene, which allows for a simple isolation of the products by precipitation followed by extraction. Various substituted benzyl alcohols smoothly undergo the transformation. The fast conversion to the carboxylic acids can be explained by the involvement of a competing Cannizzaro reaction. The scope of the dehydrogenation was further extended to linear and branched saturated aliphatic alcohols, although longer reaction times are necessary to ensure complete substrate conversions. The kinetic isotope effect of the reaction was determined to be 0.67 using 1-butanol as the substrate. A plausible catalytic cycle was characterized by DFT/B3LYP-D3 and involved coordination of the alcohol to the metal,  $\beta$ -hydride elimination, hydroxide attack on the coordinated aldehyde, and a second  $\beta$ -hydride elimination to furnish the carboxylate.



**Scheme i.** Dehydrogenation of a primary alcohol to the carboxylic acid.

## Manganese catalyzed radical Kumada-type reaction between aryl halides and aryl Grignard reagents

The reaction between aryl halides and aryl Grignard reagents catalyzed by  $\text{MnCl}_2$  has been extended to several methyl-substituted aryl iodide reagents by performing the reaction at  $120\text{ }^\circ\text{C}$  in a microwave oven (Scheme ii). A limitation of the heterocoupling process is the concomitant dehalogenation of the aryl halide and homocoupling of the Grignard reagent leading low to moderate yields of the desired heterocoupling product. The mechanism of the cross-coupling process was investigated by performing two radical trap experiments. The employment of radical scavengers such as 1,4-cyclohexadiene and 4-(2-bromophenyl)-but-1-ene revealed the presence of an aryl radical intermediate. This leads to the proposal of an  $\text{S}_{\text{RN}}1$  pathway for the coupling.

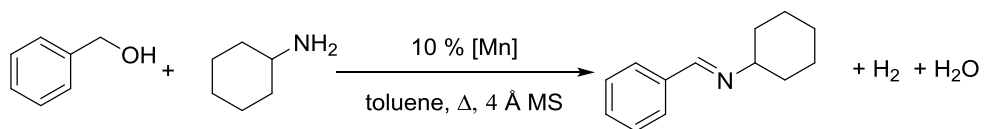


**Scheme ii.** Cross-coupling between aryl iodides and phenylmagnesium bromide catalyzed by  $\text{MnCl}_2$ .

## Study of the dehydrogenative synthesis of imines from primary alcohols and amines catalyzed by manganese complexes

An initial study of the dehydrogenative synthesis of imines catalyzed by simple and commercially available manganese complexes has been conducted (Scheme iii). Originally the low valent  $\text{CpMn}(\text{CO})_3$ ,  $\text{Mn}(\text{CO})_5\text{Br}$ , and  $\text{Mn}_2(\text{CO})_{10}$  complexes were employed for the coupling reaction between benzyl alcohol and cyclohexylamine, but these displayed only poor or no reactivity. Surprisingly when the Jacobsen complex is used as the catalyst, the reaction between benzyl alcohol and

cyclohexylamine resulted in 77% yield of the corresponding imine. Moreover gas evolution confirmed that the reaction occurs by dehydrogenation.



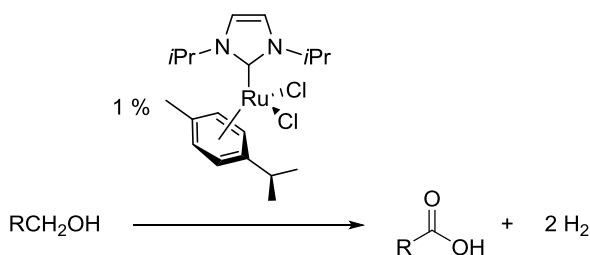
**Scheme iii.** Dehydrogenative coupling of benzyl alcohol and cyclohexylamine catalyzed by simple manganese complexes.



# Resume

## Dehydrogenativ syntese af karboxylsyrer katalyseret af et *N*-heterocyklisk ruthenium carben kompleks

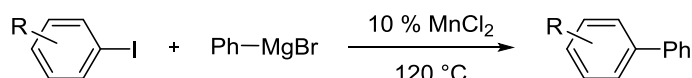
En ny metode er blevet udviklet for syntesen af karboxylsyrer via primære alkoholer og hydroxid. Reaktionen er katalyseret af det *N*-heterocykliske ruthenium carben kompleks  $[\text{RuCl}_2(\text{I}^*\text{Pr})(p\text{-cymene})]$ , hvor dihydrogen er det eneste biprodukt, der dannes (Skema 1). Den dehydrogenative reaktion udføres i toluen, hvilket muliggør en simpel isolering af produkterne ved hjælp af udfældning efterfulgt af ekstraktion. Forskellige substituerede benzyl alkoholer gennemgår problemfrit omdannelsen. Den hurtige omdannelse til karboxylsyrene kan forklares ved, at en konkurrerende Cannizzaro reaktion er involveret. Anvendelsen af dehydrogeneringen blev yderligere udvidet til at inkludere mættede lineære og forgrenede alifatiske alkoholer, dog er længere reaktionstider nødvendige for at garantere fuld omdannelse af substraterne. Den kinetisk isotop effekt for reaktionen blev bestemt til 0,67 under anvendelse af 1-butanol som substrat. En plausibel katalytisk cyklus blev karakteriseret via DFT/B3LYP-D3, og indebar koordinering af alkoholen til metallet,  $\beta$ -hydrid eliminering, angreb af hydroxid på det koordinerede aldehyd, og endnu en  $\beta$ -hydrid eliminering for at give karboxylsyren.



**Skema i.** Dehydrogenering af primære alkoholer til karboxylsyrer.

## Radikal Kumada-type reaktion mellem aryl halider og aryl Grignard reagenser katalyseret af mangan

Reaktionen mellem aryl halider og aryl Grignard reagenser katalyseret af  $\text{MnCl}_2$  er nu blevet udvidet til flere methyl-substituerede aryl iodid reagenser ved at udføre reaktionen ved  $120\text{ }^\circ\text{C}$  i en mikrobølgeovn (Skema ii). En begrænsning for den heterokoblende proces er den ledsagende dehalogenering af aryl halidet samt homokobling af Grignard reagentet, hvilket fører til et lavt til moderat udbytte af det ønskede heterokoblede produkt. Mekanismen for denne krydskoblings proces blev undersøgt ved at udføre to radikale-fælde eksperimenter. Ved at anvende radikale scavengers som fx 1,4-cyclohexadien og 4-(2-bromfenyl)-but-1-en blev det vist, at der forekommer et aryl radikal som intermediat. Dette giver anledning til fremsætningen om en  $\text{S}_{\text{RN}}1$  reaktionsvej for koblingen.

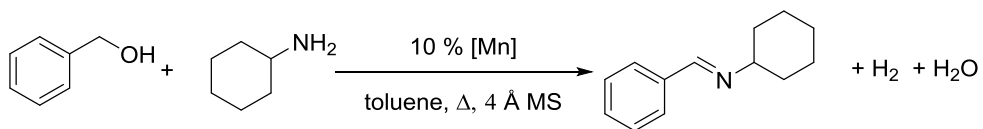


**Skema ii.** Krydskobling mellem aryl iodider og fenyl magnesium bromid katalyseret af  $\text{MnCl}_2$ .

## Studie af den dehydrogenative syntese af iminer fra primære alkoholer og aminer katalyseret af mangan komplekser

Der er blevet udført et indledende studie af den dehydrogenerende syntese af iminer katalyseret af simple og kommercielle mangan komplekser (Skema iii). Indledende blev de lav valente komplekser  $\text{CpMn}(\text{CO})_3$ ,  $\text{Mn}(\text{CO})_5\text{Br}$  og  $\text{Mn}_2(\text{CO})_{10}$  anvendt for koblings reaktionen mellem benzyl alkohol og cyklohexylamin, men disse udviste kun lav eller ingen reaktivitet. Når Jacobsen komplekset bliver brugt som katalysator, giver reaktionen mellem benzyl alkohol og cyklohexylamin

overraskende et udbytte af den korresponderende imin på 77%. Yderligere bekræftede gasudvikling, at reaktionen foregår ved dehydrogenering.



**Skema iii.** Dehydrogenativ kobling af benzyl alkohol og cyklohexylamin katalyseret af simple mangan komplekser.

# List of abbreviations

---

AAD	Acceptorless alcohol dehydrogenation
Ac	Acetyl
acac	Acetylacetonate
AD	Acceptorless dehydrogenation
ADC	Acceptorless dehydrogenative coupling
Ar	Aromatic
BDE	Bond dissociation energy
Bu	Butyl
Cy	Cyclohexyl
Cp	Cyclopentadienyl
DABCO	1,4-Diazabicyclo[2.2.2]octane
DFT	Density functional theory
DMAP	4-Dimethylamino pyridine
DMF	<i>N,N</i> -Dimethylformamide
DMSO	Dimethyl sulfoxide
DMP	Dess-Martin periodinane
DPEPhos	Bis[(2-diphenylphosphino)phenyl] ether
dppe	1,2-Bis(diphenylphosphino)ethane
dtbpf	1,1'-Bis(di- <i>tert</i> -butylphosphino)ferrocene
Et	Ethyl
ET	Electron transfer
EWG	Electron withdrawing group
GC-MS	Gas chromatography / mass spectrometry
HRMS	High resolution mass spectrometry
<i>i</i> Pr	1,3-Diisopropylimidazol-2-ylidene

<i>i</i> Pr	<i>iso</i> -Propyl
KIE	Kinetic isotope effect
<i>m</i>	Meta
MS	Mass spectrometry
NHC	N-Heterocyclic carbene
NMP	<i>N</i> -Methyl-2-pyrrolidone
NMR	Nuclear magnetic resonance
<i>o</i>	Ortho
<i>p</i>	Para
PDC	Pyridinium dichromate
PE-I	Iodo-polyethylene
PEGs	Poly(ethylene glycol)s
PEPPSI	1,3-Bis(2,6-Diisopropylphenyl)imidazol-2-ylidene][3-chloropyridyl)palladium(II) dichloride
Ph	Phenyl
ppm	Parts per million
S <sub>N</sub> 1	Unimolecular nucleophilic substitution
S <sub>N</sub> 2	Bimolecular nucleophilic substitution
rt	Room temperature
<i>t</i> Bu	<i>tert</i> -Butyl
TEMPO	(2,2,6,6-Tetramethylpiperidin-1-yl)oxy
THF	Tetrahydrofuran
TMEDA	<i>N,N,N',N'</i> -Tetramethylethylenediamine
TOF	Turn-over frequency
TON	Turn-over number
TS	Transition state

## Table of Contents

---

Acknowledgements.....	i
Abstract .....	iii
Resume .....	vi
List of abbreviations.....	ix
Table of Contents.....	xi
1 Introduction.....	1
1.1 Catalysis: general principles .....	1
1.2 The main elementary steps of a general catalytic cycle in metal catalysis.....	3
1.3 Metal catalysis of radical reactions.....	7
2 Dehydrogenative synthesis of carboxylic acids catalyzed by a ruthenium <i>N</i> -heterocyclic carbene complex.....	16
2.1 Introduction.....	16
2.2 Synthesis of carboxylic acids from catalytic oxidation of primary alcohols.....	19
2.3 Acceptorless dehydrogenations of primary alcohols .....	22
2.3.1 Ruthenium-catalyzed AAD reactions.....	24
2.3.2 Ruthenium <i>N</i> -heterocyclic carbene catalyzed dehydrogenative transformation of primary alcohols .....	28
2.4 Conclusion.....	32
2.5 Results and discussion .....	34
2.5.1 Preliminary studies and optimization of the reaction conditions.....	34
2.5.2 Substrate scope and limitations .....	36
2.5.3 Investigation of the reaction mechanism .....	43
2.6 Conclusion.....	54
2.7 Experimental section.....	55
3 Manganese catalyzed radical Kumada-type reaction between aryl halides and aryl Grignard reagents .....	64

3.1	Introduction to cross-coupling reactions: a brief retrospective on their origins and history .....	64
3.1.1	The development of transition metal catalyzed cross-coupling reactions .....	67
3.1.2	The Corriu-Kumada coupling .....	70
3.1.3	Recent examples of the Kumada reaction: a brief overview of the literature .....	72
3.2	Manganese as an alternative for catalyzing cross-coupling reactions ....	82
3.2.1	Overview of the literature on manganese catalyzed cross-coupling reactions .....	83
3.2.2	The Kumada coupling under manganese catalysis .....	85
3.3	Manganese in radical reactions .....	89
3.3.1	Participation of Mn(0), Mn(II) and Mn(III) in radical reactions .....	90
3.4	Conclusion .....	94
3.5	Results and discussion .....	95
3.5.1	Study by another PhD student .....	95
3.5.2	Optimization of the reaction conditions .....	96
3.5.3	Substrate scope and limitations .....	105
3.5.4	Investigation of the reaction mechanism .....	108
3.6	Conclusion .....	112
3.7	Experimental section .....	113
4	Study of the dehydrogenative synthesis of imines from primary alcohols and amines catalyzed by manganese complexes .....	123
4.1	Introduction .....	123
4.1.1	Manganese-catalyzed dehydrogenation reactions of primary alcohols .....	125
4.2	Conclusion .....	131
4.3	Results and discussion .....	131
4.3.1	Preliminary study .....	131
4.4	Conclusion .....	135

4.5	Experimental section.....	136
4.5.1	General methods .....	136
4.5.2	General procedure for the dehydrogenative imine synthesis catalyzed by Jacobsen complex.....	136
4.5.3	Gas development.....	136
	Publications .....	138
	Bibliography .....	139





# 1 Introduction

## 1.1 Catalysis: general principles

Chemical catalysis is the phenomenon that occurs when a substance called a catalyst reduces the free energy of the highest transition states and in this way increases the rate of a chemical transformation without being itself consumed. The efficiency of a catalyst in a process can be measured by the turnover number (TON). TON is defined as the number of moles of substrate that one mole of catalyst can convert into product before being inactivated. The turnover frequency (TOF) instead is defined as the turnover in a certain period of time. When a catalyst interacts with one or more reagents, the energy barrier of the reaction can be lowered by the stabilization of the incipient transition state. An example of this is an enzyme-catalyzed reaction.

The mechanism can be completely different and occurs with more steps. In this case the activation energy of the individual steps must be lower than that of the uncatalyzed reaction, resulting in a lower overall energy barrier. This last case usually takes place in organometallic chemistry (Figure 1.1).<sup>1</sup>

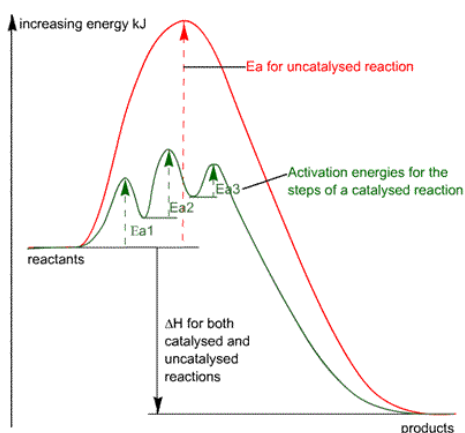
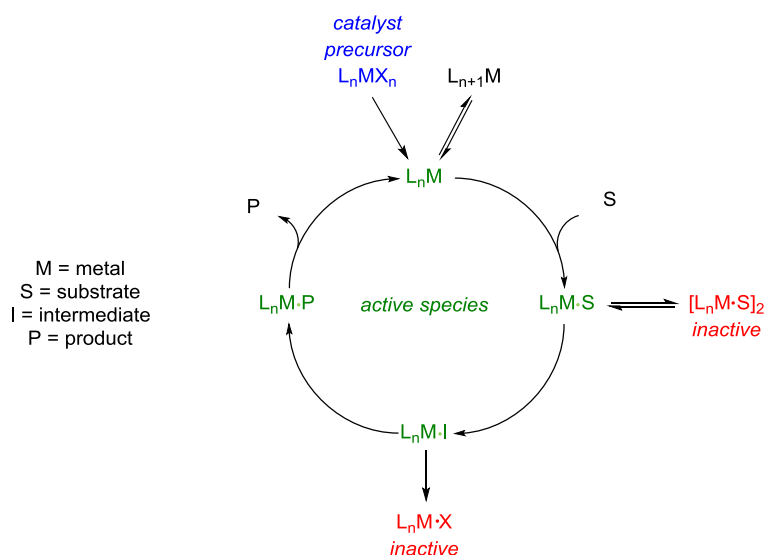


**Figure 1.1.** Reaction coordinate diagrams for an uncatalyzed and a catalyzed transformation.

A key requirement for a substance to be a catalyst is the ability to be regenerated at the end of a reaction. Hence the sum of the steps of a catalytic process is often called a *catalytic cycle*. Typically a *catalyst precursor* ( $L_nMX_n$ ) which is normally more stable than the actual catalyst is added to the reaction environment and the active species ( $L_nM$ ) is formed *in situ* by dissociation of a dative ligand (Scheme 1.1). Throughout the whole cycle, the active catalyst may decompose to non-active species. Inactivation of the catalyst could be reversible, and hence the catalytic cycle keeps on, or irreversible, and consequently it stops. At the end of the transformation the product leaves the complex  $L_nMP$ , and this regenerates the active catalyst which can bind a new substrate molecule forming the adduct  $L_nM\cdot S$  or reversible coordination to a ligand forming  $L_{n+1}M$  can take place.



**Scheme 1.1.** Example of catalytic cycle.

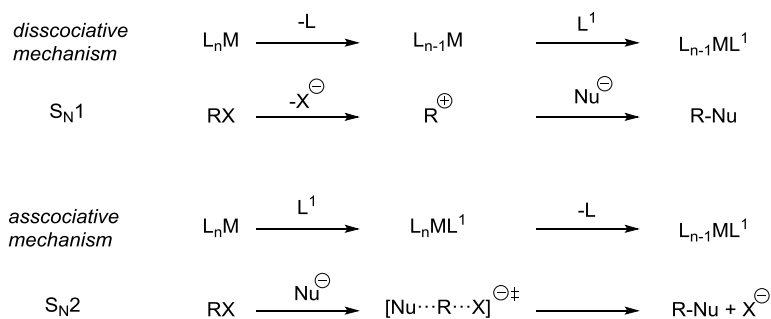
In the following a more detailed description of the individual elementary steps of the catalytic cycle is presented.

## 1.2 The main elementary steps of a general catalytic cycle in metal catalysis

In organometallic chemistry the catalyst is an organotransition metal compound which consists of organic and/or inorganic ligands coordinated to a metal center. The right choice of both metal and ligand environment is crucial to the efficiency of the catalyst for a certain reaction. The efficiency of the catalyst is expressed through its capability to enhance both the kinetics of the reaction and the selectivity toward the desired product. During the catalytic cycle the organotransition metal compound undergoes various transformations, of which some are reported below.<sup>1</sup>

### Ligand substitution

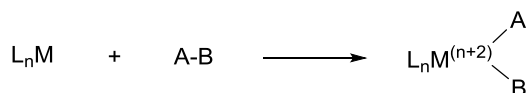
Ligand substitution is typically the first step encountered in many catalytic reactions involving transition metal complexes. It describes the replacement of a ligand that is coordinated to the metal center, with a free ligand. This phenomenon occurs mostly by a dissociative or associative mechanism (Scheme 1.2). The former is characteristic for coordinatively saturated complexes with octahedral geometry. The dissociative replacement involves an initial cleavage of a metal-ligand bond which can be compared to the nucleophilic substitution reaction  $S_N1$  that implicates the initial breakage of a bond between carbon and a leaving group. The associative mechanism, on the contrary, is typical for 16 electrons complexes with square planar geometry and resembles the nucleophilic substitution reaction  $S_N2$  although the association of a ligand to a transition metal leads to an intermediate, while an  $S_N2$  reaction goes through a transition state.<sup>1</sup>



**Scheme 1.2.** Dissociative and associative mechanisms for ligand substitution.

## Oxidative addition

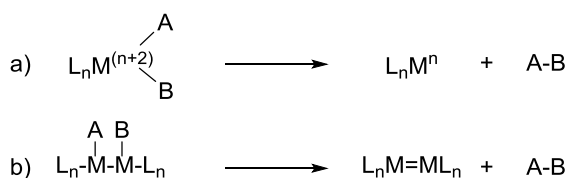
The oxidative addition is the addition of a substrate molecule to the metal complex. It implicates the bond cleavage of an organic reagent and hence the introduction of two new ligands bounded to the metal center. The consequence of this reaction is that the formal oxidation state of the metal is raised by two (Scheme 1.3). The oxidative addition can proceed by different mechanisms depending on the polarity of the reagents. In fact species that are non-polar or have a low polarity such as dihydrogen and alkanes, appear to undergo a concerted pathway resulting in *cis* selectivity while reagents that have a high polarity such as alkyl halides generally undergo a stepwise mechanism.<sup>2</sup>



**Scheme 1.3.** Schematic presentation of an oxidative addition.

## Reductive elimination

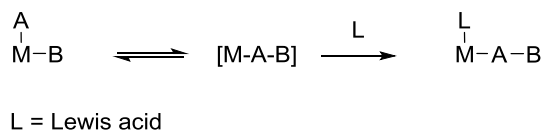
Reductive elimination is the reverse reaction of the oxidative addition where the final product is generated by a new covalent bond between two ligands bound either to one or two metal centers (Scheme 1.4). The consequence of this reaction is that the metal oxidation state is formally reduced by two. The mechanism for the reductive elimination is dependent on the metal center and the ligands which constitute the complex. Furthermore it can occur by a concerted pathway in which a three-centered transition state is formed and the stereochemistry is retained or by a radical pathway in which the stereochemical information is lost.<sup>2</sup>



**Scheme 1.4.** Formation of a new covalent bond between two ligands attached to a) the same metal center; b) different metals of a binuclear complex.

## Migratory insertion

When an unsaturated ligand A inserts into an adjacent metal-ligand bond M-B the reaction is called a migratory insertion. The insertion leaves a vacant coordination site that is often occupied by a Lewis base (L) and the final product is then generated (Scheme 1.5). The unsaturated ligand A can be carbon monoxide, carbon dioxide, an olefin, or an aldehyde. During the migratory insertion, the coordination number of the metal center and the electron count change, but the formal oxidation state of the metal remains unaffected. Furthermore the groups undergoing migratory insertion must be *cis* to each other.<sup>1</sup>

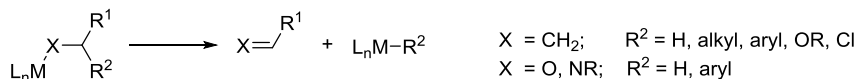


**Scheme 1.5.** Insertion of ligand A into an M-B bond and consequently coordination of a Lewis base by the metal center.

## Elimination

Elimination reactions are the reverse of the migratory insertions. They can happen by transfer of a group from the  $\alpha$ -,  $\beta$ -,  $\gamma$ -carbon atom of a covalent ligand of the metal center. The most common elimination reaction is the  $\beta$ -hydrogen elimination, which consists of the formation of a  $\pi$ -bond and a metal-hydrogen bond. Other types of  $\beta$ -elimination involving alkyl, aryl, alkoxide and halide groups are known. When  $\beta$ -hydrogens are absent,  $\alpha$ -hydrogen eliminations can be observed as well (Scheme 1.6).<sup>1</sup>

a)  $\beta$ -elimination reaction



b)  $\alpha$ -elimination reaction

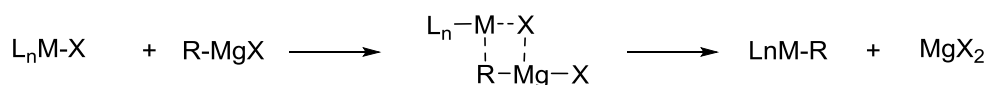


**Scheme 1.6.** a)  $\beta$ -Elimination reaction; b)  $\alpha$ -elimination reaction.

## Transmetallation

The transfer of an organic group from one metal to another is defined as transmetallation. The reaction is usually irreversible for thermodynamic and kinetic reasons. The main application of the transmetallation is the cross-coupling

reaction where it represents a fundamental step. As an example, in the Kumada coupling the transmetallation step involves the replacement of the halide or pseudohalide present in the transition organometallic complex with an aryl, vinyl or alkyl group of a magnesium reagent. A plausible mechanism would involve the initial coordination of the halogen by the magnesium core which would assist a concerted dissociation of the halogen and the organogroup delivery to the nickel/palladium center (Scheme 1.7).<sup>3</sup>

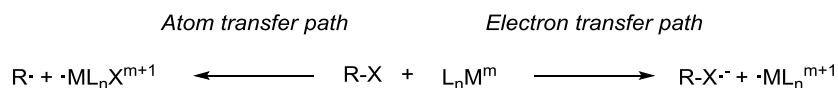


**Scheme 1.7.** Transmetallation reaction in Kumada coupling where R = aryl, vinyl, alkyl and X = halide, pseudohalide.

### 1.3 Metal catalysis of radical reactions

Depending on the electronic properties of a transition metal compound, it can be involved in a two-electron transfer catalytic cycle, whose steps were previously illustrated, or it can follow two distinct radical pathways. The first one is an electron transfer (ET) pathway in which the transition metal compound acts as the electron-donor providing one electron to an organic molecule which is the electron-acceptor. A radical anion is therefore generated from a neutral molecule and it usually fragments into a radical and an anion. In the second pathway the transition metal compound is able to perform a homolytic abstraction of an atom or a group from a non-radical precursor, leaving a radical residue (Scheme 1.8). This last path occurs when the  $\sigma$  bond between the engaged atom or group and the rest of the molecule is weak.<sup>4</sup>





**Scheme 1.8.** Possible radical interactions between transition metal complexes and organic substrates.

Since transition metals can act as initiators, catalysts or both in radical reactions, the current paragraph aims to illustrate briefly some fundamental concepts related to catalysis of radical processes where a metal is involved.

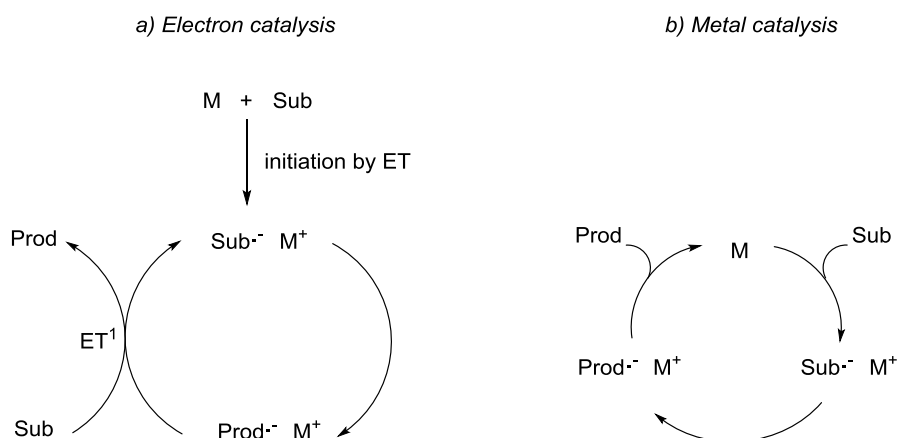
First and foremost a definition of a radical is given: a radical is an atom or compound which contains an unpaired electron. The radical species are in general highly reactive intermediates which tend to react very quickly with other molecules or with themselves, leading to dimerization or polymerization. Furthermore oxidation to a cation by loss of an electron or reduction to an anion by addition of an electron can occur.<sup>5</sup> These processes can be described by chain or non-chain mechanisms which are characterized by a series of elementary steps. Both have the initiation step in common, in which the active radical species called chain carriers are formed. The propagation step on the other hand is representative for the chain mechanism since one radical precursor generates another giving rise to a chain reaction which can be represented in a cycle. A termination reaction competes with the propagation reaction as it results in a net decrease of free radicals with consequent formation of more stable compounds by the combination of radical species. This is considered a step of non-chain mechanism.<sup>5</sup> Due to the nature of radicals these are very interesting intermediates in organic synthesis where most challenges are related to the efficiency and selectivity of their reactions.

An interesting area that recently has been developed concerns the reactions of radicals in the presence of a catalyst. Generally for transition metal catalyzed transformations such as palladium or nickel catalyzed cross-coupling reactions it is assumed that the catalyst is directly involved throughout the entire catalytic cycle.

On the contrary, since radicals and radical ions are already reactive intermediates, the catalytic cycle in radical reactions mostly consists of two parts: an innate catalyst-free part which is the reactions of radicals with themselves or with other ions or molecules, and a catalytic part which consists of radical generation and trapping.

From a mechanistic point of view the chain and non-chain difference is important. In fact, in chain reactions, a metal performs only the initiation role, while in the non-chain catalytic cycle the metal is involved at least in two different roles: initiation and termination.<sup>6</sup>

Two examples of radical catalysis where a metal is involved and an electron-transfer (ET) process occurs are the electron catalysis which is a chain mechanism and the metal catalysis being a non-chain mechanism (Scheme 1.9).

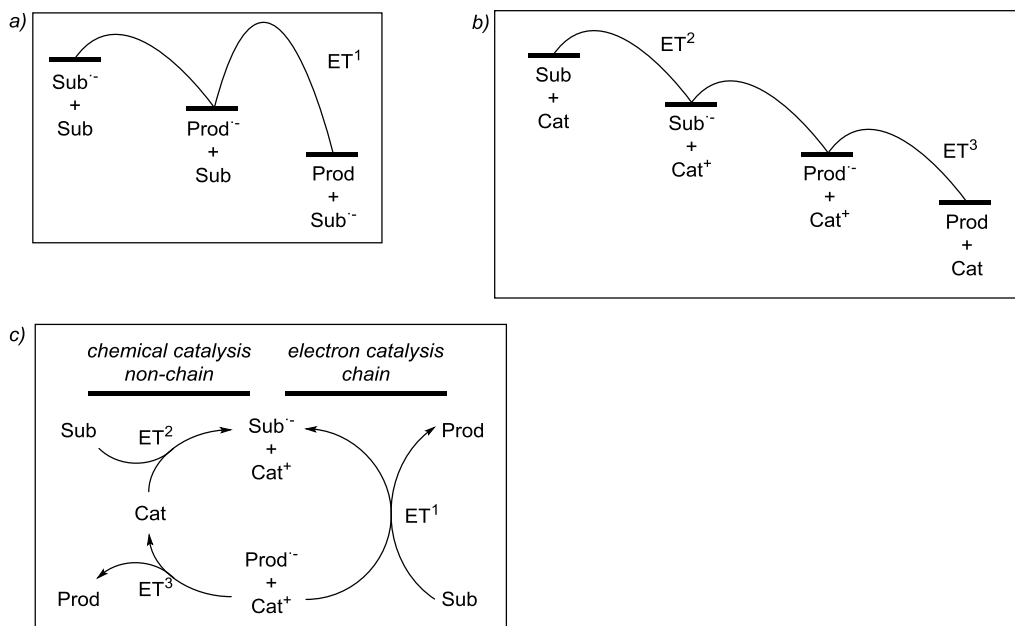


**Scheme 1.9.** a) Electron catalyzed chain cycle where the metal plays the role of initiator; b) metal catalyzed non-chain cycle.

Electron catalysis uses an electron as the catalyst for the reaction and can be initiated for instance by transition metal salts which transfer an electron to a substrate molecule generating a substrate radical anion ( $\text{Sub}^{\cdot-}$ ). This undergoes one or several steps to form the product radical anion ( $\text{Prod}^{\cdot-}$ ). At the end the extra

electron is given back to another substrate molecule to close the cycle and the initiator which is oxidized in the initiation step, is never reduced back. Moreover the oxidized form of the metal is also used as counterion for the radical anions which are produced during the transformation. In summary, this is a case of an innate chain reaction initiated by the metal and catalyzed by an electron.<sup>6</sup>

On the contrary, in the metal catalysis the transition metal is the actual catalyst. The ET transfer process from the metal to the substrate occurs directly in the first step of the catalytic cycle. The oxidized metal ( $M^+$ ) in this case is also used as counterion for all the radical species generated during the reaction. After the conversion of the radical substrate ( $Sub^{\cdot-}$ ) to the radical product ( $Prod^{\cdot-}$ ), the excess electron is transferred back from the product to the metal which is reduced to its original oxidation state ( $M$ ). However, when the electron catalysis occurs it is known that, a typical difficulty can be the electron-transfer passage  $ET^1$  from the radical product to the substrate in order to propagate the chain (Scheme 1.9, a). The  $ET^1$  step can be slow even if it is exothermic. As a solution a metal as catalyst whose redox potential fits the two ET steps of the reaction can be involved. This scenario would include that the lower oxidation state form of the catalyst would reduce the precursor ( $ET^2$ ) and the subsequent higher oxidation state form of the catalyst would oxidize the last reactive intermediate to the product ( $ET^3$ ). Hence the slow step is replaced by two fast steps mediated by the catalyst (Scheme 1.10, b).<sup>6</sup>

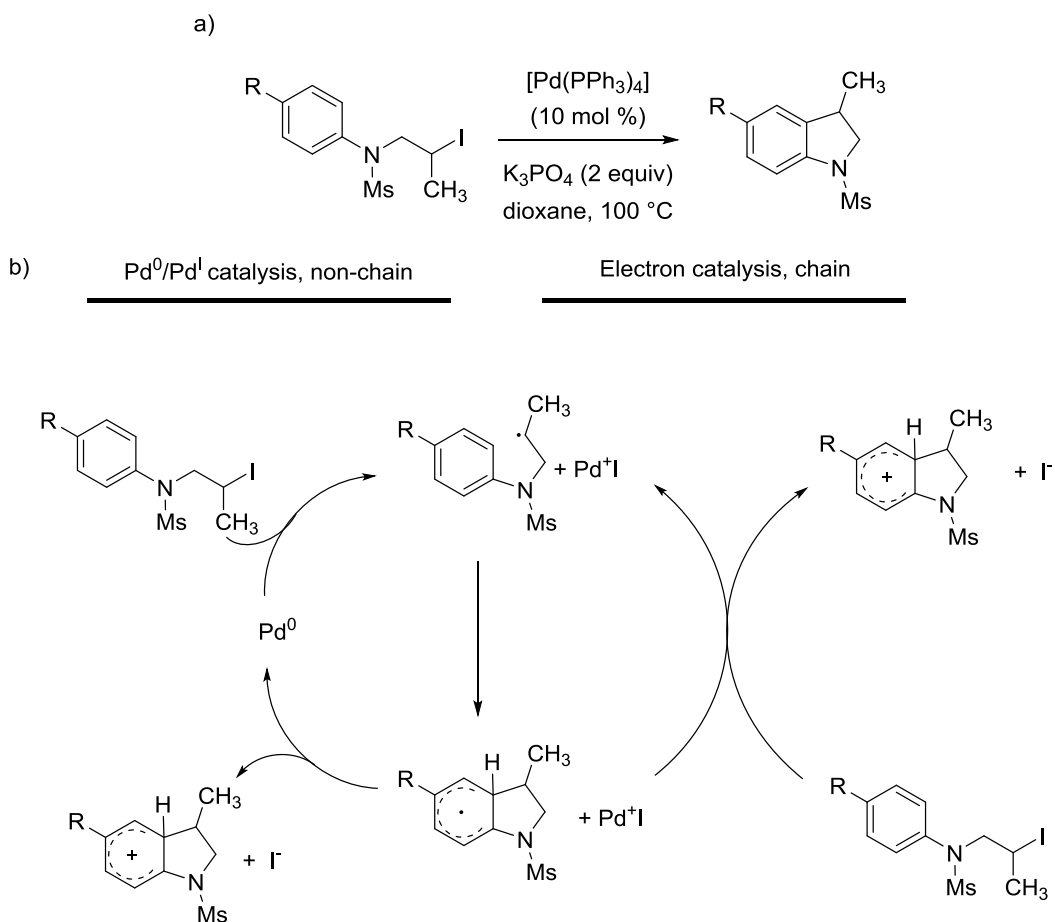


**Scheme 1.10.** Redox catalysis with a chemical catalyst: a) reaction coordinate of electron catalysis with an exothermic ET step that is too slow to support the chain; b) reaction coordinate diagram of redox catalysis cycle in which two fast steps replace the slow step; c) chemical catalysis competes with electron catalysis.<sup>6</sup>

In this case the metal catalysis is strictly connected to the electron catalysis process (Scheme 1.10, c). The different types of catalysis are in direct competition since the first step in the metal catalytic cycle ( $\text{ET}^2$ ) is also the initiation step of the electron-catalysis chain. Therefore non-chain processes are often intertwined with chain reactions and sometimes it is complicated to ascertain which mechanism if not both are operating.

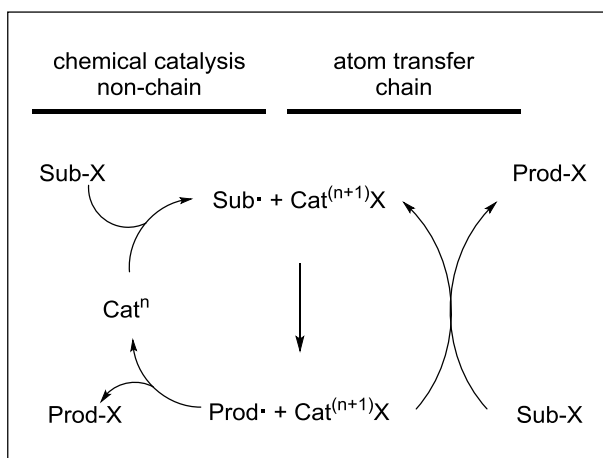
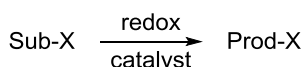
An example of an intertwined reaction is illustrated in Scheme 1.11 where Alexanian and coworkers reported a palladium-catalyzed cyclization of unactivated alkyl halides.<sup>7</sup> In this case non-chain chemical catalysis and chain electron catalysis may compete to form the product. If the non-chain mechanism prevails then the  $\text{Pd}^{(0)}/\text{Pd}^{(I)}$  redox couple is the catalyst of the reaction. On the contrary if

the chain pathway predominates, palladium simply initiates the electron-catalyzed reaction. The two mechanisms have the cyclization of an alkyl radical to a cyclohexadienyl radical in common. In the electron catalysis pathway the cyclohexadienyl radical reacts with a substrate molecule to afford a stable cyclohexadienyl cation which subsequently loses a proton providing the aromatized product. In the non-chain catalytic cycle the cyclohexadienyl radical species transfers the electron to Pd<sup>(0)</sup>I to regenerate Pd<sup>(0)</sup> and to form the cyclohexadienyl cation which undergoes deprotonation resulting in the final product.



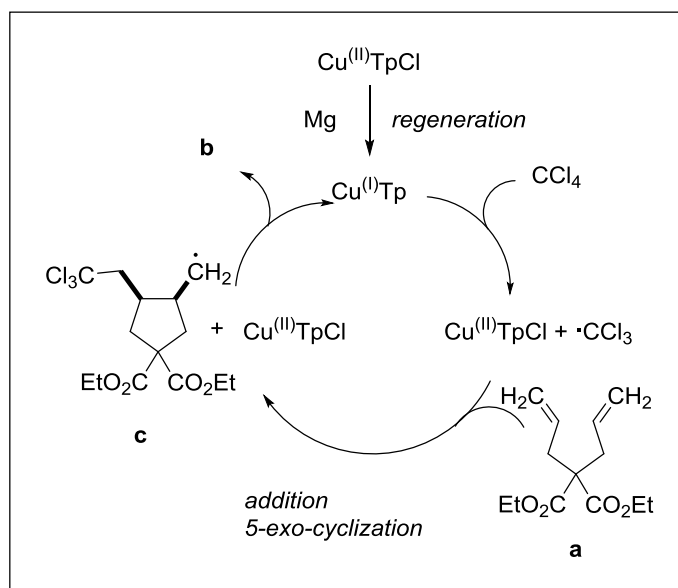
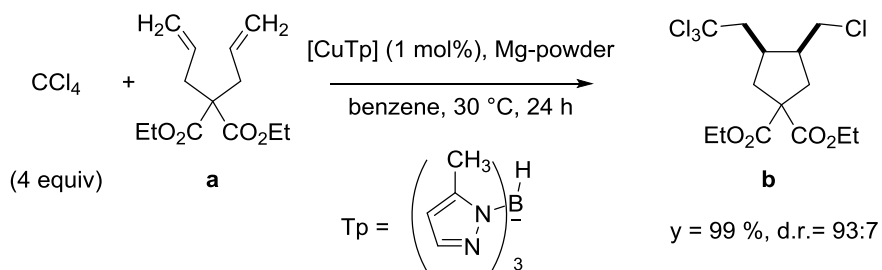
**Scheme 1.11.** Example of intertwined palladium catalysis and electron-catalysis.

Redox catalysis by metals can also occur by atom or group transfer reactions. While iodides and reactive bromides can undergo innate atom-transfer chain cycles, less reactive bromides and chlorides often need the presence of a catalyst since their direct radical transfer reactions are slow. In this case the innate chain cycle and the catalyzed cycle will also overlap and be in direct competition. Both have the halogen abstraction by the catalyst to give the radical species  $\text{Sub}\cdot$  and the formation of the transient radical  $\text{Prod}\cdot$  in common (Scheme 1.12). Afterwards one of two things can happen. If the metal catalysis non-chain predominates, the intermediate complex  $\text{Cat}^{(n+1)}\text{X}$  will react with the transient radical  $\text{Prod}\cdot$  to form the final product and thereby regenerating the catalyst. Otherwise if the atom transfer chain prevails, the transient radical  $\text{Prod}\cdot$  will react with another substrate molecule  $\text{Sub-X}$  to give the desired  $\text{Prod-X}$  and again the radical species  $\text{Sub}\cdot$ .



**Scheme 1.12.** Atom-transfer reactions. The catalytic cycle intertwines with innate atom-transfer cycle.

The most commonly employed metal catalyst in atom-transfer reactions is copper and it was extensively used in atom-transfer radical additions and cyclization processes.<sup>8</sup> A recent example of a copper-catalyzed atom-transfer addition is illustrated in Scheme 1.13.<sup>9</sup> Carbon tetrachloride reacts with ethyl bisallyl malonate under copper trispyrazolylborate (Tp) catalysis. The mechanism of the transformation involves a sequence of radical addition, cyclization and atom-transfer reactions.  $\text{Cu}^{(I)}\text{Tp}$  abstracts a Cl atom from  $\text{CCl}_4$  in the first step giving the trichloromethyl radical  $\cdot\text{CCl}_3$  and the oxidized species  $\text{Cu}^{(II)}\text{TpCl}$ . A subsequent addition of  $\cdot\text{CCl}_3$  to bisallyl malonate **a** and further 5-*exo*-cyclization, provides the primary exocyclic radical **c** which abstracts the Cl atom from  $\text{Cu}^{(II)}\text{TpCl}$  affording the final product **b**. Competing side reactions may involve the dimerization of the trichloromethyl and the cyclized radicals resulting in the accumulation of  $\text{Cu}^{(II)}\text{TpCl}$  complex and subsequent suppression of the reaction. The presence of magnesium is therefore required to restore the active  $\text{Cu}^{(I)}\text{Tp}$  complex whose concentration must remain constant.



**Scheme 1.13.** Cu-catalyzed atom-transfer addition and cyclization reaction.



## 2 Dehydrogenative synthesis of carboxylic acids catalyzed by a ruthenium *N*-heterocyclic carbene complex

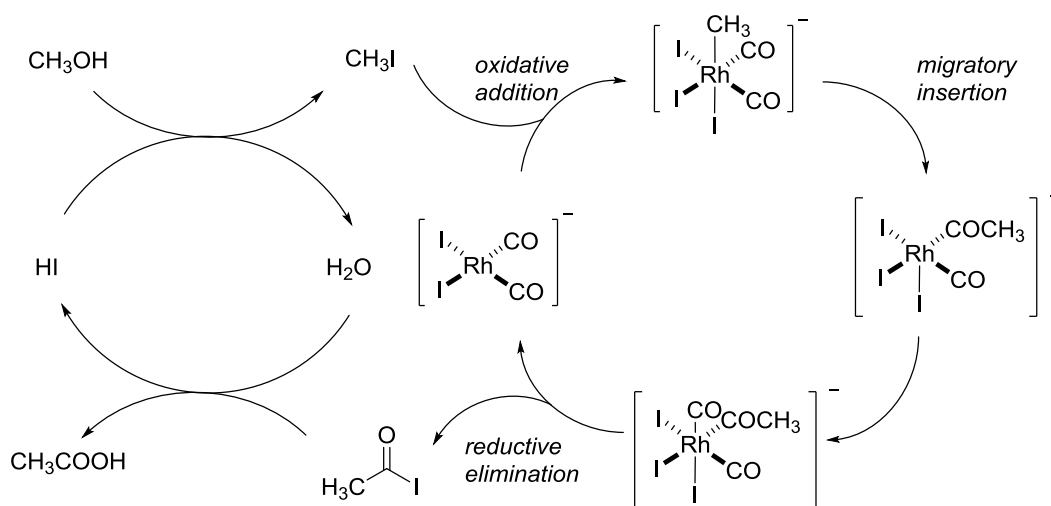
---

### 2.1 Introduction

Carboxylic acids represent an important class of compounds in organic chemistry. They are widely present in nature, and are contained in fundamental biological molecules such as amino acids and lipids. Carboxylic acids are also extensively employed in industry for the production of pharmaceuticals, food additives, polymers, and solvents. For instance fatty acids are used for coatings, acrylic and methacrylic acids are used as precursors to polymers and adhesives, citric acid is employed in beverages (etc.). Acetic acid is an important chemical reagent and is broadly used in industry for the production of cellulose acetate for photographic film and polyvinyl acetate for wood glue. Moreover it is a precursor to solvents and it is widely employed as a food additive in the food industry.

The main industrial process for manufacturing ethanoic acid was developed in 1966 by Monsanto.<sup>10</sup> This process is based on methanol carbonylation catalyzed by a rhodium complex with hydrogen iodide as the co-catalyst. The role of iodide is to convert methanol to methyl iodide which undergoes oxidative addition to *cis*-[Rh(CO)<sub>2</sub>I<sub>2</sub>]<sup>-</sup>. Coordination and insertion of carbon monoxide leads to an acyl complex which then undergoes a reductive elimination yielding the acetyl iodide and regenerating the active catalyst *cis*-[Rh(CO)<sub>2</sub>I<sub>2</sub>]<sup>-</sup>. Conclusively, acetic acid is produced by reaction of acetyl iodide with H<sub>2</sub>O and thereby also restoring HI which can re-enter the catalytic cycle (Scheme 2.1). This was previously the main industrial process, but it has now been replaced by the Cativa procedure which differs solely in the involvement of an iridium based complex [Ir(CO)<sub>2</sub>I<sub>2</sub>]<sup>-</sup>.<sup>11</sup> The development of this method brought several advantages: the use of less water in

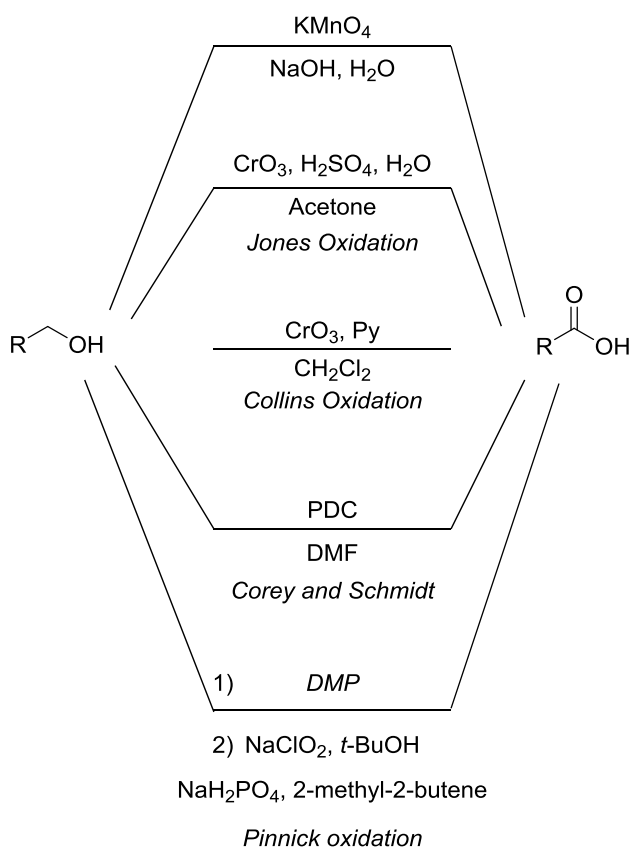
the reaction mixture, the suppression of the water gas shift reaction, as well as the decrease of byproducts such as propionic acid.



**Scheme 2.1** Monsanto process for methanol carbonylation.

Laboratory approaches to prepare carboxylic acids include procedures where primary alcohols or aldehydes are oxidized with stoichiometric amount of oxidants. Typical examples are reported below in Scheme 2.2.<sup>12</sup> The oxidation with potassium permanganate ( $\text{KMnO}_4$ ) was first investigated by Fournier in 1907 and 1909. The reaction conditions proposed by Fournier include strong alkaline aqueous environment, although this limits the scope of the reaction as not every alcohol is soluble in water. Hence, the addition of an organic co-solvent often helps the dissolution of the alcohol in the aqueous permanganate. Moreover,  $\text{KMnO}_4$  decomposes in water to manganese dioxide ( $\text{MnO}_2$ ) and dioxygen, and therefore consecutive additions of the oxidant are required during the reaction to ensure full conversion. The Jones oxidation is another traditional method which allows for the formation of carboxylic acids from primary alcohols by the employment of chromic trioxide or sodium dichromate in diluted sulfuric acid. The

chromic acid is generated *in situ* and acts as the oxidant of the transformation. This procedure was improved and a complex of chromium(VI) oxide with pyridine (Collins reagent) or pyridinium dichromate (PDC) can be used for the purpose. It is also possible to conduct a two-step oxidation in order to avoid harsh oxidation conditions and functional group incompatibility. In this case the primary alcohol is first oxidized to an aldehyde by the Dess-Martin periodinane (DMP) and subsequently undergoes a Pinnick oxidation resulting in the carboxylic acid.<sup>12</sup>

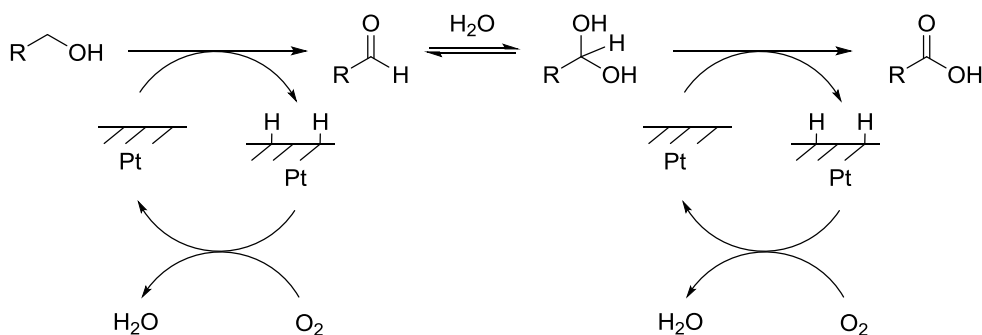


**Scheme 2.2.** Traditional methods for the oxidation of primary alcohols with stoichiometric oxidants.

## 2.2 Synthesis of carboxylic acids from catalytic oxidation of primary alcohols

Other procedures to synthesize carboxylic acids from primary alcohols employ a catalytic amount of a metal or metal complex and cheap stoichiometric oxidants such as periodate and dioxygen. The secondary oxidants oxidize the catalyst to the original oxidation state hence a new catalytic cycle can start.

The Heyns oxidation is a known reaction which employs platinum as catalyst and dioxygen as secondary oxidant (Scheme 2.3).<sup>13</sup>

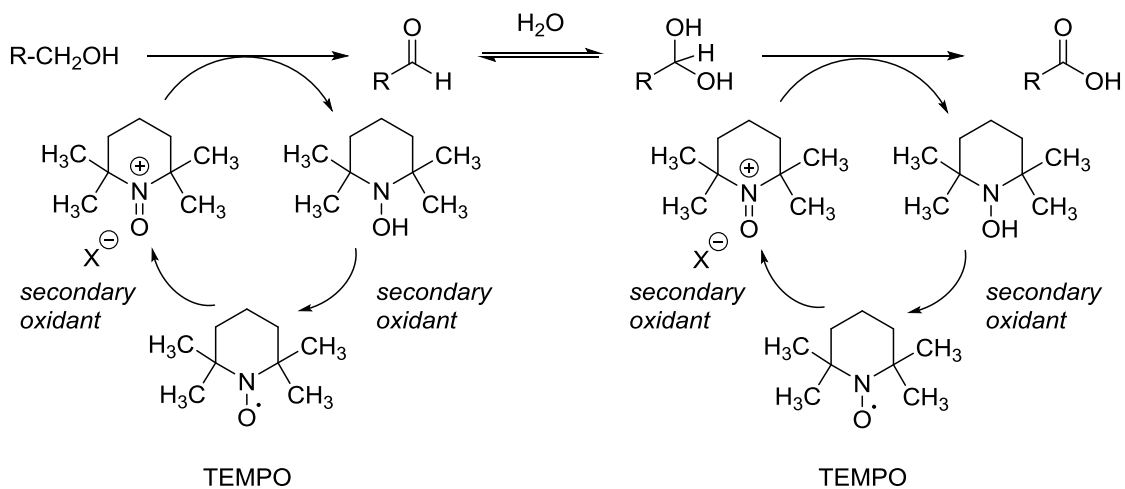


**Scheme 2.3.** Heyns oxidation mechanism where a primary alcohol is oxidized to the corresponding carboxylic acid through an aldehyde and a gemdiol as intermediates.

This reaction is normally conducted under basic condition which allows the consumption of the primary alcohol into the corresponding carboxylate salt of the carboxylic acid. Usually the process is selective towards primary alcohols under mild reaction conditions,<sup>14,15</sup> but oxidation of secondary alcohols can sometimes occur even if it represents the minor pathway.<sup>16–20</sup> Heyns oxidation is normally performed in water, but the presence of an organic co-solvent sometimes is useful as this allows for dissolution of hydrophobic alcohols. However, when an organic solvent is used as the only solvent, the reaction product is an aldehyde.<sup>13</sup>

Another known procedure provides the formation of carboxylic acids by the use of ruthenium tetroxide ( $\text{RuO}_4$ ) as the catalyst and periodate being added to re-oxidize the low-valent ruthenium compounds to the active species for a new catalytic cycle.  $\text{RuO}_4$  was already known to be a strong oxidizing agent and it was already employed in oxidation reactions in stoichiometric amount early in the 1950s, but it is a toxic and explosive compound and appropriate precautions must be taken to handle it. A catalytic amount of  $\text{RuO}_4$  associated with periodate as secondary oxidant was first investigated by Pappo and Becker in the oxidation of alkenes and alkynes<sup>12</sup> and was later extended to primary alcohols in 1968 by Roberts and co-workers.<sup>21</sup> The catalytic use of this reagent makes the oxidative procedure a safer and cheaper way to oxidize organic compounds. This preparative method underwent several modifications concerning the secondary oxidant and the solvent employed in the process. Sharpless's modification consists in the use of a two-phase solvent mixture of water/MeCN/ $\text{CCl}_4$ . Acetonitrile helped to prevent the inactivation of the catalyst thanks to its capability in forming complexes with low valent ruthenium species and in restoring the active  $\text{RuO}_4$ .<sup>21</sup> Moreover, it was found that  $\text{CCl}_4$  which is a toxic solvent can be replaced by ethyl acetate.  $\text{NaIO}_4$  is the secondary oxidant used in most cases, although  $\text{H}_5\text{IO}_6$  is sometimes recommended for a more facile reaction.<sup>22-25</sup> In most of the cases the hydrated form of  $\text{RuCl}_3$  is employed as the ruthenium precursor  $\text{RuO}_4$ . Instead of  $\text{RuO}_4$  it is possible to use ruthenate ( $\text{RuO}_4^{2-}$ ) or perruthenate ( $\text{RuO}_4^-$ ) salts which are mild oxidants. For instance tetrapropylammonium perruthenate (TPAP) in the presence of *N*-methylmorpholine-*N*-oxide as secondary oxidant can be employed for the synthesis of carboxylic acids.<sup>26-28</sup>

Furthermore the oxidation of primary alcohols to carboxylic acids can be conducted by the participation of an organic molecule as catalyst. A very useful organic molecule is the stable radical 2,2,6,6-tetramethylpiperidine-1-oxyl (TEMPO) which is usually oxidized to the active oxoammonium cation by a secondary oxidant (Scheme 2.4).<sup>12</sup>



**Scheme 2.4.** General accepted mechanism for the TEMPO mediated transformation of a primary alcohol to a carboxylic acid.

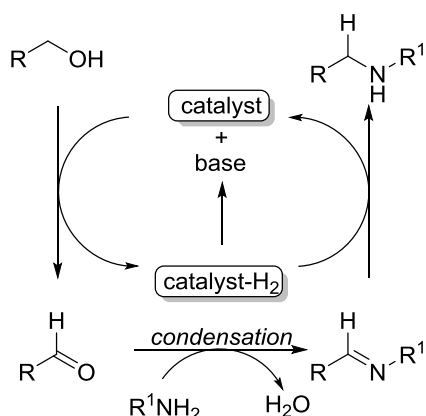
Occasionally TEMPO can inhibit the oxidation of the aldehyde to the acid if the mechanism follows a radical pathway. In this case the secondary oxidant for the transformation of the primary alcohol to the aldehyde fulfills the role of a primary oxidant at the second stage generating the acid. The procedure with TEMPO as the catalyst underwent several improvements since the discovery. Anelli's method requires treatment of primary alcohols with 4-MeO-TEMPO in  $\text{CH}_2\text{Cl}_2/\text{water}$  mixture with sodium hypochlorite ( $\text{NaClO}$ ) in the presence of sodium bicarbonate ( $\text{NaHCO}_3$ ) and potassium bromide ( $\text{KBr}$ ).<sup>29</sup> A limitation of this method is the employment of  $\text{NaClO}$  as a stoichiometric oxidant which can result in chlorination reactions for some sensitive substrates. This issue is overcome by Zhao's procedure in which  $\text{NaClO}$  is instead used in catalytic amounts<sup>30</sup> while sodium chlorite ( $\text{NaClO}_2$ ), which is employed in the oxidation transformation in stoichiometric quantity, has two roles: it oxidizes the intermediate aldehyde to the corresponding carboxylic acid and regenerates  $\text{NaClO}$ .<sup>31</sup> A further important variation is represented by Epp and Widlansky's procedure in which the transformation of primary alcohols to carboxylic acids is conducted by using

bis(acetoxy)iodobenzene (PhI(OAc)<sub>2</sub>) as a stoichiometric secondary oxidant. This method avoids the employment of inorganic salts and the only byproducts produced from the reaction are iodobenzene and acetic acid.<sup>32</sup>

### 2.3 Acceptorless dehydrogenations of primary alcohols

As previously reported, traditional dehydrogenations of primary alcohols are performed using toxic strong oxidants that results in stoichiometric toxic waste. The recent development of acceptorless dehydrogenation (AD) reactions helps to circumvent these issues. In fact AD processes are catalyzed by metal complexes and no additional oxidants are used. Very importantly is the only by-product is hydrogen gas which is liberated during the transformation.<sup>33</sup> This aspect is also very important for a renewable energy angle since hydrogen is considered a valuable energetic resource which may replace fossil fuels in the future.<sup>34</sup> The major challenge with hydrogen is the difficulty in storage. It has a low ignition energy considering that small amounts are easily flammable in contact with air, and it has a strong propensity to escape containment. A solution to these problems can be the use of liquid organic hydrogen carriers (LOHCs) which can store or release hydrogen through catalytic hydrogenation or dehydrogenation processes.<sup>34</sup>

Furthermore, in terms of synthetic strategies the hydrogen generated by AD reactions can be consumed directly *in situ* to hydrogenate an unsaturated intermediate derived from a condensation reaction. This method is called “hydrogen autotransfer” or “hydrogen borrowing” of which an example is reported in Scheme 2.5.<sup>33, 34</sup>



**Scheme 2.5.** Example of hydrogen autotransfer: the catalyst dehydrogenates the alcohol and formally transfers hydrogen to an unsaturated intermediate. The process occurs with no evolution of hydrogen gas and with water as the only by-product.

Over the last few years different transition metal complexes based on iridium and rhodium, have been used for the acceptorless alcohol dehydrogenation (AAD) reactions. For instance Fujita and Yamaguchi reported in 2011 the dehydrogenative synthesis of aldehydes from primary alcohols by using 2 mol% of Cp\*Ir catalyst with a C-N chelating ligand (complex **a**, Figure 2.1).<sup>35</sup> If a bipyridine-based ligand **b** is employed instead dissolution of the catalyst in water is possible, and the procedure is feasible in aqueous media.<sup>36</sup> [Rh(trop)<sub>2</sub>N)-(PPh<sub>3</sub>)] has proven to give dehydrogenative coupling of primary alcohols with water, methanol, and amines to form carboxylic acids, methyl carboxylates and amides (complex **c**, Figure 2.1). The presence of a hydrogen acceptor such as cyclohexanone or methylmethacrylate is needed for this reaction.<sup>37</sup> Another rhodium-catalyst whose activity towards dehydrogenation reactions was recently discovered, is complex **d** which can be successfully used for the dehydrogenative coupling of benzyl alcohols and aliphatic alcohols to produce esters.<sup>38</sup>



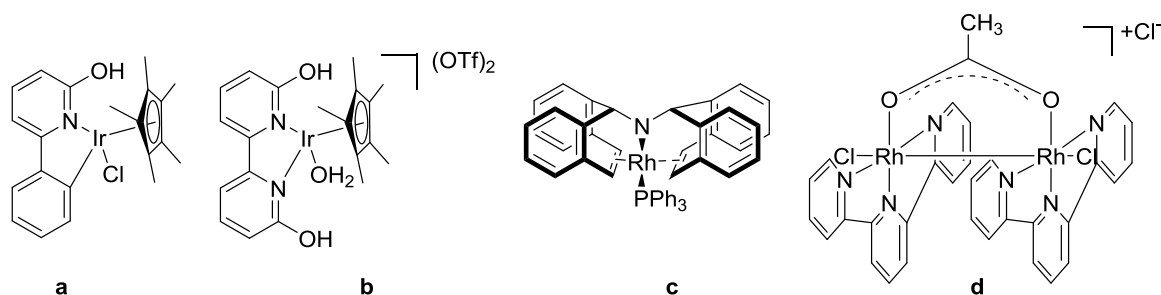
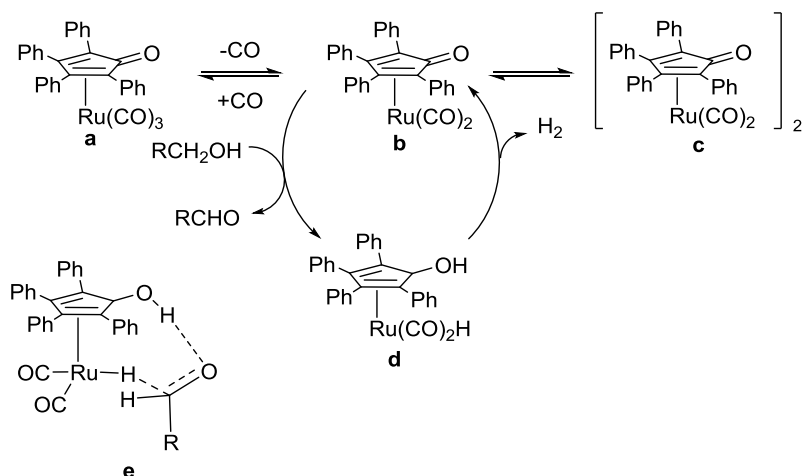


**Figure 2.1.** Catalysts employed for the dehydrogenative transformations of primary alcohols by Fujita and Yamaguchi (**a**, **b**),<sup>35, 36</sup> Grützmacher (**c**);<sup>37</sup> Wang and Xiao (**d**).<sup>38</sup>

### 2.3.1 Ruthenium-catalyzed AAD reactions

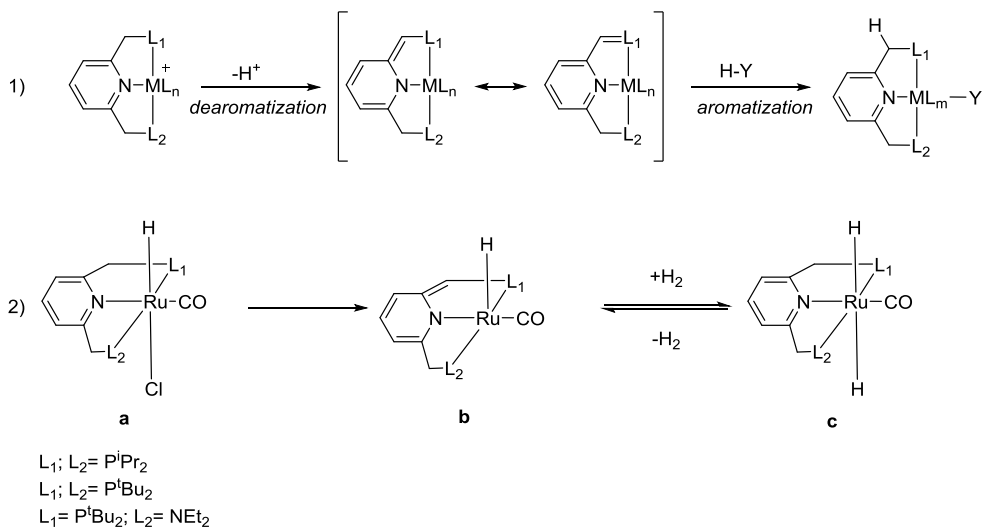
The activity of ruthenium complexes towards dehydrogenation reactions was already known from the studies conducted by Shvo and co-workers. Their first approaches employed  $\text{Ru}_3(\text{CO})_{12}$  as the catalyst precursor for the transformations of alcohols and aldehydes into esters in the presence of diphenyl acetylene as a hydrogen acceptor which is reduced to a mixture of *cis* and *trans* stilbene and 1,2-diphenylethane.<sup>39,40</sup> Subsequent insights on these dehydrogenation reactions have highlighted that phenyl acetylene not only has the function of hydrogen acceptor, but it has a fundamental role in the activation of the catalyst. In fact, reaction of phenyl acetylene with  $\text{Ru}_3(\text{CO})_{12}$  forms a tetracyclone ligand *in situ* and generates  $(\eta^4\text{-tetracyclone})(\text{CO})_3\text{Ru}$  (**a**) as well as the dimeric form  $[(\eta^4\text{-tetracyclone})(\text{CO})_2\text{Ru}]_2$  (**c**). These two ruthenium complexes are employed as catalyst precursors for the dehydrogenative synthesis of esters and ketones respectively from primary and secondary alcohols without any hydrogen acceptor (Scheme 2.6).<sup>41</sup>



**Scheme 2.6.** Complexes **a** and **c** are catalyst precursors which can be interconverted by the loss or addition of CO. Furthermore, the loss of CO from **a** or the dissociation of **c** provides the same structure **b** which has a free coordination site and is the actual catalyst involved in Shvo's reactions. Complex **b** oxidizes the alcohol to the aldehyde which is the intermediate of the reaction. The resulting dihydride complex **d** subsequently can lose dihydrogen restoring complex **b**. Structure **e** represents the transition state according to the outer-sphere mechanism.<sup>42,43</sup>

Recently Milstein and co-workers have been developing various procedures where primary alcohols are involved in the synthesis of esters,<sup>44–46</sup> amides,<sup>47–50</sup> imines,<sup>51,52</sup> and acetals.<sup>53–55</sup> The novelty of Milstein's procedures lies in the use of ruthenium pincer complexes composed of PNP or PNN ligands. In fact the protons at the phosphine arms of these ligands are easily removable by a base due to the relatively low resonance energy of pyridine (28 kcal/mol) and the stabilization of the dearomatized ligand by the metal center.<sup>56,57</sup> The dearomatized complexes generated can activate chemical bonds by cooperation between the metal and the ligand thereby again undergo aromatization by a reaction with H-Y where Y= H, OH, OR, NH<sub>2</sub>, NR<sub>2</sub>, C (Scheme 2.6).<sup>56,57</sup> The oxidation state of the metal is not altered during this process. As an example the reversible reaction with dihydrogen of the dearomatized complex **b** resulting in the aromatized *trans*-dihydride complex **c** is shown in Scheme 2.6.<sup>56</sup> This type of metal-ligand cooperation by

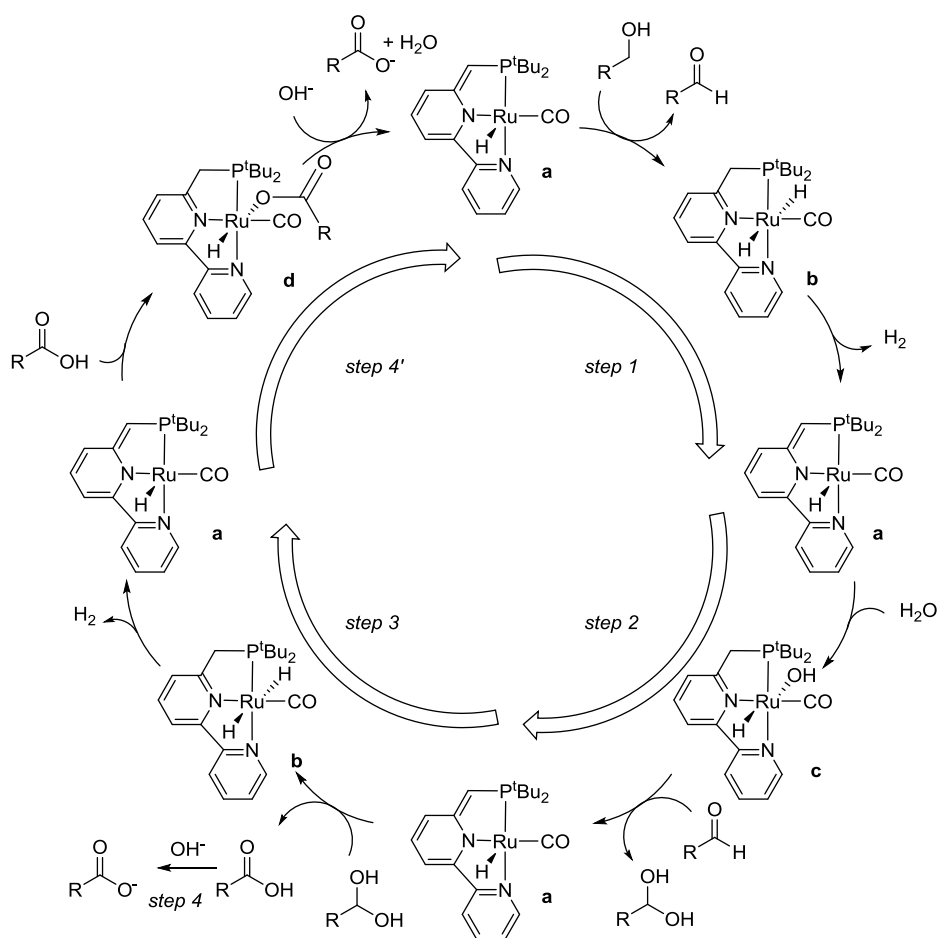
aromatization and dearomatization of pyridine- and acridine-based pincer complexes plays a key role in the catalytic dehydrogenation transformations presented by Milstein.



**Scheme 2.6.** 1) General metal-ligand cooperation by aromatization-dearomatization; 2) dearomatization of PNP and PNN pincer complexes and their reversible reactions with  $H_2$  to give aromatized complexes **c**.

In 2013 Milstein and co-workers presented a reaction for the dehydrogenative synthesis of carboxylic acids.<sup>58</sup> A low catalyst loading (0.2 mol%) of a ruthenium PNN pincer complex is used for the purpose and the reaction is conducted in basic aqueous solution in absence of a hydrogen scavenger. The reaction mechanism was first analyzed by the authors and further investigation by computational calculations showed that the process pass through an overall four step mechanism with the formation of an aldehyde and a gemdiol as intermediates (Scheme 2.7).<sup>59</sup> At the end of every step complex **a** is regenerated. The first step is characterized by the dehydrogenation of the primary alcohol to the aldehyde with the formation of a *trans*-dihydro ruthenium complex **b** followed by release of  $H_2$ . Water addition

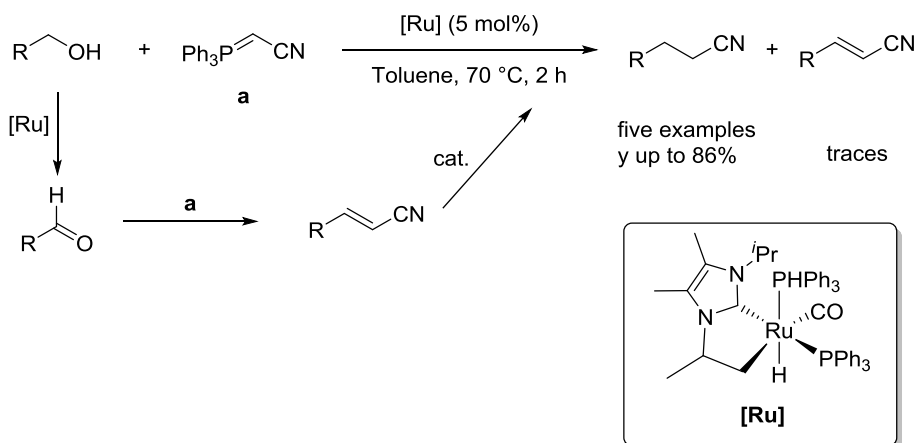
in step 2 results in complex **c** which then leads to the concerted transfer of  $\text{OH}^-$  and a hydrogen atom to the aldehyde providing a gem-diol as an intermediate. A dehydrogenation of the gem-diol follows to form the carboxylic acid and the *trans*-dihydro ruthenium complex **b** which releases  $\text{H}_2$  to restore complex **a**. In step 4 the carboxylic acid is deprotonated by the base into the carboxylate, since the acid would otherwise coordinate to complex **a** giving ruthenium complex **d**. Anyway, in this last case the base results in the deprotonation of the acid to the corresponding carboxylate and leads to the initial complex **a** (step 4).



**Scheme 2.7.** Proposed four-steps overall mechanism for the formation of a carboxylate anion with the active complex **a**.

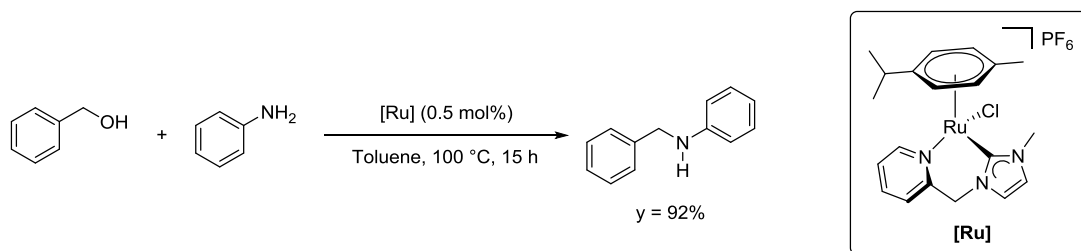
### 2.3.2 Ruthenium *N*-heterocyclic carbene catalyzed dehydrogenative transformation of primary alcohols

The importance of ruthenium in organometallic catalysis mostly lies in the features of *N*-heterocyclic carbenes (NHCs) as ligands. NHCs display higher thermal stability and stronger  $\sigma$ -donating properties increasing the catalytic activity over phosphine or amines as ligands.<sup>60</sup> Ruthenium *N*-heterocyclic carbene complexes (Ru-NHC) have been extensively utilized in organometallic chemistry for metathesis reactions.<sup>61</sup> Only recently these complexes have found different applications. The Beller group was one of the first to exploit the potentials of NHC ligands in ruthenium catalyzed transfer hydrogenation reactions.<sup>62</sup> More specifically Beller and co-workers reported the 2-propanol-based reduction of acetophenone to form 1-phenylethanol by an *in situ* prepared ruthenium catalyst from  $[\text{Ru}(\text{cod})(2\text{-methylallyl})_2]$  and an imidazolium salt  $[\text{IPrH}][\text{Cl}]$  in the presence of a base. Optimization of the reaction conditions included the employment of different NHC ligands attached to the ruthenium center. This has resulted in a large number of interesting catalysts which can be used in the direct hydrogenation reactions of C=O and C=C bonds.<sup>63–66</sup> A field of particular interest in which NHC ruthenium complexes have been largely used is the dehydrogenative transformations of alcohols. In particular the so-called borrowing hydrogen reactions allow the temporary oxidation of alcohols to aldehydes and ketones which are subsequently utilized for the formation of C-C and C-N bonds. As an example Williams and co-workers reported in 2007 an indirect Wittig reaction where the Ru-NHC species catalyzed first the dehydrogenation of a primary alcohol to the aldehyde. The alkene intermediate formed by Wittig reaction of the aldehyde with (triphenylphosphoranylidene) acetonitrile undergoes subsequent hydrogenation catalyzed by the Ru-NHC species to provide the final saturated hydrocarbon product (Scheme 2.8).<sup>67</sup>



**Scheme 2.8.** Indirect Wittig reaction reported by Williams and co-workers.

Valerga and co-workers in 2012 described the alkylation of aryl amines with alcohols to afford the amine products by the use of Ru-picolyl-NHC complexes (Scheme 2.9).<sup>68</sup>

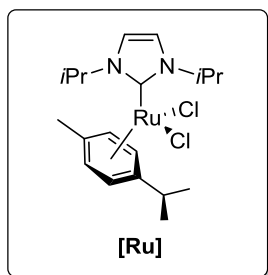
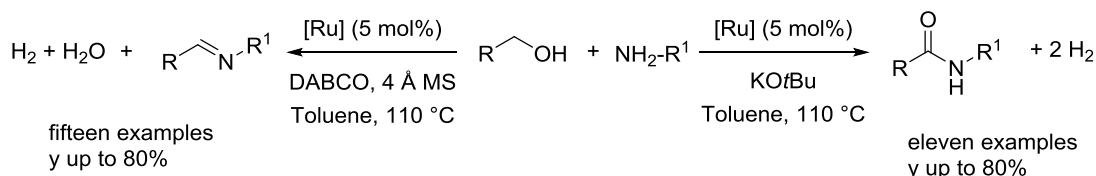


**Scheme 2.9.** Alkylation of aniline with benzyl alcohol catalyzed by Ru-picolyl-NHC complex.

The use of benzylamine under the reaction conditions allowed for the formation of the corresponding imine as the product. This suggested that a hemiaminal was generated as intermediate during the reaction and subsequently underwent dehydration to form the imine product.<sup>68</sup>

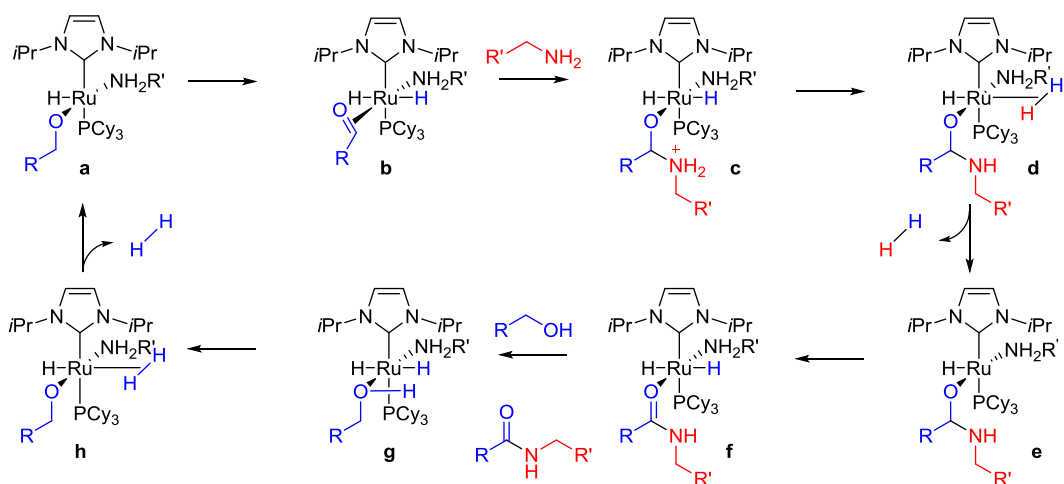
During the same period R. Madsen and co-workers reported the dehydrogenative synthesis of imines from primary alcohols and amines catalyzed by the complex  $[\text{Ru}(p\text{-cymene})(\text{I}^i\text{Pr})\text{Cl}_2]$ . Also in this case the hemiaminal is formed as the

intermediate during the reaction (Scheme 2.10, a).<sup>69</sup> Previous studies conducted by the authors have demonstrated that  $[\text{Ru}(\textit{p}\text{-cymene})(\textit{iPr})\text{Cl}_2]$  complex in the presence of tricyclohexylphosphine ( $\text{PCy}_3$ ) and  $\text{KO}^t\text{Bu}$  gave rise to amides in good to excellent yield (Scheme 2.10, b).<sup>70,71</sup>



**Scheme 2.10.** Madsen's and co-workers dehydrogenative synthesis of imines (a) and amides (b) by the employment of the complex  $[\text{Ru}(\textit{p}\text{-cymene})(\textit{iPr})\text{Cl}_2]$ .

The mechanism for the amide formation has been studied in detail by experimental and computational methods. It is believed to proceed through the aldehyde and the hemiaminal as intermediates (Scheme 2.11).<sup>72</sup>

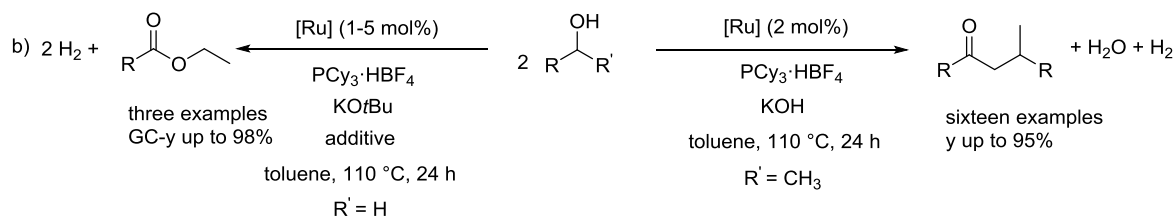
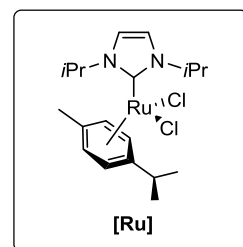
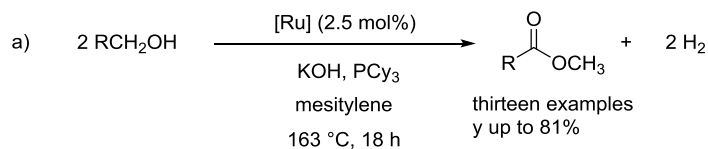


**Scheme 2.11.** Mechanism for the amide formation catalyzed by complex  $[\text{Ru}(\textit{p}\text{-cymene})(\textit{iPr})_2\text{Cl}_2]$ .

Firstly both the *p*-cymene ligand and the two chlorides are lost being replaced by coordination of a hydride, an alkoxide, and an amine providing complex **a**. Subsequent  $\beta$ -hydride elimination affords the *trans*-dihydro complex **b** where an aldehyde now is coordinated to the ruthenium center. The amine addition to the coordinated aldehyde affords the protonated hemiaminal as the intermediate producing complex **c**. The following proton transfer to the hydride and dihydrogen evolution provides complex **e** which undergoes  $\beta$ -hydride elimination with consequent amide formation generating complex **f**. The amide so formed is then released by the complex **f** and a second molecule of alcohol is coordinated to the ruthenium center resulting in complex **g**. The catalytic cycle ends with a second evolution of dihydrogen and the regeneration of complex **a**.

The scope of  $[\text{Ru}(\textit{p}\text{-cymene})(\textit{iPr})_2\text{Cl}_2]$  has also been extended to the synthesis of esters when primary alcohols are treated with the Ru-complex,  $\text{PCy}_3$  and KOH in refluxing mesitylene (Scheme 2.12, a).<sup>73</sup> The reaction conditions for the direct condensation of primary alcohols into esters were further optimized and extended to the dehydrogenative self-coupling of secondary alcohols into the corresponding ketones (Scheme 2.12, b).<sup>74</sup>



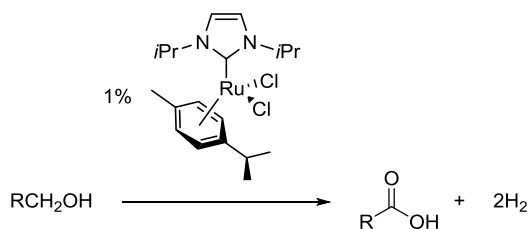


**Scheme 2.12.**  $[\text{Ru}(p\text{-cymene})(i\text{Pr})\text{Cl}_2]$  catalyzes homodimerization of primary alcohols to esters (a) and self-condensation of secondary alcohols to ketones (b).

## 2.4 Conclusion

Carboxylic acids remain valuable tools in organic chemistry due to their easy conversion into different functional groups. They can be synthesized from primary alcohols by the use of stoichiometric oxidizing agents which generates a stoichiometric amount of waste at the end of the oxidation reactions. In the last years R. Madsen's group has been developing more benign catalytic transformations for the oxidation of primary alcohols where a stoichiometric oxidizing agent is not utilized. In fact, the transformations can now occur under dehydrogenative conditions where the ruthenium catalyst liberates hydrogen gas from the alcohol. The method was used to synthesize amides, imines and esters and can be also extended to the synthesis of carboxylic acids since their formation were observed during the optimization of the ester synthesis from primary alcohols. For this project the optimization of the reaction conditions has been

carried out and demonstrated the possibility to achieve the acids with a relatively low catalyst loading (Scheme 2.13).



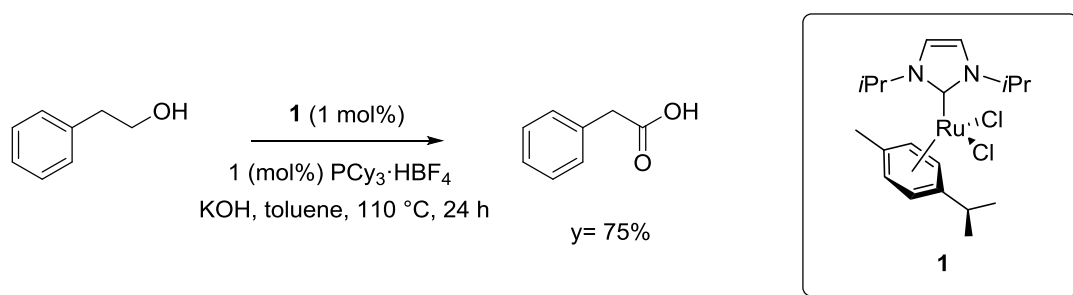
**Scheme 2.13.** Dehydrogenative synthesis of carboxylic acids from primary alcohols catalyzed by [Ru(*p*-cymene)(IPr)Cl<sub>2</sub>].

In the next results and discussions section, the substrate scope and limitations of the dehydrogenative synthesis of primary alcohols to carboxylic acids catalyzed by [Ru(*p*-cymene)(IPr)Cl<sub>2</sub>] will be presented together with a mechanistic investigation for the reaction.<sup>75</sup>

## 2.5 Results and discussion

### 2.5.1 Preliminary studies and optimization of the reaction conditions

Complex **1** was used earlier as a precatalyst for the dehydrogenative self-condensation of 2-phenylethanol into the corresponding ester.<sup>74</sup> The reaction was carried out under strongly basic conditions by using  $\text{KtBuO}$  and  $\text{Mg}_3\text{N}_2/\text{K}_3\text{PO}_4$ .<sup>74</sup> However when the bases were substituted with a stoichiometric amount of  $\text{KOH}$ , the product changed to the carboxylic acid. In this way, 2-phenylethanol was converted into phenylacetic acid in 75% yield in refluxing toluene. (Scheme 2.14).



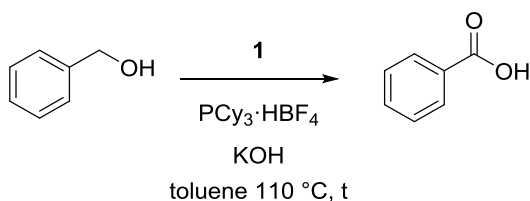
**Scheme 2.14.** Dehydrogenative oxidation of 2-phenylethanol with complex **1**.

Furthermore, it was found that when polar solvents such as dioxane, diglyme, and *tert*-amyl alcohol were used, transformation of the primary alcohol to the corresponding acid was not completed after 24 h. The inhibition of the ruthenium catalyst by the carboxylate salt which is soluble in these solvents could be a plausible explanation. When the reaction was performed in the presence of a high boiling point solvent such as xylene, the yield of phenylacetic acid dropped to 20%. It was furthermore demonstrated that the employment of  $\text{LiOH}$  and  $\text{NaOH}$  as the base or the replacement of the phosphine with  $\text{PPh}_3$  or  $\text{dppp}$ , resulted in the lower conversion of 2-phenylethanol.

These preliminary results encouraged the development of a new dehydrogenative method for the formation of carboxylic acids which represents the main discussion in this dissertation. For the further optimization of the oxidation reaction benzyl alcohol was chosen as the test substrate instead of 2-phenylethanol as it was observed that 2-phenylethanol underwent C-C cleavage with subsequent formation of toluene and formic acid as a collateral reaction.<sup>76</sup> The catalytic procedure was carried out in refluxing toluene under a flow of argon with 1 mol% of complex **1** in the presence of 1 mol% PCy<sub>3</sub>·HBF<sub>4</sub> as the ligand as well as 1.2 equivalent of KOH as the base. In earlier studies conducted in our research group of the dehydrogenative amidation reaction catalyzed by complex **1**, problems with reproducibility were found. These were attributed to the direct employment of PCy<sub>3</sub> which is easily oxidized by air. Moreover, it was discovered that commercial samples of PCy<sub>3</sub> from various suppliers contain different amounts of impurities as phosphine oxide and phosphites which are difficult to remove.<sup>72</sup> This issue was overcome by the employment of the more stable PCy<sub>3</sub>·HBF<sub>4</sub> salt,<sup>77</sup> and it was therefore selected for the current work.

As already stated, the employment of a stoichiometric amount of KOH was necessary to ensure full conversion of the alcohol affording 79% of benzoic acid product after 6 h (entry 1, Table 1). Interestingly employing 2 and 5 equivalent of KOH the yield of the benzoic acid dropped to 55% and 31% respectively (entry 2-3, Table 1). The catalyst loading was furthermore investigated discovering that lower loadings (entry 4-5, Table 1) provided a decrease in acid yield together with an increase in reaction time.

**Table 2.1.** Benzoic acid formation catalyzed by complex **1** in the presence of different equivalents of KOH and catalyst loading.



entry	catalyst loading [mol%]	KOH [equiv]	t [h]	BnOH conv.(%)	Isolated yield [%]
1	1	1.2	6	97	79
2	1	2	6	97	55
3	1	5	6	65	31
4	0.5	1.2	18	94	60
5	0.1	1.2	40	70	39[a]

All reactions were performed on a 2.5 mmol scale of benzyl alcohol in 5 mL of toluene. Benzyl alcohol conversion was determined by GC-MS analysis using dodecane (1.3 mmol) as internal standard. <sup>[a]</sup> Yield calculated by NMR.

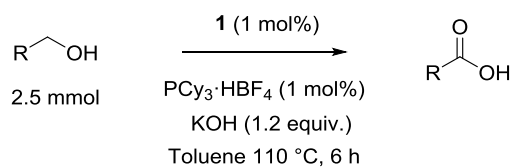
Thus, the optimal conditions for the oxidative transformation of benzyl alcohol to benzoic acid remain 1 mol% of complex **1**, 1 mol% of  $\text{PCy}_3 \cdot \text{HBF}_4$ , and 1.2 equivalent of KOH in refluxing toluene under a flow of argon. The carboxylic acid first precipitates in the organic solvent as the potassium salt followed by protonation to the acid using hydrochloric acid.

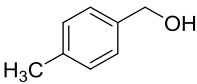
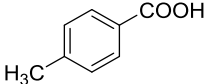
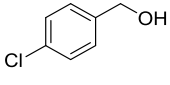
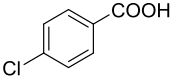
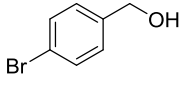
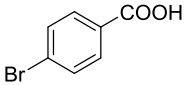
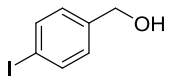
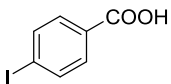
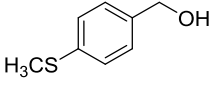
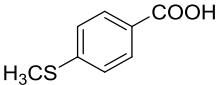
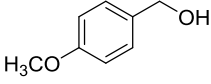
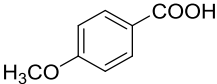
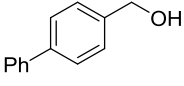
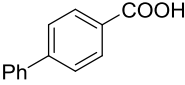
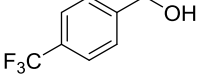
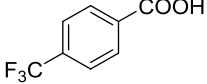
## 2.5.2 Substrate scope and limitations

With the optimized conditions in hand, the scope of the dehydrogenative oxidation with several primary alcohols was investigated. Based on the satisfactory result obtained with benzyl alcohol, various *p*-substituted benzyl alcohols were chosen

as substrates and converted into the corresponding *p*-substituted benzoic acids (Table 2.2). All the reactions reported in Table 2.2 were monitored by GC-MS and in all cases the substrates were fully converted after 6 h. Using *p*-methyl- and *p*-chlorobenzyl alcohol under the dehydrogenative conditions, the corresponding carboxylic acids were obtained in high yields, 88% and 82% respectively (entry 1-2). *p*-Bromo- and *p*-iodobenzyl alcohol afforded the products in slightly lower yields (entry 3-4). This can be explained to the formation of benzoic acid which in both cases were derived from a competing reductive dehalogenation. 5% of benzoic acid was generated in the reaction of *p*-bromobenzyl alcohol, while 12% was formed when *p*-iodobenzyl alcohol underwent the corresponding transformation. Good yields were also achieved with methoxy or methylthio as substituents in the *para*-position (entry 5-6). The GC-MS spectra for these reactions also contained additional traces of the decarbonylation products and the aldehydes. These same side products were also observed when *p*-phenyl- and *p*-(trifluoromethyl)benzyl alcohol were employed as substrates, alongside the carboxylic acids which were formed in moderate and good yields (entry 7-8). In light of the previous discussion the observation of aldehyde species can affirm this to be an intermediate in the dehydrogenative oxidation.

**Table 2.2.** Dehydrogenative oxidation of benzyl alcohols.



entry	substrate	product	isolated yield [%]
1			88
2			82
3			70 <sup>[a]</sup>
4			67 <sup>[b]</sup>
5			67
6			60
7			49
8			67

<sup>[a]</sup> <sup>1</sup>H-NMR shows the presence of 5% of benzoic acid. <sup>[b]</sup> <sup>1</sup>H-NMR shows 12% of benzoic acid alongside the product.

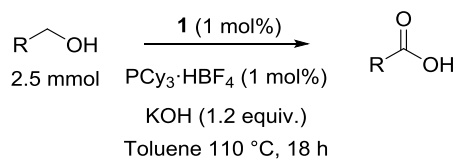
Attempts to perform the oxidation method described so far with other benzylic substrates were also made, but these yielded exclusively undesired products (results not shown). In case of *p*-hydroxybenzyl alcohol the reaction stopped at the aldehyde species. A likely explanation could be that the phenol group ( $pK_a \sim 10$ ) is deprotonated by KOH during the reaction, which could electronically disfavour a hypothetical nucleophilic attack of the base on the aldehyde to eventually generate the benzoic acid. A second attempt where the base was increased to 2 equivalents was made, but in this instance the reaction also stopped at the aldehyde level. When 2-(2-pyridyl)ethanol was employed as the substrate, elimination occurred and 2-vinylpyridine was obtained as the product. An explanation may lie in the acidity of the benzylic hydrogens which are enhanced by the presence of the nitrogen in the aromatic ring. Furthermore, methyl *p*-(hydroxymethyl) benzoate was immediately hydrolyzed by KOH resulting in *p*-(hydroxymethyl) benzoic acid and no oxidation of the alcohol was observed. The explanation could be precipitation of the corresponding potassium benzoate which would render the alcohol inaccessible to the dehydrogenation.

In order to verify the versatility of the oxidation reaction linear, branched, and cyclic aliphatic primary alcohols were subjected to the reaction conditions (Table 2.3). Full conversion of the aliphatic alcohols was obtained after 18 h indicating a lower reactivity of primary alcohols compared to benzylic alcohols.

Linear aliphatic primary alcohols such as 1-decanol and 1-nonanol afforded carboxylic acids in 82% and 71% yields, respectively (entry 1-2). Substrates with substituents in position 3 as 3-phenyl-1-propanol and 3-methyl-1-pentanol were also successfully converted to the corresponding 3-phenylpropionic acid and 3-methylpentanoic acid in 72% and 84% yield, respectively (entry 3-4). When a methoxy group is present in position 2 as in the case of 2-methoxyethanol, the yield found for the corresponding acid was 51%.



**Table 2.3.** Dehydrogenative oxidation of aliphatic primary alcohols.



entry	substrate	product	isolated yield [%]
1			82
2			71
3			72
4			84
5			51
6			60
7			60
8			62
9			88
10			76

In this case GC-MS spectra did not show side-products which could justify the moderate yield obtained. 2-Ethyl-1-butanol and cyclopentylmethanol were also subjected to the reaction conditions giving rise to the related carboxylic acids in good yields (entry 6-7). Interestingly, the dehydrogenation of 5-hexen-1-ol afforded the saturated hexanoic acid as the major product in 62% yield (entry 8). This can be attributed to the release of hydrogen in the reaction environment which can easily be used *in situ* for a further hydrogenation. Moreover, it could be intriguing to conduct the reaction on substrates with a chiral center in the 2 position since the formation of the aldehyde as the intermediate could cause the loss of the stereochemical information. Notably, (*S*)-2-methyl-1-butanol afforded the completely racemic 2-methylbutanoic acid (entry 9). The experiment was also conducted on (-)-*cis*-myrtanol, a more peculiar substrate with a specific geometric constraint. The full conversion of (-)-*cis*-myrtanol resulted in the complete inversion of configuration giving rise to the thermodynamically more stable (+)-*trans*-dihydromyrtenic acid (entry 10). The inverted configuration has been assigned through a 2D-Nuclear Overhauser Effect Spectroscopy (NOESY) experiment. In this case several important peak correlations were found and are highlighted in Figure 2.2. In particular the correlation between the  $\alpha$ -proton H<sup>a</sup> and one of the methyl groups present in the molecule has been decisive to the assignment of the structure configuration. It appears that deprotonation in the  $\alpha$  position occurs readily which would cause a loss of the stereochemistry resulting in racemization or as in the case of (-)-*cis*-myrtanol in the total inversion of configuration.

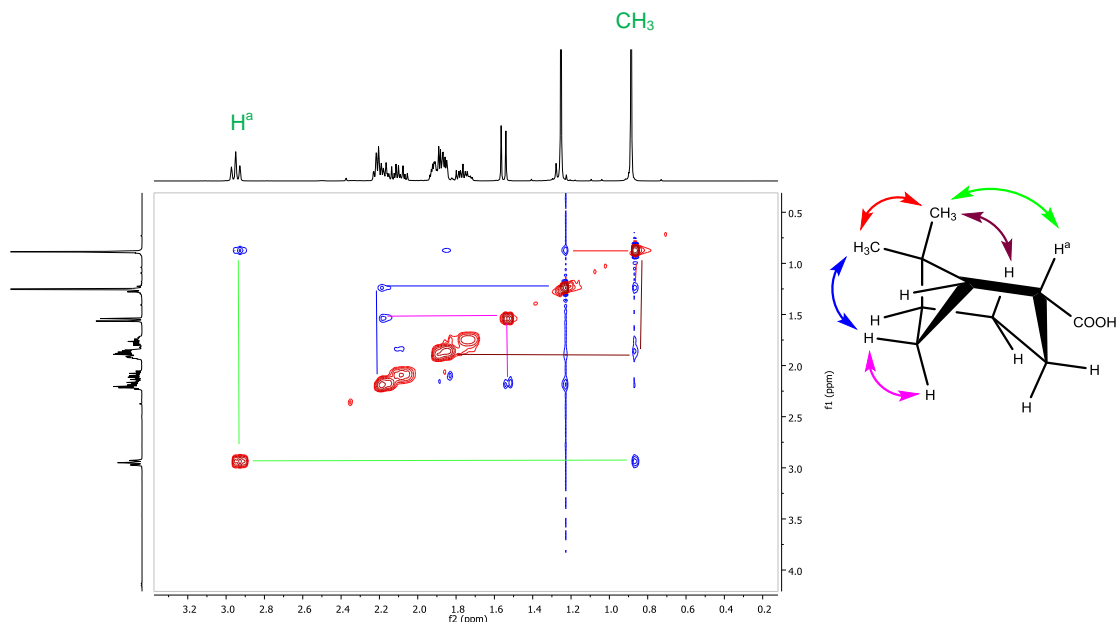


**Figure 2.2.** 2D-NOESY of (+)-*trans*-dihydromyrtenic acid.

The dehydrogenation of aliphatic primary alcohols in general demonstrated moderate to good yields. Moreover, in principle the aldehyde intermediate could undergo an aldol condensation as a collateral reaction, but this was not observed in any of the examples reported in Table 2.3. All the products in table 2.2 and 2.3 were easily isolated without the need for flash chromatography. The initially formed potassium salt of the acid precipitated from the toluene solution and was separated by filtration, followed by treatment with aqueous hydrochloric acid, extraction with ethyl acetate and removal of the solvent. This yielded sufficiently pure carboxylic acids where no further purification was necessary.

A further extension of the reaction scope was the employment of diols as substrates since these compounds have already shown a propensity to undergo lactonization under dehydrogenative esterification conditions with complex **1**.<sup>73</sup> Hence, 1,4-butanediol, 1,4-pentanediol, and 1,8-octanediol were subjected to the oxidation conditions of this work. In general, all the reactions at the end presented a mixture of compounds which were not separated (results not shown). 1,4-Butanediol and 1,4-pentanediol yielded a mixture of butyrolactones and

monocarboxylic acids which were probably generated from the hydrolysis by KOH. This is also confirmed by a test reaction between  $\gamma$ -butyrolactone and 1.2 equivalent of KOH in refluxing toluene which was monitored by GC-MS giving rise to 82% conversion of the lactone. The employment of a longer chain diol as 1,8-octanediol resulted in 40% of conversion only affording a mixture of the monocarboxylic and dicarboxylic acids as products. Attempts to use 2 mol% of complex **1** gave same results for all of three examples.

A further step forward in the study of the current transformation of primary alcohols into carboxylic acids would be the employment of water as a reaction solvent. Unfortunately, when benzyl alcohol reacted with complex **1** in water as the solvent the formation of only 14% of benzoic acid was observed. A probable explanation may lie to the low stability of the catalytic system in water and the need for a higher boiling point solvent for the reaction to be thermodynamically favored. In fact, and not surprisingly, running the reaction with toluene, but lowering the temperature to 50 and 80 °C resulted in no product formation.

### 2.5.3 Investigation of the reaction mechanism

The transformation of primary alcohols to carboxylic acids presented in the current work is believed to proceed via a dehydrogenation of the alcohol to the aldehyde based on previous studies conducted in our research group of the dehydrogenative imination, amidation, and esterification.<sup>69,70,72-74</sup> In this case the aldehyde is possibly attacked by a OH<sup>-</sup> species to form a hydrate anion from which the carboxylic acid is then generated by further dehydrogenation. This process is accompanied by production of two equivalents of hydrogen. Several experiments were carried out in order to clarify the reaction mechanism.

## Hydrogen development

The evolution of hydrogen during the reaction was measured by conducting a standard reaction in which 1.5 mmol of benzyl alcohol was converted into benzoic acid in a Schlenk tube connected to a burette filled with water. In this case 3 mmol of dihydrogen are expected at the end of the dehydrogenation. A total gas volume of 64 mL was collected which corresponded to approximately 2.7 mmol according to the ideal gas law. This confirmed that two equivalents of dihydrogen are released during the reaction (Figure 2.3).

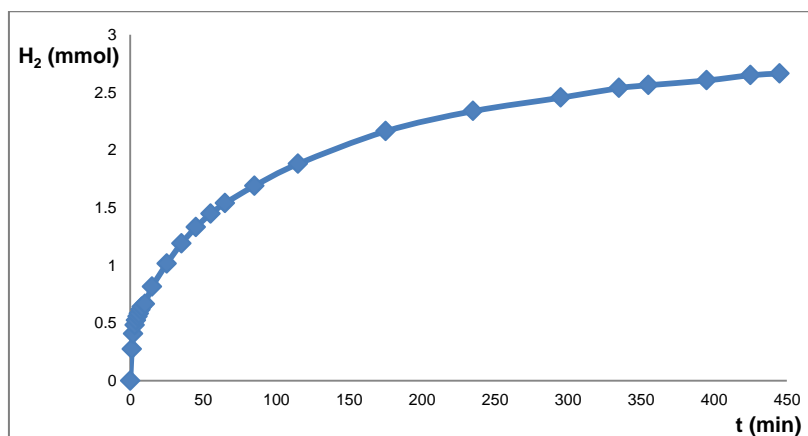
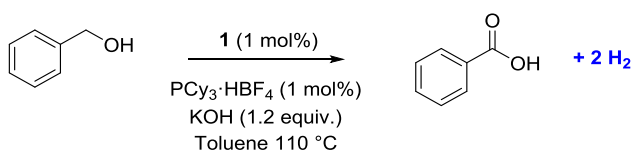
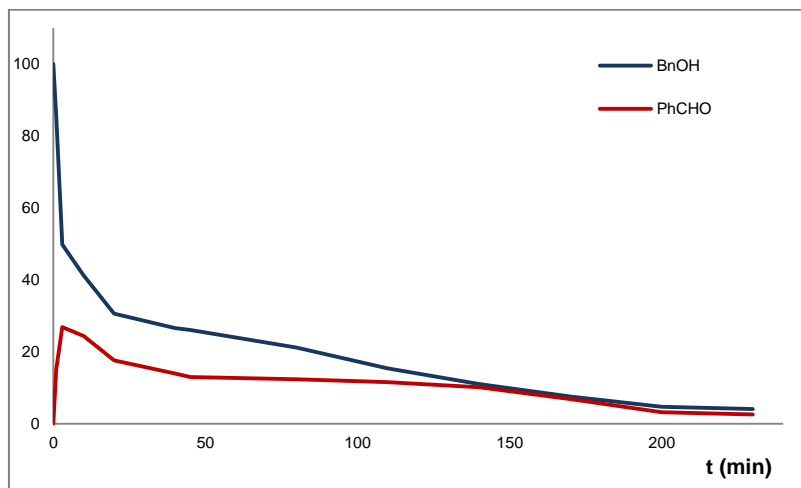


Figure 2.3. Hydrogen gas development as a function of time.

## Evidence for the aldehyde as a reaction intermediate

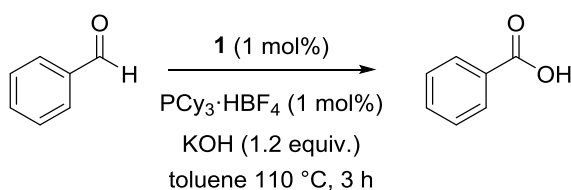
The formation of the aldehyde intermediate was verified by monitoring the oxidation reaction of benzyl alcohol by GC measurements. The graph in Figure 2.4 shows the monitored yields of benzyl alcohol and benzaldehyde as a function of

time. It can be seen that benzaldehyde is formed at the very beginning of the reaction and up to 26% accumulated in the reaction mixture.



**Figure 2.4.** Benzaldehyde formation during the oxidation of benzyl alcohol.

A further confirmation of the benzaldehyde participation to the reaction was provided by letting benzaldehyde react with **1** under standard oxidation conditions affording the product benzoic acid in 72% yield (Scheme 2.15).



**Scheme 2.15.** Dehydrogenative oxidation of benzaldehyde to benzoic acid.

Interestingly, following the reaction by GC-MS gave evidence of a rapid conversion of benzaldehyde into a mixture of benzyl alcohol and benzoic acid. This result is shown in Figure 2.5 where it is evident that after ten minutes benzaldehyde is converted into 34% of benzyl alcohol followed by a sluggish further conversion to benzoic acid.

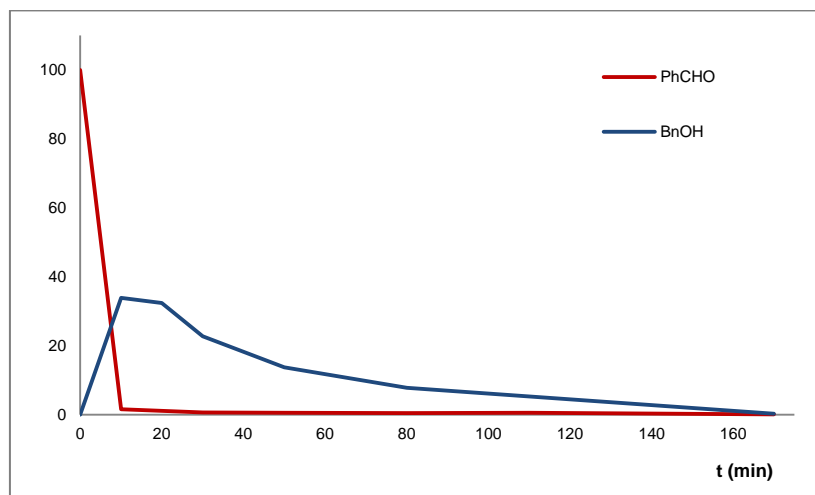
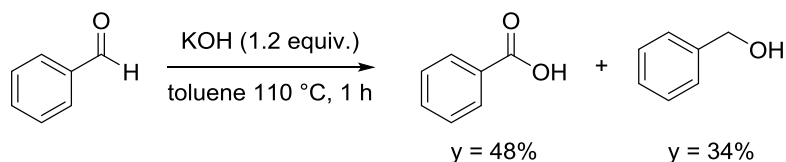


**Figure 2.5.** Benzaldehyde dehydrogenative oxidation generates benzyl alcohol.

This result was very interesting and displayed the possibility that an aldehyde disproportionation could interfere with the reaction mechanism. In fact a Cannizzaro<sup>78,79</sup> reaction seemed to be a plausible secondary reaction as this can easily occur since a non-enolizable aldehyde and stoichiometric amounts of KOH are used in the oxidation conditions examined. Therefore, benzaldehyde was also reacted with KOH in the absence of complex **1** affording a mixture of benzyl alcohol and benzoic acid in 34% and 48% yield respectively as calculated by <sup>1</sup>H NMR (Scheme 2.16).



**Scheme 2.16.** Cannizzaro reaction of benzaldehyde.

The Cannizzaro reaction seems to have a significant role in the dehydrogenation of benzyl alcohols to benzoic acids. This parallel reaction may be also the

explanation for the shorter reaction time of these substrates as compared to the reaction time of aliphatic alcohols.

### Attempts to perform Hammett study and determine the kinetic isotopic effect

Kinetic experiments are essential in order to have a more complete picture of a reaction mechanism. Mechanistic investigation experiments for the dehydrogenative amidation catalyzed by complex **1** have previously been conducted by Makarov *et al.* clarifying the related mechanism as well as DFT calculations.<sup>72</sup> Inspired by this, a Hammett study for the oxidation reaction under consideration was also attempted and competition experiments with *p*-substituted benzyl alcohols were examined. However, no linear correlation between the  $\sigma$  values for the different *para* substituents and the rate constants was obtained. The non-linearity of the Hammett plot could be reasoned by the contribution of different mechanisms to the overall transformation to the carboxylic acid including the Cannizzaro reaction (Figure 2.6).

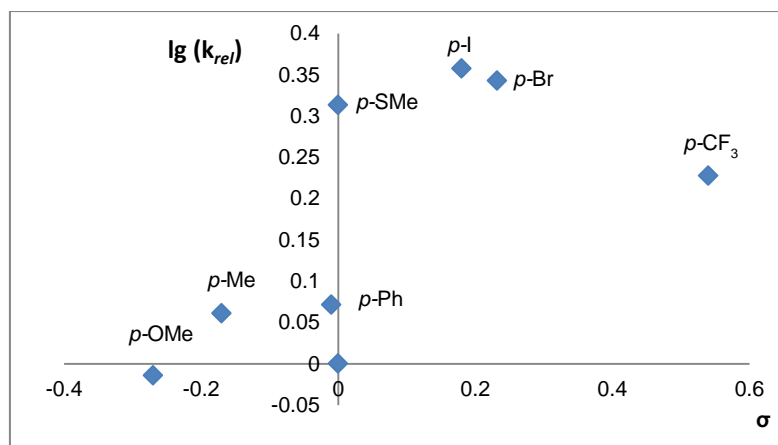
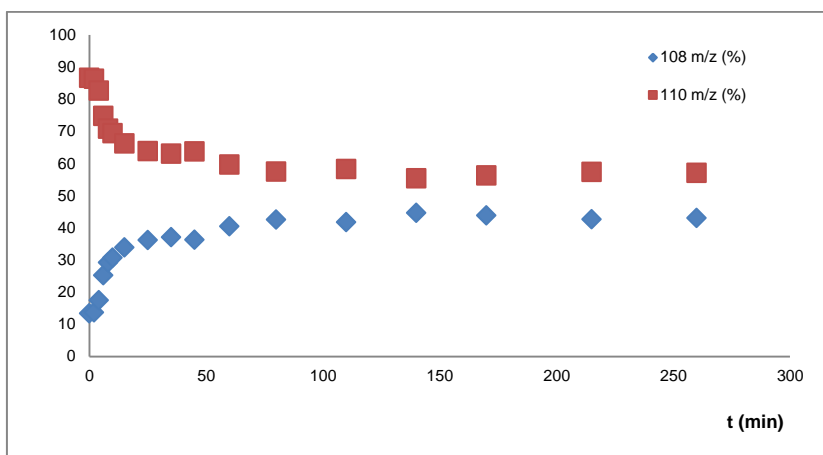


Figure 2.6. Hammett plot with  $\sigma$  values.



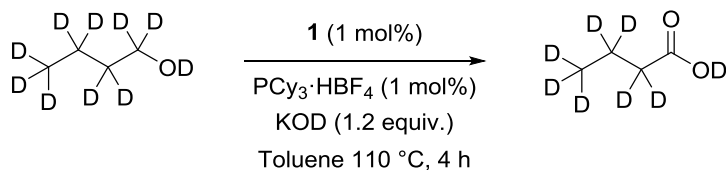
Furthermore, the study of the kinetic isotopic effect (KIE) for the amidation reaction catalyzed by **1**, exhibited rapid scrambling of hydrogen and deuterium when an equimolar mixture of benzyl alcohol and  $\alpha,\alpha$ - $d_2$ -benzyl alcohol was used. This phenomenon was attributed to a reversible step at the beginning of the reaction, which involved  $\beta$ -hydride elimination and a migratory insertion.<sup>72</sup> Additionally it was demonstrated that toluene was not implicated in the scrambling. This also determined that a ruthenium-dihydride species was involved in the catalytic cycle. Hence for this study the KIE was calculated by measuring the initial rates of the two reactions where deuterated substrates and non-deuterated substrates were separated. Perdeutero-1-butanol ( $C_4D_9OD$ ) and  $N,N$ - $d_2$ -benzylamine ( $BnND_2$ ), 1-butanol and benzyl amine proved to be ideal substrates for these non-competitive experiments and a KIE of 2.29 was obtained in the amidation.<sup>72</sup>

In light of this information, attempts to perform a similar KIE study were made for the dehydrogenative oxidation of primary alcohols to carboxylic acids under examination. As suspected this reaction also exhibited a scrambling of hydrogen and deuterium when  $\alpha,\alpha$ - $d_2$ -benzyl alcohol was allowed to react with 1.2 equivalent of KOH and complex **1** in refluxing toluene. This phenomenon was measured by GC-MS and illustrated in Figure 2.7. The percentages of the peak areas corresponding to the mass of the  $\alpha,\alpha$ - $d_2$ -benzyl alcohol (110 m/z) and the non-deuterated benzyl alcohol (108 m/z) as functions of time is reported. During the reaction the area of the peak corresponding to the non-deuterated alcohol increased while the one related to the deuterated alcohol decreased until an equilibrium is reached. Hence the scrambling of hydrogen and deuterium which occurs in  $\alpha,\alpha$ - $d_2$ -benzyl alcohol is probably due to a quick equilibrium through  $\beta$ -hydride elimination.



**Figure 2.7.** Observation of scrambling for  $\alpha,\alpha$ - $d_2$ -benzyl alcohol.

Consequently to determine the KIE for the oxidation reaction, two separate experiments were set up: one with deuterated 1-butanol- $d_{10}$  and potassium deuteroxide (KOD) and one with 1-butanol and KOH (Scheme 2.17). The conversion of the substrates in time calculated by GC-MS allowed for extrapolation of the  $\ln\left(\frac{C}{C_0}\right)$ , where C represents the concentration of substrate at a certain time and  $C_0$  is the substrate concentration at  $t = 0$ . By plotting  $\ln\left(\frac{C_H}{C_{H(0)}}\right)$  vs  $\ln\left(\frac{C_D}{C_{D(0)}}\right)$  an experimental KIE of 0.67 was obtained (Figure 2.8). This very low value suggested that the deuterated substrate reacted 1.5 times faster than the non-deuterated counterpart. This result may indicate that the basicity or the nucleophilicity of the base plays an important role in the rate determining step considering that deuteroxide ion is more basic than hydroxide ion.<sup>80</sup>



**Scheme 2.17.** Non-competitive experiment to determine the KIE with perdeutero-1-butanol. Same conditions were applied to 1-butanol where KOH (1.2 equiv.) was used instead of KOD.

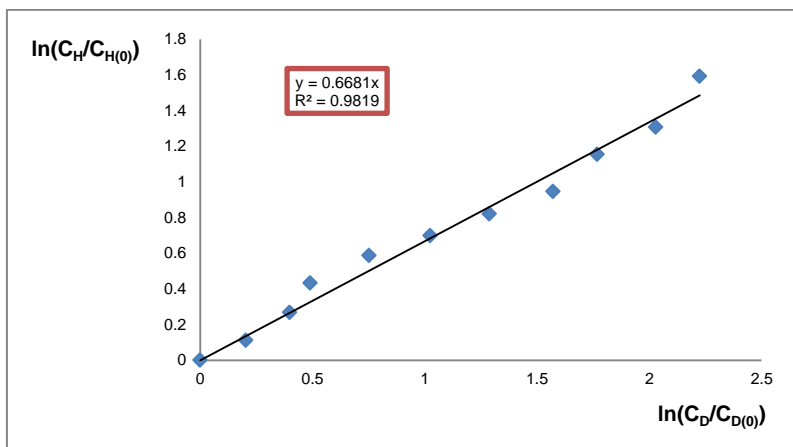


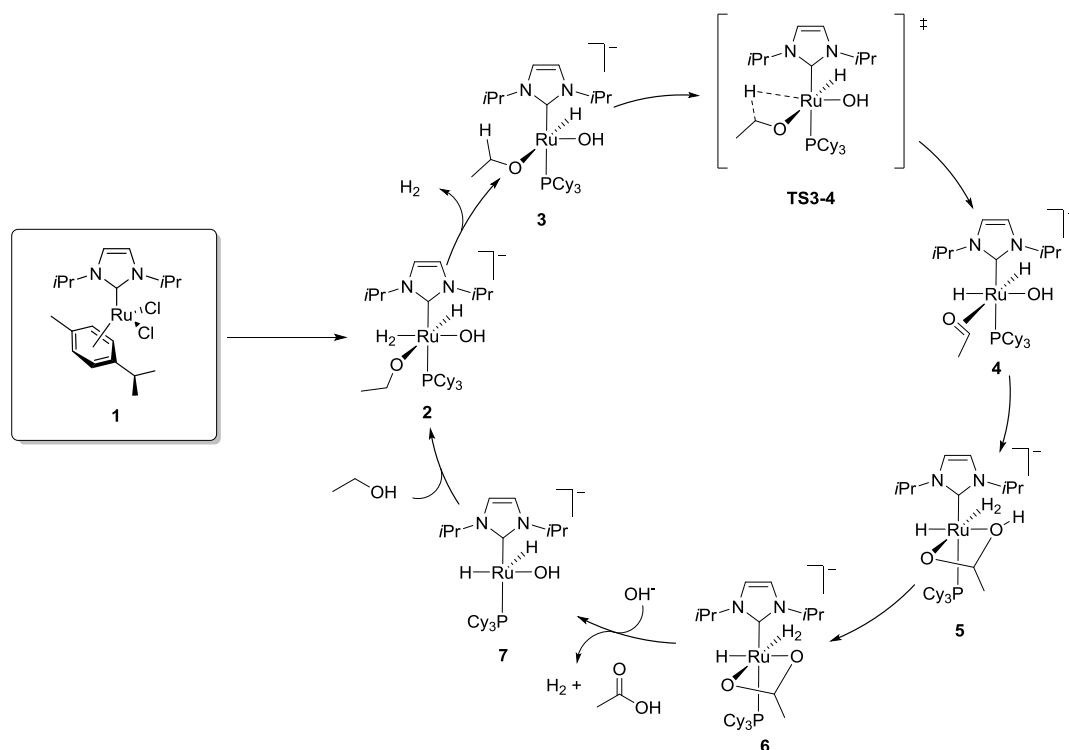
**Figure 2.8.** Determination of KIE by plotting the initial rates of the reactions involving 1-butanol and 1-butanol- $d_{10}$ .

### The proposed catalytic cycle

A more in-depth understanding of the reaction mechanism could be obtained through computational studies to accompany the experimental investigations conducted so far. The mechanistic analysis by the employment of DFT calculations was performed in collaboration with Dr. Peter Fristrup and Dr. Ilya Makarov.

The proposed catalytic cycle for the oxidation reaction of primary alcohols to carboxylic acids is reported in Scheme 2.18. As it was previously underlined, benzyl alcohol can react through a Cannizzaro reaction for the formation of benzoic acid. For this reason ethanol was chosen as a model substrate for the theoretical study as it would conceivably follow the ruthenium catalyzed pathway. Moreover, the hydroxide ion solvated with water molecules was used instead of free hydroxide because it was demonstrated that this solvated system provides results which are closer to the experimental data.<sup>81</sup> Even if the solvent used for the reaction is toluene, the reaction system is not completely free of water since KOH contains 0.35-0.55 equivalent of  $H_2O$  per equivalent of hydroxide depending on the base quality. The hydroxide ion can also be solvated by the alcohol molecules

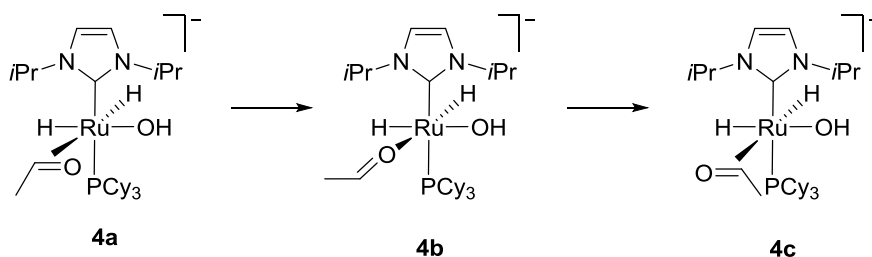
present in the reaction mixture. This fact indicates that it is probable that hydroxide ion is solvated during the entire course of the catalytic cycle.



**Scheme 2.18.** Proposed mechanism for the formation of carboxylic acid from primary alcohol. **TS3-4** is one of the highest energy transition states of the catalytic cycle due to the breakage of the C-H bond which leads to the formation of the aldehyde.

During the initiation step the dichloride ruthenium precatalyst **1** loses the *p*-cymene ligand. According to the literature the two chlorines are believed to be replaced by a hydride and an alkoxide derived from the oxidative addition of the ethanol. This leads to a highly electronically unsaturated 12- $e^-$  complex<sup>82</sup> which is then converted into the more stable 16- $e^-$  complex **2** by coordination of a phosphine molecule and a hydroxide ion. At this point the loss of dihydrogen generates a free coordination site in complex **3** which should be *cis* to the alkoxide allowing the  $\beta$ -hydride elimination to occur. Notably, the orientation of the ligands in complex **3**,

where  $\text{PCy}_3$  and NHC are in the apical positions while alkoxide, hydroxide and hydride lie in one plane, is the most stable, and complex **3** has the lowest energy respect to all the possible isomers. This is also valid for complex **4** which is next formed by a  $\beta$ -hydride elimination. In complex **4** the aldehyde is coordinated to the ruthenium center by the  $\pi$ -system of the carbonyl group. The *cis* orientation of the aldehyde respect to the hydroxide grants a nucleophilic attack of the hydroxide to the aldehyde, however, the aldehyde complex should isomerize in order to give the proper orientation of the aldehyde to the hydroxide previous to nucleophilic attack (Scheme 2.19).



**Scheme 2.19.** Isomerization of the aldehyde complex **4a** which goes through the formation of the higher energy complex **4b**. Here the aldehyde is coordinated to ruthenium through the oxygen. In complex **4c** the distances of the Ru-O and the Ru-C bonds are calculated to be comparable but the bond between ruthenium and the carbonyl carbon elongates as the hydroxide comes closer to it.

The nucleophilic attack of the hydroxide ion on the aldehyde results in a hemiacetal complex **5**. This allows for a deprotonation of the *cis*-hydride affording complex **6**. At this point dihydrogen is lost from complex **6** and a spontaneous  $\beta$ -hydride elimination occurs resulting in the carboxylate and the dihydride-complex **7** which is the most stable complex of the catalytic cycle even though it is coordinatively unsaturated. The reason for this can be found in the favorable electron donating properties of all the five ligands coordinated to the ruthenium center. Interestingly, it was observed from the optimization of complex **7** that the alcohol does not coordinate to ruthenium since it is a weak electron-donor. Anyway, the alcohol is deprotonated by the hydride affording the alkoxide species,

and coordination to ruthenium happens affording complex **2** which is ready for a new catalytic cycle.

The kinetic isotopic effect was also investigated through calculations where  $\text{OD}^-$  and  $\text{CH}_3\text{CD}_2\text{OD}$  were used in place of  $\text{OH}^-$  and ethanol. Additionally, the hydrogen atoms which are generated from these substrates were replaced by deuterium during the whole catalytic cycle. Notably from this study it was possible to demonstrate that the first part of the catalytic cycle has a higher energy barrier due to the breakage of the C-H/D bond (**TS3-4**,  $42.8 \text{ kJ}\cdot\text{mol}^{-1}$  for C-D bond vs  $38.4 \text{ kJ}\cdot\text{mol}^{-1}$  for C-H bond). Relative Gibbs free energies were also calculated from the transition states for the addition of the hydroxide to the aldehyde and were found to be virtually identical (**TS4-5**  $53.0 \text{ kJ}\cdot\text{mol}^{-1}$  for C-D bond vs  $52.7 \text{ kJ}\cdot\text{mol}^{-1}$  for C-H) (Figure 2.9). This can be a further explanation for the experimental KIE obtained (0.67) which is different from the calculated value (1.08). Consequently the difference in basicity and nucleophilicity between  $\text{OH}^-$  and  $\text{OD}^-$  can again explain the difference between the experimental and the calculated values.

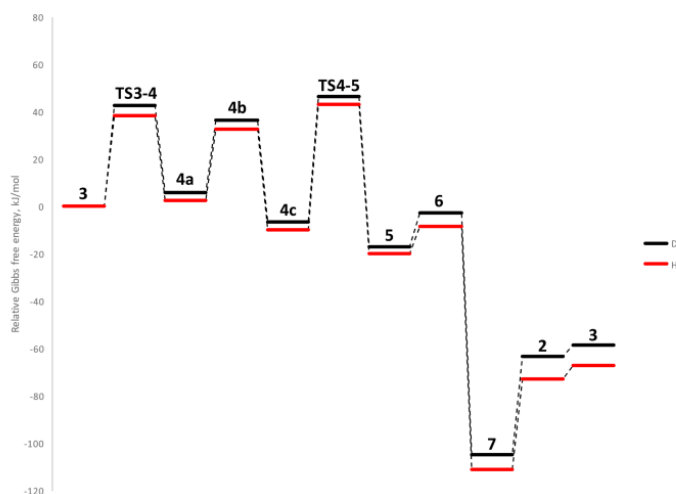


**Figure 2.9.** Energy profile for proposed catalytic cycle with partially deuterated substrates in black and fully deuterated substrates in red.<sup>75</sup>

## 2.6 Conclusion

In conclusion a new method for the dehydrogenative synthesis of carboxylic acids from primary alcohols was developed. The procedure utilizes of 1 mol % of the ruthenium *N*-heterocyclic carbene complex  $\text{RuCl}_2(\text{I}^i\text{Pr})(p\text{-cymene})$  as precatalyst which has already been successfully employed in the dehydrogenative synthesis of amides, esters, and imines. Moreover, this versatile oxidation reaction allowed the use of a wide variety of benzylic and aliphatic alcohols for the synthesis of carboxylic acids in moderate to high yields. Additionally, the reaction permits an easy isolation of the products without the use of chromatography, distillation, or recrystallization. DFT calculations were conducted in parallel to the experimental studies in order to gain more detailed information about the reaction mechanism and to allow the proposal of a plausible catalytic cycle.

## 2.7 Experimental section

### General methods

All solvents were of HPLC grade and were not further purified, all chemicals were bought from Sigma Aldrich. NMR spectra were recorded on a Bruker Ascend 400 spectrometer.  $\text{CDCl}_3$  and  $\text{DMSO-}d_6$  were used as solvents for NMR measurements. Chemical shifts were measured relative to the signals of residual  $\text{CHCl}_3$  ( $\delta_{\text{H}}$  7.26 ppm) and  $\text{CDCl}_3$  ( $\delta_{\text{C}}$  77.16 ppm) or to the signals of residual  $\text{CHD}_2\text{SOCD}_3$  ( $\delta_{\text{H}}$  2.50 ppm) and  $(\text{CD}_3)_2\text{SO}$  ( $\delta_{\text{C}}$  39.52 ppm). HRMS measurements were made using ESI with TOF detection.

Multiplicity are reported as s = singlet, d = doublet, t = triplet, q = quintet, tt = triplet of triplets, m = multiplet, br. s = broad singlet, while coupling constants are shown in Hz.

$\text{RuCl}_2(\text{I}^i\text{Pr})(p\text{-cymene})$  was synthesized according to the reported procedure.<sup>83</sup> Kinetic experiments were monitored by gas chromatography on a Shimadzu GCMS-QP2012S instrument equipped with an Equity-5, 30 × 0.25mm × 0.25 $\mu\text{m}$  column. Dodecane was used as the internal standard.

### General Procedure for Oxidation of Primary Alcohols

A Schlenk tube was charged with complex **1**<sup>83</sup> (11.5 mg, 0.025 mmol),  $\text{PCy}_3\text{-HBF}_4$  (9.2 mg, 0.025 mmol), KOH (168 mg, 3 mmol) and a stir bar. A cold finger was attached and the tube was evacuated and refilled three times with argon. The primary alcohol (2.5 mmol) (and sometimes 1.3 mmol of dodecane as internal standard) in toluene (5 mL) was added and the Schlenk tube was placed in a preheated oil bath ( $T = 120\text{ }^\circ\text{C}$ ). The reaction was monitored by GC until completion and the Schlenk tube was then removed from the oil bath and cooled to room temperature. Ethyl acetate (5 mL) was added and the white precipitate



filtered off and washed with pentane (15 mL) and ethyl acetate (15 mL). The precipitate was dissolved in water (5 mL) and acidified to pH 1 with saturated aqueous HCl. The aqueous layer was extracted with ethyl acetate (3 × 10 mL). The combined organic layers were dried over Na<sub>2</sub>SO<sub>4</sub> and concentrated *in vacuo* to give the corresponding acid as a pure compound by <sup>1</sup>H NMR.

## Gas Development

Following the general procedure for oxidation of primary alcohols, benzyl alcohol (108.1 mg, 1.5 mmol), complex **1** (6.9 mg, 0.015 mmol), PCy<sub>3</sub>·HBF<sub>4</sub> (5.6 mg, 0.015 mmol), KOH (102.1 mg, 1.8 mmol), and 3.0 mL of toluene were added to a Schlenk tube. The tube was connected to a buret filled with water and stirred at 120 °C. The bottom of the burette was further connected to a water reservoir with a large surface area. The volume increase was measured as a function of time. At the end of the reaction, 64.0 mL was collected corresponding to 2.7 mmol of molecular hydrogen according to the ideal gas law.

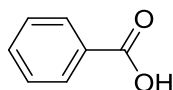
## Determination of the KIE

Two Schlenk tubes were charged separately with complex **1** (11.5 mg, 0.025 mmol), PCy<sub>3</sub>·HBF<sub>4</sub> (9.2 mg, 0.025 mmol) and a stir bar. In the first Schlenk tube, KOH (170.6 mg, 3 mmol) was added and a cold finger was attached. The tube was evacuated and refilled with argon three times. Then 1-butanol (186.8 mg, 2.5 mmol) and dodecane (1.3 mmol) were dissolved in 5.0 mL of toluene and added to the tube. In the same way, KOD (171.3 mg, 3 mmol, 1-butanol-*d*<sub>10</sub> (212.2 mg, 2.5 mmol), dodecane (1.3 mmol) and toluene (5 mL) were added to the second Schlenk tube. The reactions were stirred in the same oil bath at 120 °C and aliquots of 0.05 mL were taken out in a period of 4 hours, diluted with 1.5 mL of CH<sub>2</sub>Cl<sub>2</sub> and analyzed by GC-MS. The KIE was determined to be 0.67.

## Synthesis $\alpha,\alpha$ - $d_2$ - benzyl alcohol<sup>84</sup>

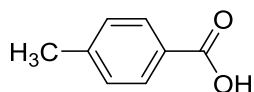
To a stirred suspension of  $\text{LiAlD}_4$  (11 mmol) in THF (20 mL) at 0 ° C was added a solution of methyl benzoate (11 mmol) in  $\text{Et}_2\text{O}$  (10 mL). The reaction was stirred at room temperature and was monitored by TLC to determine the consumption of the benzoate. The reaction mixture was quenched at 0 ° C with 1N HCl and then extracted with ethyl acetate (3 x 10 mL). The combined organic layers were dried over  $\text{Na}_2\text{SO}_4$  and concentrated in vacuo to give the corresponding  $\alpha,\alpha$ - $d_2$ - benzyl alcohol as a colorless oil in 69 %.

## Benzoic acid



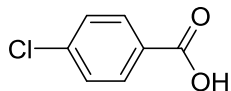
Isolated as a white solid in 79% yield.  $^1\text{H}$  NMR (400 MHz,  $\text{CDCl}_3$ ):  $\delta$  = 7.47–7.51 (m, 2 H), 7.63 (tt, 2 H,  $J$  = 1.3, 6.9 Hz), 8.13–8.15 (m, 2 H).  $^{13}\text{C}$  NMR (100 MHz,  $\text{CDCl}_3$ ):  $\delta$  = 128.7, 129.5, 130.4, 134.0, 172.5 ppm. The observed chemical shifts are in accordance with the literature values.<sup>85</sup>

## *p*-Methylbenzoic acid



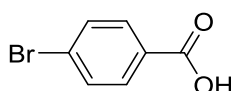
Isolated as a light purple solid in 88% yield.  $^1\text{H}$  NMR (400 MHz,  $\text{DMSO}-d_6$ ):  $\delta$  = 2.36 (s, 3 H), 7.29 (d, 2 H,  $J$  = 8.5 Hz), 7.83 (d, 2 H,  $J$  = 8.5 Hz), 12.77 (brs, 1 H) ppm.  $^{13}\text{C}$  NMR (100 MHz,  $\text{DMSO}-d_6$ ):  $\delta$  = 21.1, 128.0, 129.1, 129.3, 143.0, 167.3 ppm. The observed chemical shifts are in accordance with the literature values.<sup>85</sup>

### ***p*-Chlorobenzoic acid**



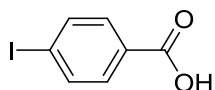
Isolated as a white solid in 82% yield.  $^1\text{H}$  NMR (400 MHz,  $\text{DMSO-}d_6$ ):  $\delta = 7.57$  (m, 2 H), 7.94 (m, 2 H), 13.18 (brs, 1 H) ppm.  $^{13}\text{C}$  NMR (100 MHz,  $\text{DMSO-}d_6$ ):  $\delta = 128.8, 129.7, 131.2, 137.8, 166.5$  ppm. The observed chemical shifts are in accordance with the literature values.<sup>85</sup>

### ***p*-Bromobenzoic acid**



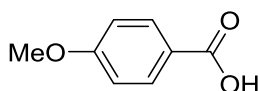
Isolated as a white solid in 70% yield.  $^1\text{H}$  NMR (400 MHz,  $\text{CDCl}_3$ ):  $\delta = 7.70\text{--}7.72$  (m, 2 H), 7.85–7.87 (m, 2 H), 13.18 (brs, 1 H) ppm.  $^{13}\text{C}$  NMR (100 MHz,  $\text{CDCl}_3$ ):  $\delta = 126.9, 130.0, 131.3, 131.7, 166.6$  ppm. The observed chemical shifts are in accordance with the literature values.<sup>85</sup>

### ***p*-Iodobenzoic acid**



Isolated as a yellowish solid in 67% yield.  $^1\text{H}$  NMR (400 MHz,  $\text{CDCl}_3$ ):  $\delta = 7.68\text{--}7.70$  (m, 2 H), 7.88–7.90 (m, 2 H), 13.13 (brs, 1 H) ppm.  $^{13}\text{C}$  NMR (100 MHz,  $\text{CDCl}_3$ ):  $\delta = 101.2, 130.3, 131.1, 137.6, 164.2, 167.0$  ppm. The observed chemical shifts are in accordance with the literature values.<sup>85</sup>

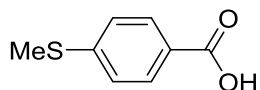
### ***p*-Methoxybenzoic acid**



Isolated as a white solid in 60% yield.  $^1\text{H}$  NMR (400 MHz,  $\text{CDCl}_3$ ):  $\delta = 3.88$  (s, 3 H), 6.93–6.97 (m, 2 H), 8.05–8.08 (m, 2 H) ppm.  $^{13}\text{C}$  NMR (100 MHz,  $\text{CDCl}_3$ ):  $\delta =$

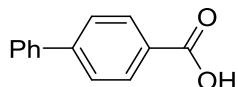
55.6, 113.9, 121.8, 132.5, 164.2, 171.2 ppm. The observed chemical shifts are in accordance with the literature values.<sup>85</sup>

### ***p*-(Methylthio)benzoic acid**



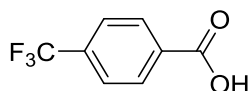
Isolated as a yellow pale solid in 67% yield. <sup>1</sup>H NMR (400 MHz, DMSO-*d*<sub>6</sub>):  $\delta$  = 2.52 (s, 3 H), 7.33 (d, 2 H, *J* = 8.5 Hz), 7.85 (d, 2 H, *J* = 8.5 Hz), 12.83 (brs, 1 H) ppm. <sup>13</sup>C NMR (100 MHz, DMSO-*d*<sub>6</sub>):  $\delta$  = 14.0, 124.9, 126.7, 129.7, 144.8, 167.1 ppm. The observed chemical shifts are in accordance with the literature values.<sup>86</sup>

### **Biphenyl-4-carboxylic acid**



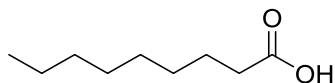
Isolated as a white solid in 49% yield. <sup>1</sup>H NMR (400 MHz, DMSO-*d*<sub>6</sub>):  $\delta$  = 7.43 (m, 1 H), 7.50 (m, 2 H), 7.73 (m, 2 H), 7.80 (m, 2 H), 8.02 (m, 2 H), 12.98 (brs, 1 H) ppm. <sup>13</sup>C NMR (100 MHz, DMSO-*d*<sub>6</sub>):  $\delta$  = 126.8, 126.9, 128.3, 129.1, 129.6, 130.0, 139.0, 144.3, 167.2 ppm. The observed chemical shifts are in accordance with the literature values.<sup>87</sup>

### ***p*-(Trifluoromethyl)benzoic acid**



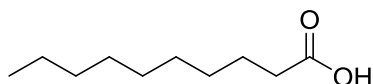
Isolated as a white solid in 67% yield. <sup>1</sup>H NMR (400 MHz, DMSO-*d*<sub>6</sub>):  $\delta$  = 7.87 (d, 2 H, *J* = 8.2 Hz), 8.13 (d, 2 H, *J* = 8.2 Hz), 13.47 (brs, 1 H) ppm. <sup>13</sup>C NMR (100 MHz, DMSO-*d*<sub>6</sub>):  $\delta$  = 123.8 (q, *J* = 271.6 Hz), 125.6 (q, *J* = 3.7 Hz), 130.1, 132.5 (q, *J* = 32.0 Hz), 134.6, 166.2 ppm. The observed chemical shifts are in accordance with the literature values.<sup>88</sup>

### Nonanoic acid



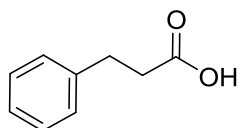
Isolated as a colorless oil in 82% yield.  $^1\text{H}$  NMR (400 MHz,  $\text{CDCl}_3$ ):  $\delta$  = 0.88 (t, 3 H  $J$  = 6.7 Hz), 1.27–1.35 (m, 10 H), 1.63 (q, 2 H,  $J$  = 7.6 Hz), 2.34 (t, 2 H,  $J$  = 7.6 Hz) ppm.  $^{13}\text{C}$  NMR (100 MHz,  $\text{CDCl}_3$ ):  $\delta$  = 14.2, 22.8, 24.8, 29.2, 29.3, 31.9, 34.2, 180.5 ppm. The observed chemical shifts are in accordance with the literature values.<sup>89</sup>

### Decanoic acid



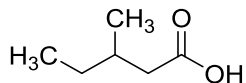
Isolated as a colorless oil in 71% yield.  $^1\text{H}$  NMR (400 MHz,  $\text{CDCl}_3$ ):  $\delta$  = 0.88 (t, 3 H  $J$  = 6.9 Hz), 1.21–1.35 (m, 12 H), 1.60–1.67 (m, 2 H), 2.35 (t, 2 H,  $J$  = 7.4 Hz) ppm.  $^{13}\text{C}$  NMR (100 MHz,  $\text{CDCl}_3$ ):  $\delta$  = 14.3, 22.8, 24.8, 29.2, 29.4, 29.5, 32.0, 33.9, 178.9 ppm. The observed chemical shifts are in accordance with the literature values.<sup>90</sup>

### 3-Phenylpropanoic acid



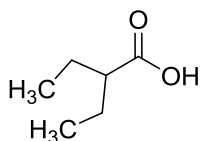
Isolated as a white solid in 72% yield.  $^1\text{H}$  NMR (400 MHz,  $\text{CDCl}_3$ ):  $\delta$  = 2.65 (m, 2 H), 2.92 (t, 2 H,  $J$  = 7.6 Hz), 7.16–7.28 (m, 5 H), 11.55 (brs, 1 H) ppm.  $^{13}\text{C}$  NMR (100 MHz,  $\text{CDCl}_3$ ):  $\delta$  = 30.7, 35.8, 126.5, 128.4, 128.7, 140.3, 179.6 ppm. The observed chemical shifts are in accordance with the literature values.<sup>90</sup>

### 3-Methylpentanoic acid



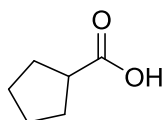
Isolated as a transparent brownish oil in 84% yield. <sup>1</sup>H NMR (400 MHz, CDCl<sub>3</sub>):  $\delta$  = 0.90 (t, 3 H,  $J$  = 7.4 Hz), 0.96 (d, 3 H,  $J$  = 6.7 Hz), 1.19–1.30 (m, 1 H), 1.34–1.45 (m, 1 H), 1.83–1.95 (m, 1 H), 2.14 (dd, 1 H,  $J$  = 8.0, 15.0 Hz), 2.35 (dd, 1 H,  $J$  = 6.0, 15.0 Hz), 11.64 (brs, 1 H) ppm. <sup>13</sup>C NMR (100 MHz, CDCl<sub>3</sub>):  $\delta$  = 11.4, 19.4, 29.4, 31.9, 41.4, 180.4 ppm. The observed chemical shifts are in accordance with the literature values.<sup>91</sup>

### 2-Ethylbutyric acid



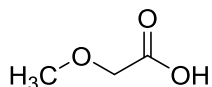
Isolated as a colorless oil in 60% yield. <sup>1</sup>H NMR (400 MHz, CDCl<sub>3</sub>):  $\delta$  = 0.94 (t, 6 H,  $J$  = 7.4 Hz), 1.50–1.71 (m, 4H), 2.20–2.27 (m, 1 H) ppm. <sup>13</sup>C NMR (100 MHz, CDCl<sub>3</sub>):  $\delta$  = 11.9, 24.9, 48.8, 182.8 ppm. The observed chemical shifts are in accordance with the literature values.<sup>92</sup>

### Cyclopentanecarboxylic acid



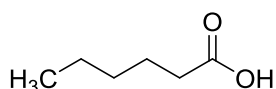
Isolated as a colorless oil in 60% yield. <sup>1</sup>H NMR (400 MHz, CDCl<sub>3</sub>):  $\delta$  = 1.53–1.96 (m, 8 H), 2.72–2.80 (m, 1 H), 11.22 (brs, 1 H) ppm. <sup>13</sup>C NMR (100 MHz, CDCl<sub>3</sub>):  $\delta$  = 25.9, 30.1, 43.8, 183.5 ppm. The observed chemical shifts are in accordance with the literature values.<sup>93</sup>

### Methoxyacetic acid



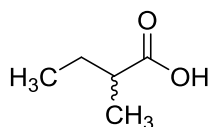
Isolated as a colorless oil in 51% yield.  $^1\text{H}$  NMR (400 MHz,  $\text{CDCl}_3$ ):  $\delta = 3.45$  (s, 3 H), 4.07 (s, 2 H), 9.66 (brs, 1 H) ppm.  $^{13}\text{C}$  NMR (100 MHz,  $\text{CDCl}_3$ ):  $\delta = 59.5, 69.3, 175.4$  ppm. The observed chemical shifts are in accordance with the literature values.<sup>94,95</sup>

### Hexanoic acid



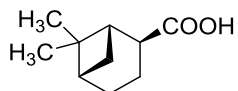
Isolated as a colorless oil in 66% yield (includes 4% of 5-hexenoic acid according to NMR).  $^1\text{H}$  NMR (400 MHz,  $\text{CDCl}_3$ ):  $\delta = 0.88\text{--}0.92$  (m, 3 H), 1.28–1.36 (m, 4 H), 1.60–1.68 (m, 2 H), 2.35 (t, 2 H,  $J = 7.6$  Hz) ppm.  $^{13}\text{C}$  NMR (100 MHz,  $\text{CDCl}_3$ ):  $\delta = 14.0, 22.4, 24.5, 31.3, 34.2, 180.4$  ppm. The observed chemical shifts are in accordance with the literature values.<sup>90</sup>

### 2-Methylbutanoic acid



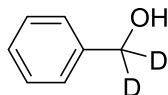
Isolated as a colorless oil in 88% yield.  $^1\text{H}$  NMR (400 MHz,  $\text{CDCl}_3$ ):  $\delta = 0.95$  (t, 3 H,  $J = 7.0$  Hz), 1.18 (d, 3 H,  $J = 7.5$  Hz), 1.45–1.55 (m, 1 H), 1.66–1.77 (m, 1 H), 2.36–2.44 (m, 1 H) ppm.  $^{13}\text{C}$  NMR (100 MHz,  $\text{CDCl}_3$ ):  $\delta = 11.7, 16.5, 26.7, 41.0, 183.6$  ppm. The observed chemical shifts are in accordance with the literature values.<sup>96</sup>

### (1S,2S,5S)-6,6-Dimethylbicyclo[3.1.1]heptane-2-carboxylic acid



Isolated as a brownish sheer oil in 76% yield.  $[\alpha]_D +1.9$  (*c* 1.0, EtOAc).  $^1\text{H}$  NMR (400 MHz,  $\text{CDCl}_3$ ):  $\delta$  = 0.87 (s, 3 H), 1.23 (s, 3 H), 1.53 (d, 1 H,  $J$  = 10.0 Hz), 1.70–1.80 (m, 1 H), 1.83–1.92 (m, 3 H), 2.03–2.21 (m, 3 H), 2.93 (t, 1 H,  $J$  = 9.0 Hz) ppm.  $^{13}\text{C}$  NMR (100 MHz,  $\text{CDCl}_3$ ):  $\delta$  = 16.7, 20.4, 23.9, 24.3, 26.5, 39.3, 40.2, 41.3, 43.8, 183.3 ppm. HRMS:  $m/z$  calcd for  $\text{C}_{10}\text{H}_{17}\text{O}_2$  169.1223  $[\text{M} + \text{H}]^+$ , found 169.1217. The observed chemical shifts are in accordance with the literature values.

### $\alpha,\alpha\text{-d}_2$ -benzyl alcohol



Isolated as a colorless oil in 69% yield.

$^1\text{H}$  NMR (400 MHz,  $\text{CDCl}_3$ ):  $\delta$  = 7.39–7.28(m, 5 H) ppm.  $^{13}\text{C}$  NMR (100 MHz,  $\text{CDCl}_3$ ):  $\delta$  = 127.2, 127.8, 128.7, 140.9 ppm. The observed chemical shifts are in accordance with the literature values.<sup>84</sup>

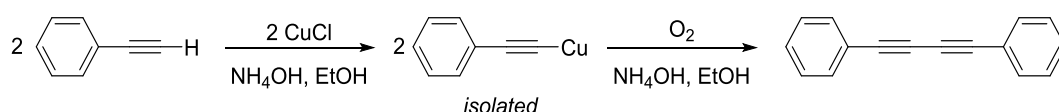


# 3 Manganese catalyzed radical Kumada-type reaction between aryl halides and aryl Grignard reagents

## 3.1 Introduction to cross-coupling reactions: a brief retrospective on their origins and history

Transition metal catalyzed cross-coupling transformations are of fundamental significance in organic synthesis, since they provide the straightforward formation of carbon-carbon or carbon-heteroatom bonds. The genesis of these processes can be found in the oldest metal-promoted homocouplings which have been known since the 19<sup>th</sup> century.<sup>97</sup>

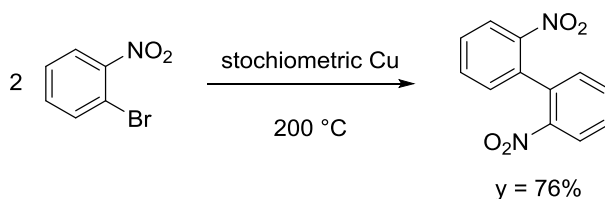
The first example of a coupling process involved copper as the metal promoter and was reported in 1869 by Carl Glaser.<sup>2</sup> He observed the oxidative formation of symmetric diynes by the use of copper chloride and two terminal alkynes. In fact when copper(I) phenylacetylide was exposed to air it underwent oxidative dimerization and diphenyldiacetylene was obtained as the product (Scheme 3.1).<sup>3</sup>



**Scheme 3.1.** The Glaser reaction.

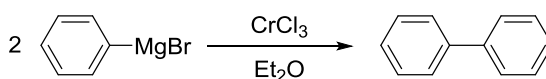
Further studies on the copper-mediated couplings resulted in the Ullmann reaction in 1901,<sup>100</sup> featuring a C(sp<sup>2</sup>)-C(sp<sup>2</sup>) bond formation between two aromatic nuclei. In particular Ullmann reported the dimerization of 1-bromo- and 1-chloro-2-nitrobenzene in the presence of finely divided copper to give a biaryl product with the elimination of copper halide (Scheme 3.2). The traditional version of the

Ullmann reaction suffered from various limitations such as the employment of electron deficient aryl halides and high temperature (above 200 °C).



**Scheme 3.2.** The Ullmann homocoupling exemplified by 1-bromo-2-nitrobenzene.

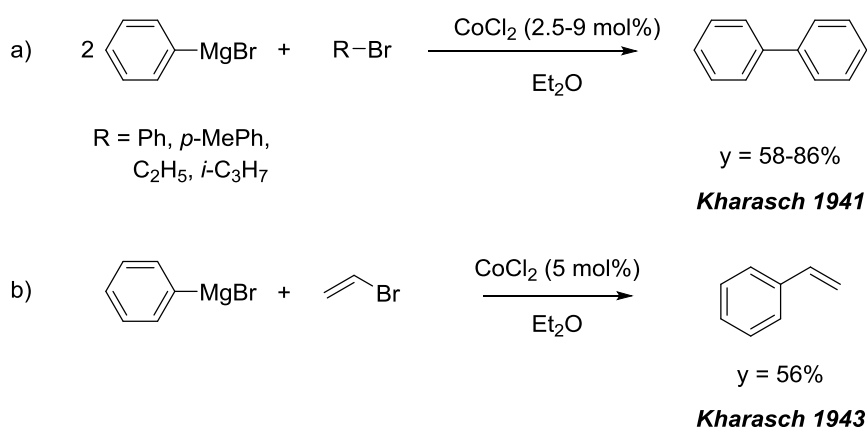
During the same period, interesting discoveries were also made in the alkali and alkali earth organometallic field. In particular Bennett and Turner in 1914 investigated the reaction between chromium(III) chloride and phenylmagnesium bromide.<sup>101</sup> Their original aim was to isolate an organometallic derivative of chromium, but a large quantity of biphenyl was instead obtained in the reaction, showing that a stoichiometric amount of chromium(III) chloride promoted the dimerization of phenylmagnesium bromide (Scheme 3.3). Later Krizewsky and Turner discovered that copper(II) chloride had a similar behavior as chromium(III) chloride for the homocoupling reaction.<sup>102</sup>



**Scheme 3.3.** Bennett and Turner dimerization of phenylmagnesium bromide.

The aforementioned discoveries had a great impact on the organic chemistry at that time, although they were strictly limited to the use of stoichiometric amounts of metal reagents and to the formation of symmetrical products. These limitations were overcome with the advent of catalysis facilitating selective catalytic methods which today are considered of great importance by the academic and industrial communities. Kharasch was one of the first chemist who investigated the transition

metal catalyzed C(sp<sup>2</sup>)-C(sp<sup>2</sup>) coupling.<sup>103</sup> In 1941 he described the results obtained when an aryl Grignard reagent is treated with an organohalide in the presence of a catalytic amount of cobalt(II) chloride (Scheme 3.4, a). The product of the reaction was the biphenyl adduct which derived exclusively from the Grignard reagent, while the organohalide took part as the oxidizing agent. In this scenario the cobalt(II) chloride was reduced by the Grignard reagent and then re-oxidized to the original oxidation state by the organohalide.

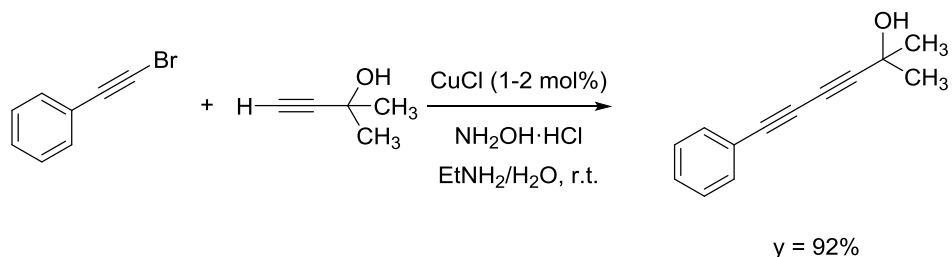


**Scheme 3.4.** The first examples of metal catalyzed couplings reported by Kharasch.

Further studies on cobalt as metal promoter of the coupling reaction resulted in the cross-coupling between a vinyl bromide and an organomagnesium species catalyzed by 5 mol % of CoCl<sub>2</sub> (Scheme 3.4, b).<sup>104</sup> The Kharasch coupling was extremely limited in substrate scope and functional group compatibility, however it provided concrete possibilities to condense two different structural fragments and to use catalytic quantities of transition metals to form carbon-carbon bonds.

### 3.1.1 The development of transition metal catalyzed cross-coupling reactions

In 1955 Cadiot and Chodkiewics reported an example of a cross-coupling where copper was used as the metal promoter.<sup>105,106</sup> As it was the case for the Glaser coupling this procedure reported the construction of 1,3-butadiyne compounds. The difference between these two methods is the amount of CuCl applied in the procedure and the use of structurally different molecules giving rise to an unsymmetrical product. The Cadiot-Chodkiewics reaction utilized 1-haloalkyne as the electrophile, a terminal alkyne as the nucleophile, 1-2 mol % of CuCl, and a suitable amine to eventually offer a cross-coupling compound as the product (Scheme 3.5). This method has been used extensively to synthesize a wide range of diacetylenic compounds.<sup>107,108,109</sup> The Cadiot-Chodkiewics process is sometimes affected by the formation of homocoupling byproducts, particularly when both of the alkynes involved in the reaction bear substituents of similar electronic effects. Furthermore the reaction proceeds in the presence of hydroxylamine hydrochloride to keep the copper salt in a low oxidation state.

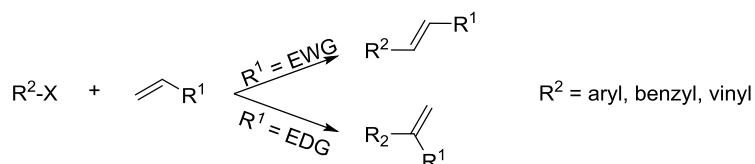


**Scheme 3.5.** Cadiot-Chodkiewicz C(sp)-C(sp) coupling.

A real and crucial change that has marked the history of cross-coupling processes occurred with the disclosure of palladium-based complexes as optimum catalysts for these transformations thanks to their efficiency and high selectivity. From the 1970's palladium catalysis plays a vital role in the organometallic chemistry and it is considered one of the most reliable methods for the formation of C-C bond.

Great contributions made by Heck, Negishi and Suzuki in this field revolutionized the scenery of organic synthesis and they were awarded the Nobel Prize in chemistry in 2010. Scheme 3.6 shows a short outline of the well-known cross-couplings named after their discoverers.

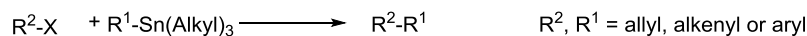
**Mizoroki-Heck**



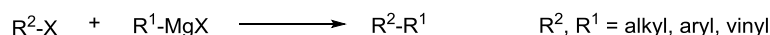
**Sonogashira**



**Miyaura-Kosugi-Stille**



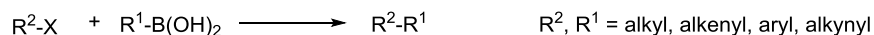
**Kumada-Corriu**



**Negishi**



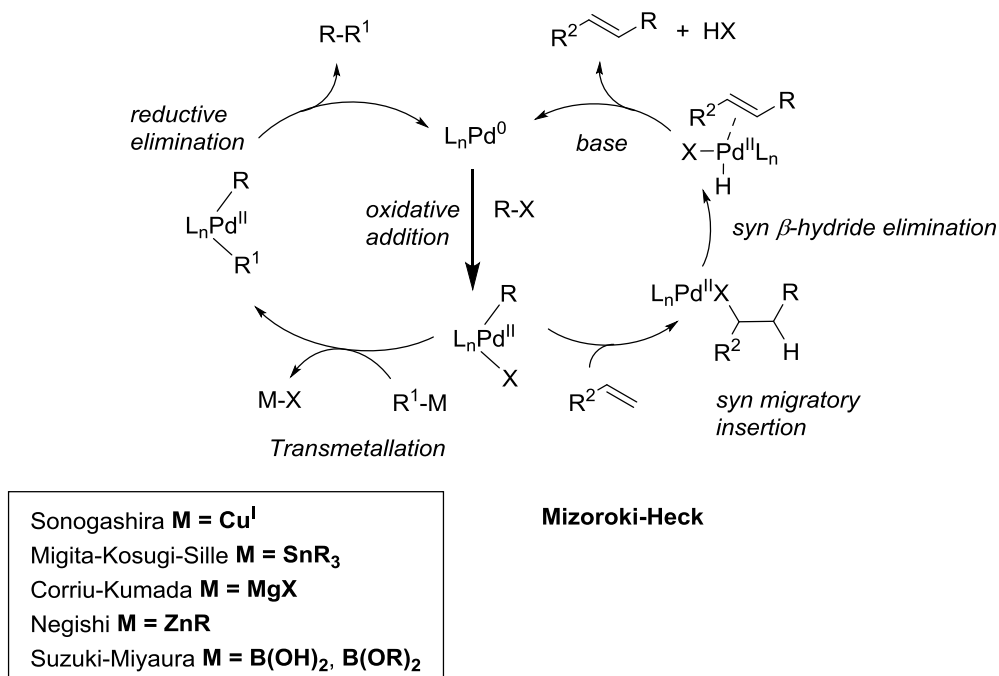
**Suzuki-Miyaura**



**Scheme 3.6.** Palladium catalyzed cross-coupling reactions

The generally accepted mechanism for the Pd-catalyzed cross-coupling reactions is depicted in Scheme 3.7. The basic steps are well established including initiation by oxidative addition of the organic halide or pseudohalide to the Pd<sup>(0)</sup> species, followed by a transmetalation step through the involvement of an organometallic

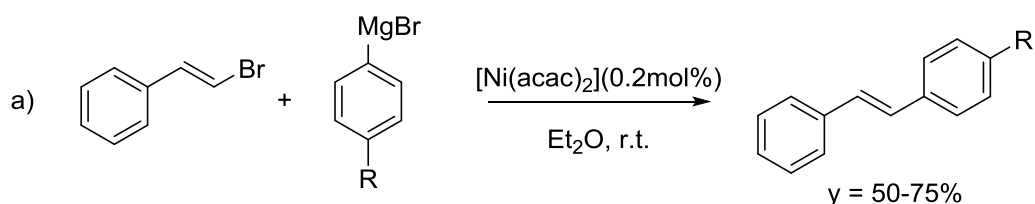
partner. The obtained intermediate  $R-Pd^{(II)}-R^1$  undergoes reductive elimination providing the product by carbon-carbon bond formation and regeneration of the active  $Pd^{(0)}$  species. The Mizoroki-Heck reaction follows a different pathway than the other cross-couplings after the oxidative addition step. In this reaction the olefin coordinates to palladium, followed by a migratory insertion of the olefin complex which leads to the formation of an alkylpalladium intermediate. When the olefin contains an electron withdrawing group (EWG) the insertion produces an alkylpalladium intermediate in which the group itself is located  $\alpha$  to the metal center. Subsequently  $\beta$ -hydride elimination occurs forming the alkene product. Finally the hydro halide (or pseudo halide) complex reacts with a base to eliminate  $HX$  and regenerate the starting  $Pd^{(0)}$  species.<sup>110</sup>



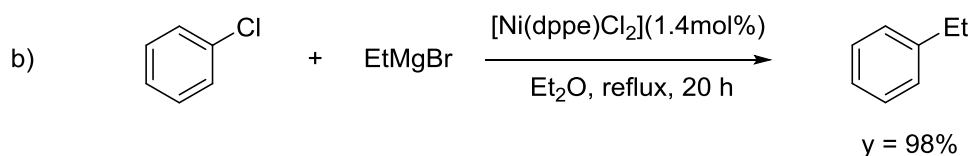
**Scheme 3.7.** General catalytic cycles for cross-coupling reactions catalyzed by palladium.

### 3.1.2 The Corriu-Kumada coupling

The reaction between an aryl or vinyl halide with a Grignard reagent in the presence of a catalytic amount of  $\text{Ni}(\text{dppe})\text{Cl}_2$  or  $\text{Ni}(\text{acac})_2$  was independently discovered in 1972 by Corriu and Kumada and allows the preparation of unsymmetrical products. This makes the cross-coupling processes particularly interesting from a synthetic point of view (Scheme 3.8).<sup>111,112</sup> In particular the novelty introduced by Kumada consisted in the employment of phosphine ligands to modulate the reactivity of the metal center. In 1976 Kumada reported that “the catalytic activity of the nickel complexes depends strongly upon the nature of the ligands” moreover “bidentate phosphines as ligand exhibit much higher catalytic activity than unidentate ones”.<sup>113</sup>



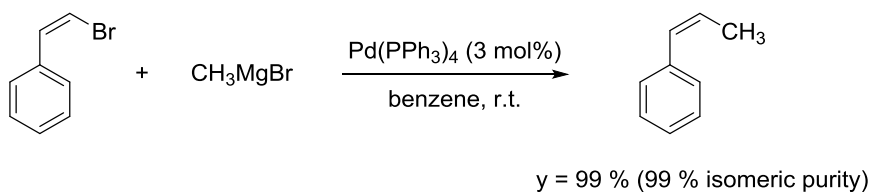
R = 4-MeOC<sub>6</sub>H<sub>4</sub>, 4-MeC<sub>6</sub>H<sub>4</sub>, 3-MeC<sub>6</sub>H<sub>4</sub>, 4-BrC<sub>6</sub>H<sub>4</sub>, 2,4-Me<sub>2</sub>C<sub>6</sub>H<sub>3</sub>



**Scheme 3.8.** a) Corriu cross-coupling catalyzed by  $\text{Ni}(\text{acac})_2$  1972. b) Kumada cross-coupling catalyzed by  $\text{Ni}(\text{dppe})\text{Cl}_2$  1972.

Even if the Grignard reagents are poorly tolerant towards some functional groups, their easy commercial availability or simple preparation together with the mild reaction conditions utilized, make the Corriu-Kumada reaction particularly

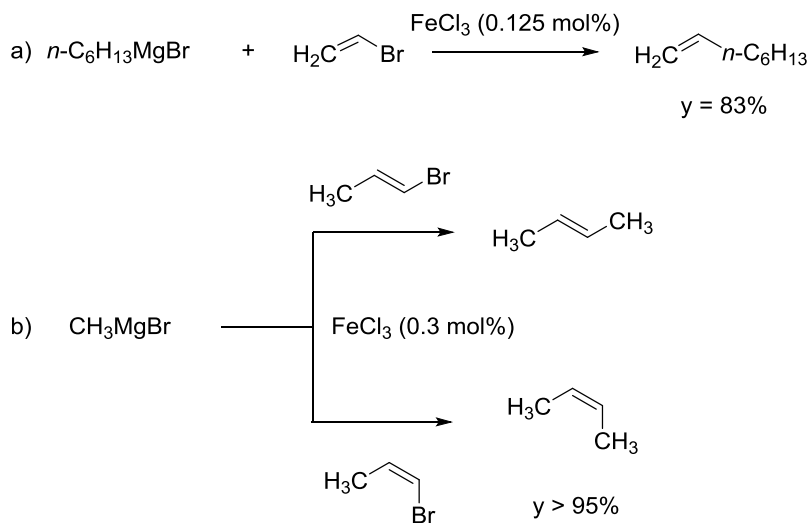
intriguing and widely studied until this day. In fact, since it was discovered, the method underwent several enhancements thanks to the development of new metal complexes. Shortly after the initial discovery, Murahashi described a stereoselective cross-coupling reaction between vinyl halides and Grignard reagents catalyzed by tetrakis(triphenylphosphine)palladium(0), Pd(PPh<sub>3</sub>)<sub>4</sub> (Scheme 3.9).<sup>114</sup>



**Scheme 3.9.** Murahashi stereoselective cross-coupling.

During the same period studies conducted by Kochi and co-workers described the activity of iron salts in similar cross-coupling reactions. In particular a procedure for the coupling of Grignard reagents with alkenyl halides using a catalytic amount of FeCl<sub>3</sub> was reported.<sup>115,116</sup> The method is stereoselective since methyl magnesium bromide reacted with *cis*- and *trans*-1-propenyl bromide to afford *cis*- and *trans*-2-butene respectively (Scheme 3.10). Furthermore Kochi established that iron 1,3-diketones were the most effective precatalysts thanks to their stability and ease of handle.<sup>117,118</sup>

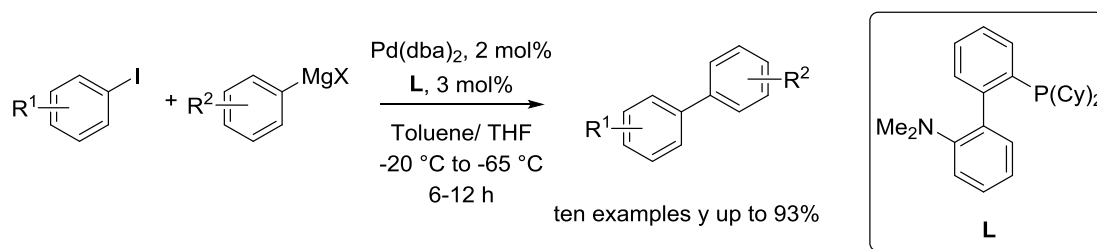




**Scheme 3.10.** Fe(III) catalyzed cross-coupling reactions reported by Kochi.

### 3.1.3 Recent examples of the Kumada reaction: a brief overview of the literature

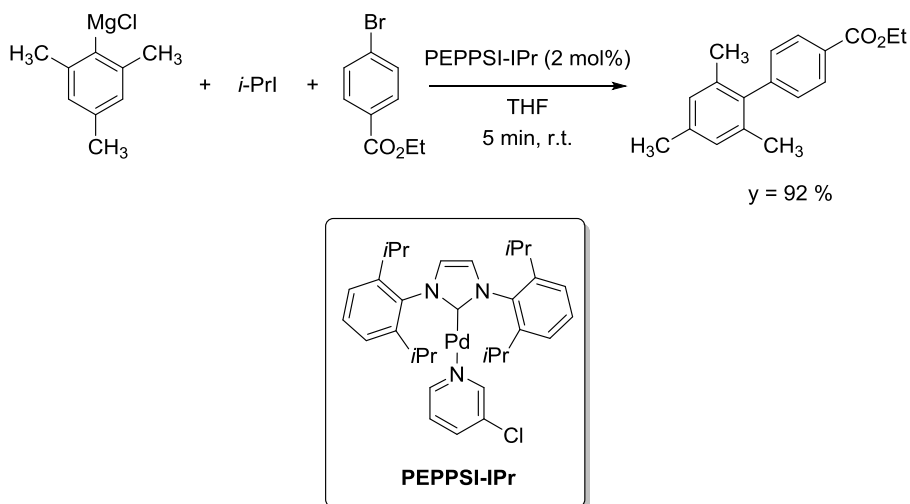
Generally published Kumada coupling processes have been catalyzed by Ni- and Pd-complexes. The problem of poor compatibility of sensitive functional groups with highly reactive Grignard reagents has been a limiting factor for the scope of the reaction. This has consequently given rise to protocols with softer nucleophilic reagents such as organozinc, organotin and organoboron compounds. However, progressive developments of the experimental conditions and the chemistry of ligands have led to the discovery of optimal reaction conditions allowing the employment of a wide variety of functional groups and minimizing the formation of side products. Recently, Buchwald and co-workers reported that functionalized aryl and hetero-aryl iodides could react with an arylmagnesium halide at low temperature in the presence of an appropriate ligand leading to the desired cross-coupling product (Scheme 3.11).<sup>119</sup>



**Scheme 3.11.** Pd catalyzed Kumada reaction of aryl iodides with Grignard reagent.

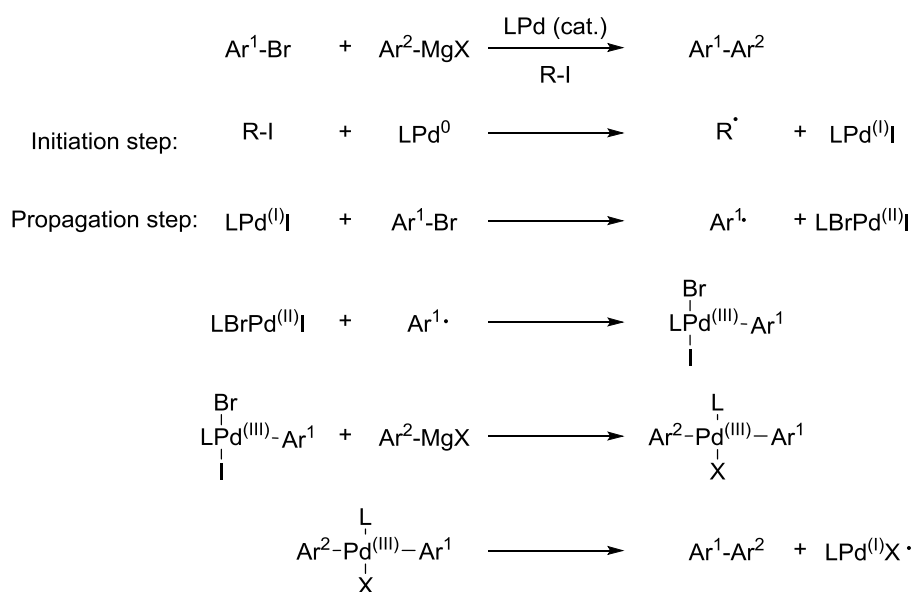
Most of the Kumada couplings follow the classical pathway of oxidative addition, transmetallation and reductive elimination as shown in Scheme 3.7.

In 2009 Knochel reported a radical cross-coupling reaction between an aryl bromide and an aryl Grignard reagent in the presence of an alkyl iodide.<sup>120</sup> The use of an allyl iodide significantly increased the functional group tolerance of this process. Moreover this method could be extended to functionalized organomagnesium compounds with a low stability at room temperature (Scheme 3.12).



**Scheme 3.12.** Radical Kumada coupling reported by Knochel.

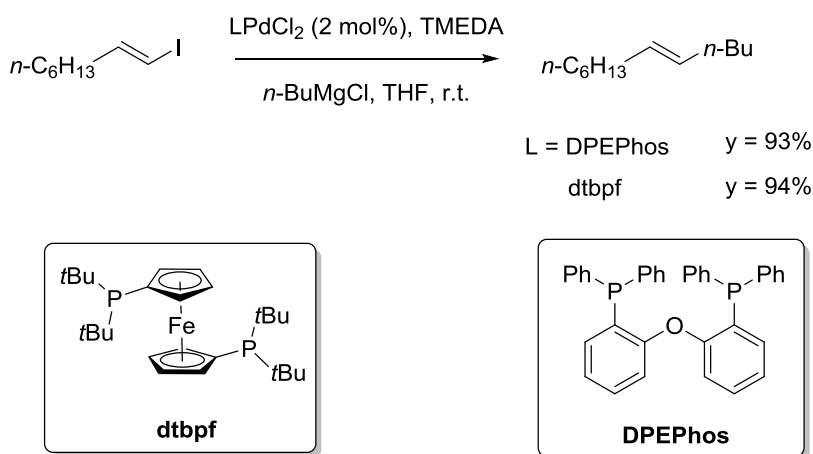
Based on the results of his studies and on previous works, Knochel proposed a radical mechanism in which the initiation step involved the reaction between the alkyl iodide RI and the palladium(0) precatalyst [LPd]<sup>(0)</sup> to afford the radical R· and [LPdI]<sup>(0)</sup> as intermediates. The propagation step immediately after provided the reaction between [LPdI]<sup>(0)</sup> and the aryl bromide Ar<sup>1</sup>-Br resulting in the aryl radical (Ar·) which is then trapped by the palladium complex [LPdX<sub>2</sub>]<sup>(II)</sup>. The formed palladium(III) species [ArLPdX<sub>2</sub>]<sup>(III)</sup> undergo a ligand exchange with the aryl Grignard reagent Ar<sup>2</sup>MgBr. Subsequently, a reductive elimination of the resultant diarylpalladium(III) halide provides the desire coupling product and regenerates palladium(I) as the radical chain carrier (Scheme 3.13).<sup>120</sup>



**Scheme 3.13.** Radical mechanism proposed by Knochel for the Pd-catalyzed cross-coupling reaction between an aryl bromide and an aryl Grignard.

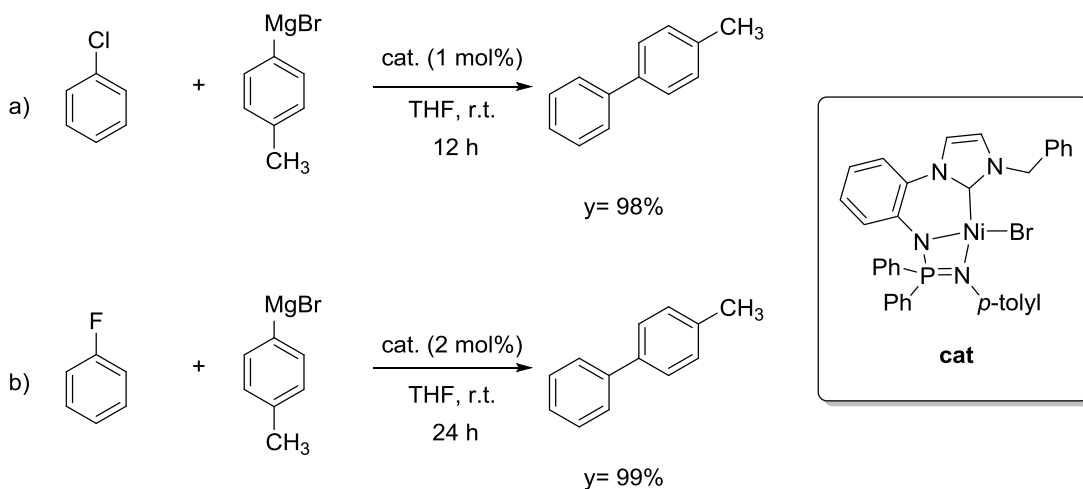
The importance of ligands in the reaction medium to avoid the formation of side products was emphasized in 2014 by Lipshutz and co-workers.<sup>121</sup> Here it was reported that a Pd-catalyzed reaction between an alkenyl halide and an alkyl Grignard reagent supported by a mixture of tetramethylethylenediamine (TMEDA)

and a sterically hindered bidentate phosphine ligand such as dtbpf or DPEPhos provided a selective formation of the desired alkene. Furthermore efficient control of the pathways that lead to undesired products was obtained, such as the dehalogenated product resulting from the competing  $\beta$ -hydride elimination or the homocoupling product that derived from the alkenyl substrate (Scheme 3.14).



**Scheme 3.14.** Example of Pd-catalyzed coupling of alkenyl iodide with alkylmagnesium bromide.

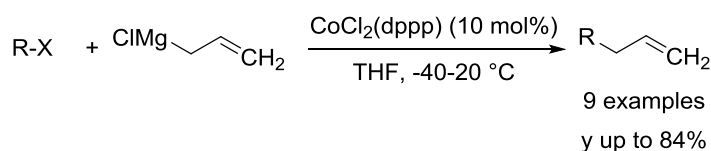
Of particular interest is that many examples of Kumada couplings reported in the literature in the past decades involve organic bromides and iodides as the electrophiles while organic chlorides and fluorides are generally considered poor electrophiles.<sup>122</sup> Generally the behavior of the metal center towards these particular substrates is modulated by the presence of a certain ligand. An example being the *N*-heterocyclic carbene-based pincer nickel complexes which can activate not only aryl C-Cl bonds, but also aryl C-F bonds and thereby catalyzing cross-couplings with aryl Grignard reagents very efficiently (Scheme 3.15).<sup>123</sup>



**Scheme 3.15.** Kumada coupling between a) phenyl chloride and b) phenyl fluoride with *p*-tolylmagnesium bromide catalyzed by a pincer nickel complex.

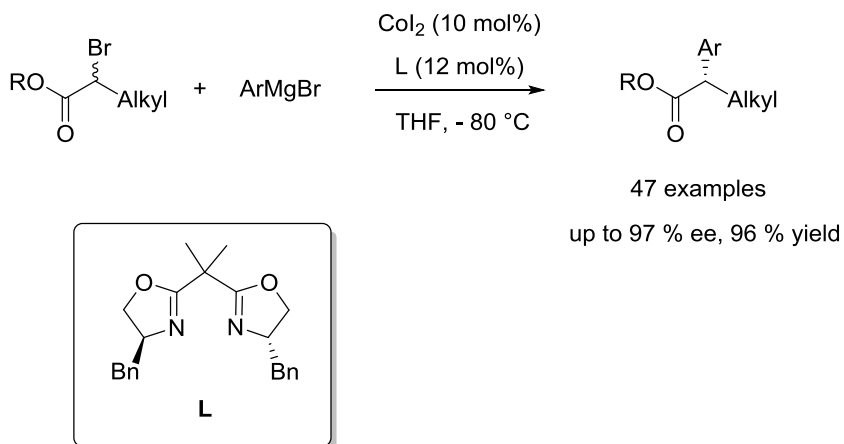
The nickel complexes together with the palladium counterparts are the most commonly employed catalysts in applied chemistry due to their efficient cross-couplings of organometallics with aryl halides. Despite this fact, they are not immune from disadvantages regarding the high cost and the toxicity of their complexes. For this reason, considering that this way to form a new carbon-carbon bond, in particular when a C(sp<sup>2</sup>) center is involved, has an enormous impact in the industry, many chemists nowadays have focused their attention on the search for valid alternative catalysts which can satisfy both economic and ecological aspects. Fortunately transition metals as cobalt<sup>124</sup>, iron<sup>118</sup> and copper<sup>125</sup>, available either as salts or complexes, have proved to be good alternatives and additionally have found to be effective and tolerant with respect to numerous functional groups. Although the catalytic activity of cobalt salts towards cross-coupling processes has been well known since the first experiments conducted by Kharasch and coworkers, several improvements have been made in the cobalt-catalyzed cross-coupling reactions since then. A selection of these progresses can be found in a work published in 2002 by Oshima and co-workers, who reported the

cobalt catalyzed cross-coupling reaction of primary, secondary and tertiary alkyl halides with allylic Grignard reagents (Scheme 3.16).<sup>126</sup> At that time the employment of alkyl halides as electrophiles was a limiting factor for the Kumada coupling reaction for two reasons. Firstly, the oxidative addition of these substrates was much slower than that of aryl and vinyl halides. Secondly, alkyl palladium or alkyl nickel could undergo  $\beta$ -hydride elimination.<sup>126</sup> According to the authors, the oxidative addition step occurred through an electron transfer mechanism from an electron-rich allyl cobalt complex to the alkyl halide.



**Scheme 3.16.** Cobalt catalyzed allylation of alkyl halides.

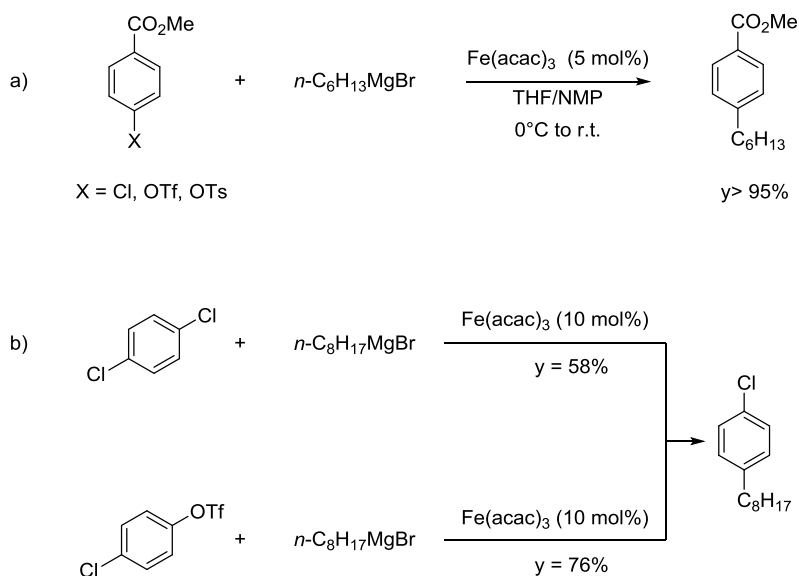
The capability of cobalt catalysts to perform a synthesis of an asymmetric compound was further emphasized by Walsh and co-workers in 2014.<sup>127</sup> The authors discovered that  $\text{CoI}_2$ , supported by a bisoxazoline as ligand, can enantioselectively catalyze a Kumada reaction between racemic  $\alpha$ -bromo esters and aryl Grignard reagents (Scheme 3.17).



**Scheme 3.17.** Cobalt catalyzed asymmetric Kumada coupling.

The procedure above has been applied for the synthesis of (*S*)-fenoprofen, a non-steroidal anti-inflammatory drug, and for the synthesis of (*S*)-*ar*-turmerone that exhibit antiproliferative and antitumor activity.<sup>127</sup>

Due to the abundance and lower toxicity of iron catalysts these were also recently considered as valuable alternatives to complexes or salts of palladium and nickel. As previously outlined by the work of Kochi, iron salts have demonstrated to be effective for forming new carbon-carbon bonds (see paragraph 3.1.2). Despite the considerable potential of iron, the real leap forward in its chemistry regarding cross-coupling reactions, took place in 2002 when Fürstner and Leitner developed a procedure for iron-catalyzed cross-coupling reactions of aryl chlorides, triflates and tosylates with alkyl magnesium bromides in THF/NMP (Scheme 3.18).<sup>128</sup> Instead, aryl iodides and bromides primarily led to the formation of the reduced product. Afterwards the possibility to selectively conduct a monoalkylation on aromatic rings bearing more than one halide or pseudohalide has been proven (Scheme 3.18).<sup>129</sup>

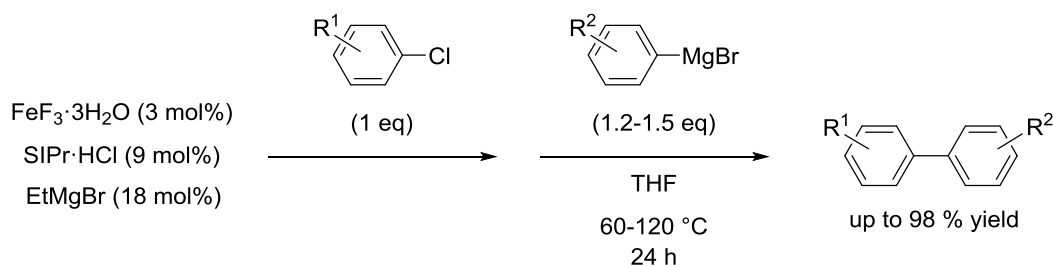


**Scheme 3.18.** Fe(acac)<sub>3</sub> catalyzed a) Kumada coupling reaction between an aryl halide or pseudohalide and hexylmagnesium bromide b) selective monoalkylation of 1,4-dichlorobenzene and 4-chlorophenyl trifluoromethanesulfonate.

A synthetic application of this method can be found in the total synthesis of the spermidine alkaloid (-)-isooncinotine and the olfactory macrocycle (+)-muscopyridine.<sup>130,131</sup> However the employment of iron catalysts for the Kumada cross-coupling between two aryl substrates remained limited by the homocoupling of the Grignard reagent and the use of electron-deficient aryl halides.<sup>132</sup> A solution to minimize the formation of the homocoupling product has been suggested by Nakamura and co-workers in 2007. The authors stated that a combination of iron fluoride salts (FeF<sub>3</sub>) with an *N*-heterocyclic carbene ligand could suppress the homocoupling reaction.<sup>133</sup> The homocoupling was predominant when FeCl<sub>3</sub>, either with or without the *N*-heterocyclic carbene ligand, was employed in the cross-coupling process, while it was suppressed if FeCl<sub>3</sub> was pretreated with KF, meaning that the fluoride anion played a significant role in controlling the homocoupling route (Scheme 3.19).

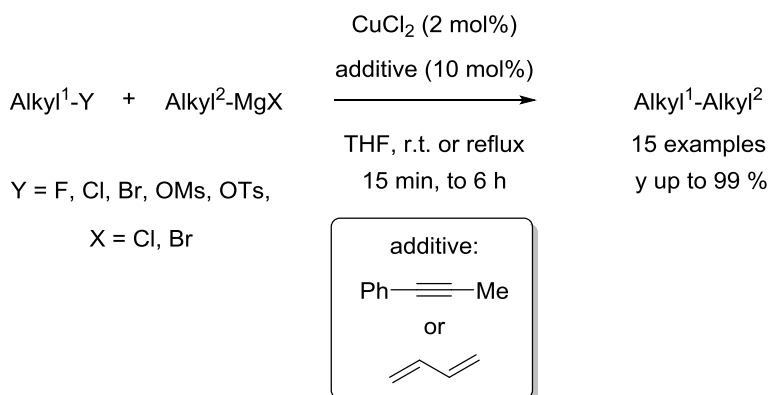


The nonprecious metal copper is nowadays considered a very attractive alternative due to its abundance and low cost. At the beginning of the twentieth century (see paragraph 3.1.2), copper was often employed as the coupling agent but it was outclassed by palladium in the cross-coupling reactions, and the use of copper has remained confined as co-catalyst in the Sonogashira and Stille coupling.



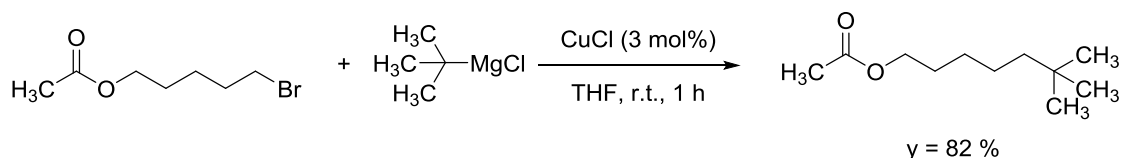
**Scheme 3.19.** Iron-catalyzed selective biaryl coupling reaction.<sup>36</sup>

Recently new methodologies have been developed for the copper mediated formation of carbon-carbon bonds. As an example Kambe and co-workers in 2007 described the copper-catalyzed cross-coupling reaction of alkyl chlorides with Grignard reagents in the presence of 1-phenylpropyne as an additive. The alkyl chlorides were known to be less reactive than the corresponding bromides and iodides probably caused by the strong C-Cl bond. Furthermore, the method can be extended to alkyl fluorides, mesylates and tosylates (Scheme 3.20).<sup>134,135</sup>



**Scheme 3.20.** Cu-catalyzed cross-coupling reaction between Grignard reagents and alkyl chlorides, fluorides, mesylates and tosylates.

Other procedures have also been recently developed for alkyl-alkyl cross-coupling reactions. The right choice of catalysts and ligands solved the reluctance of alkyl halides as electrophiles to undergo oxidative addition. The issue related to the alkyl-metal intermediates to suffer  $\beta$ -hydrogen elimination was also solved.<sup>136–139</sup> However, the use of more sterically bulky nucleophiles such as secondary or tertiary alkyls, still has to be perfected.<sup>140–143</sup> In fact bulky nucleophiles hardly underwent transmetalation but instead were isomerized to unwanted products. Some progress regarding this limitation was published in 2012 by Hu and co-workers where they described a copper-based method for the coupling of secondary and tertiary Grignard reagents with functionalized alkyl halides and tosylates (Scheme 3.21).<sup>144</sup>



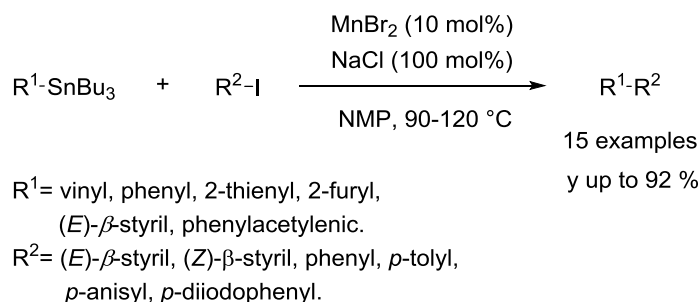
**Scheme 3.21.** Cu-catalyzed cross-coupling reaction between *tert*-butylmagnesium chloride and 5-bromopentyl acetate.

### 3.2 Manganese as an alternative for catalyzing cross-coupling reactions

It was previously highlighted that iron, cobalt and copper can be employed as sustainable alternatives to precious palladium and toxic nickel. Through ongoing search for eco-friendly, efficient, and also economic methodologies, the attention of the chemical community in particular has been turned to first-row transition metals such as iron and manganese. However, unlike iron, the catalytic potentials of manganese have remained quite unexplored for a long time, and only in the recent years a growing number of publications came along. Manganese is the 12<sup>th</sup> most abundant element in the Earth's crust where it is naturally present in rocks, soil, water, food, and in most of all living organisms. Approximately 12 milligrams of manganese is contained in the human body, mostly in the bones, liver and kidneys.<sup>145</sup> Manganese has an important role in biology since it acts as cofactor for a large number of enzymes. Furthermore, it is necessary for the nervous system, reproductive hormone functions, and it acts as an antioxidant intervening on free radicals as to prevent cell damages.<sup>146,147</sup> Manganese exists in several oxidation states, from -3 to +7 and therefore it confers a great redox power. Manganese compounds with high oxidation states such as  $\text{Mn(IV)O}_2$  and  $\text{KMn(VII)O}_4$ , are well known to be strong oxidizing agents. On the other hand its compounds with low oxidation states such as organomanganese(II) halides react in a 1,2-addition to aldehydes and ketones and furthermore exhibit reactivity toward carbon dioxide, sulfur dioxide and isocyanates.<sup>148–150</sup> Therefore manganese is a very interesting transition metal which constitutes a good candidate for the development of alternative catalytic systems for cross-coupling reactions. Of the few examples in the literature concerning manganese catalyzed cross-couplings some, with particular attention to the Kumada coupling, are mentioned below.

### 3.2.1 Overview of the literature on manganese catalyzed cross-coupling reactions

Compared to the reported Heck, Suzuki, Negishi, Stille and Sonogashira couplings catalyzed by palladium, very few examples have been presented using manganese as the catalyst. A Stille cross-coupling reaction performed by manganese has been reported by Kang and co-workers in 1997. This work demonstrates the possibility to couple organostannanes with alkynyl or aryl iodides by the employment of simple  $\text{MnBr}_2$  as the catalyst together with  $\text{NaCl}$  as an additive and NMP as solvent (Scheme 3.22).<sup>151</sup> The method works well without using palladium and in general temperatures between 90 and 120°C are needed for the reaction to take place.

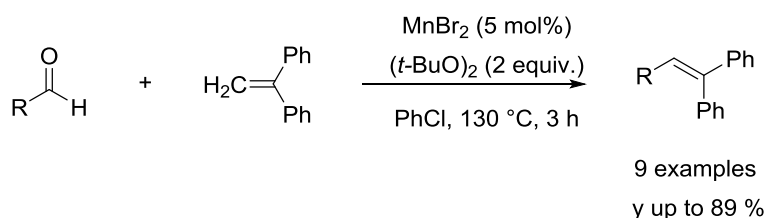


**Scheme 3.22.** Mn-catalyzed cross-coupling of organostannanes and organic iodides.

Jiang and co-workers in 2008 described a Suzuki coupling reaction catalyzed by manganese.<sup>152</sup> In particular the authors claimed that hydroxyapatites ( $\text{Ca}_{10}(\text{PO}_4)_6(\text{OH})_2$ , HAP) supported Mn catalyst (MnHAP) can synthesize biaryls through a cross-coupling of aryl bromides with aryl boronic acids in low to moderate yields. The reaction is conducted in a mixture of DMF/ $\text{H}_2\text{O}$  under reflux conditions. The structure of the employed catalyst is not given, but a fluorine-exchanged HAP-supported manganese catalyst (MnFAP) is found to be the

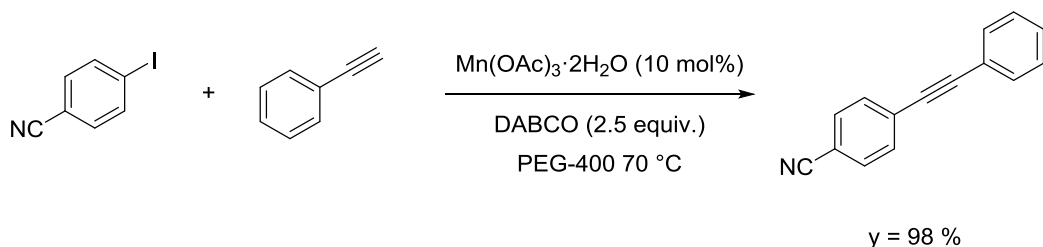
optimal catalyst for this method. A Mn(II) complex is believed to be the active species that takes part in the reaction.

Very recently Li and co-workers outlined the development of a radical alkyl-Heck-type reaction of different aliphatic aldehydes via a decarbonylation where again a simple manganese salt,  $\text{MnBr}_2$ , is used as the catalyst (Scheme 3.23).<sup>153</sup> By now it is known that the aryl or alkenyl-Heck reactions have a wide spectrum of available and well-functioning substrates, while the alkyl-Heck coupling still suffers from oxidative addition to  $\text{sp}^3$ -hybridized electrophiles and  $\beta$ -hydrogen elimination. The employment of compounds containing a carbonyl group as alkyl donors such as aldehydes, which are inexpensive and readily available, allows the extent of the substrates scope for the alkyl-Heck coupling to be extended.<sup>153</sup>



**Scheme 3.23.** Mn-catalyzed alkyl-Heck type reaction via oxidative decarbonylation of aldehydes.

An example of a manganese-catalyzed Sonogashira reaction was first reported by Wu and co-workers in 2016.<sup>154</sup> The procedure described by the authors presents mild and green conditions: the coupling between aryl iodides and aryl acetylenes being supported by  $\text{Mn}(\text{OAc})_3 \cdot 2\text{H}_2\text{O}$  as catalyst, DABCO as additive and poly(ethylene glycol)s (PEGs) as solvent. Furthermore the reaction is tolerant to moisture and air. Various functionalized diphenylacetylenes are synthesized through this strategy in moderate to good yields (Scheme 3.24).

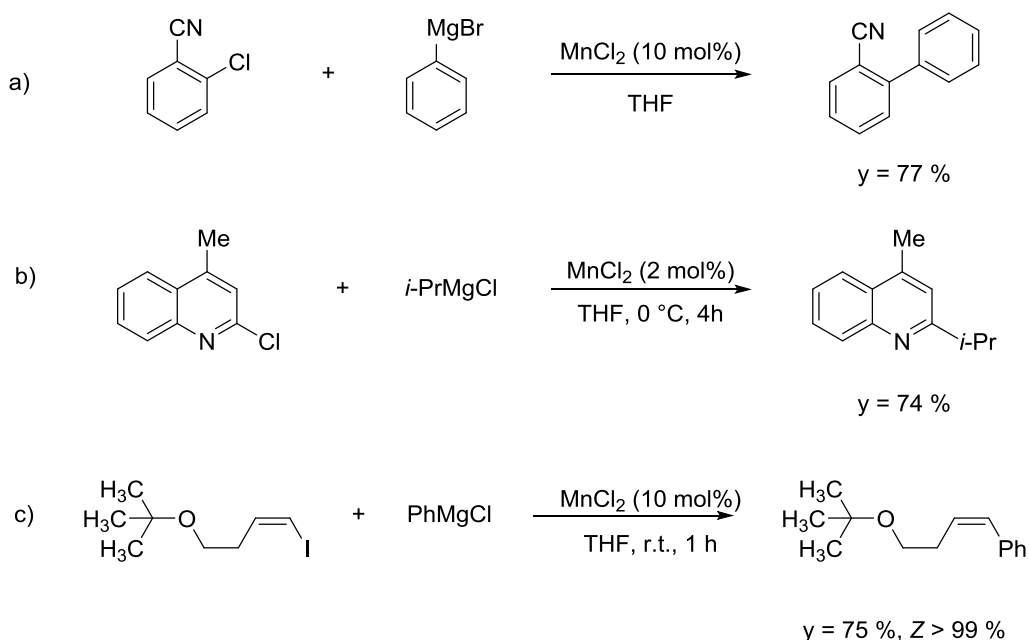


**Scheme 3.24.** Manganese catalyzed Sonogashira coupling of 4-iodobenzonitrile and phenylacetylene.

### 3.2.2 The Kumada coupling under manganese catalysis

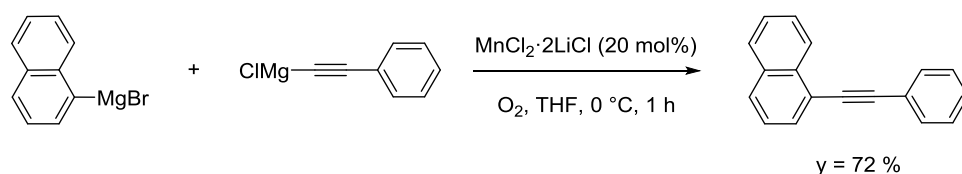
The Kumada coupling catalyzed by manganese is more documented in the literature than the couplings previously mentioned. A plausible reason is probably due to the reactivity of Grignard reagents towards manganese to form organomanganese species. In fact the transmetalation Mg/Mn constitutes the first step in all of the reactions involving Grignard reagents catalyzed by manganese and takes place very quickly.<sup>155</sup> Various strategies for the cross-coupling reactions under manganese catalysis with the involvement of Grignard reagents have been reported in the last few years. Particularly the Cahiez research group explored this topic extensively. For instance he disclosed the possibility to form biaryl compounds from the coupling between *ortho*- or *para*-activated aryl chlorides and phenylmagnesium bromide in the presence of 10 mol% of  $MnCl_2$  as the catalyst and THF as the solvent. Moreover the method has been extended to alkyl Grignard reagents with success and in general is performed under mild conditions and gives good to excellent yields of the cross-coupling products (Scheme 3.25, a).<sup>156</sup> Further research carried out by Cahiez and co-workers has led to the discovery of a chemoselective reaction between *ortho*-acylated aryl chlorides and phenylmagnesium chloride catalyzed by 10 mol% of  $MnCl_2$ . A limitation of this method was that the use of more responsive Grignard reagents, such as butylmagnesium chloride, which would preferably give nucleophilic addition to the carbonyl group of the substrate. To overcome this issue and to widen the scope of

the reaction, the authors employed a stoichiometric amount of the organomanganese reagents which were prepared *in situ* from  $\text{MnCl}_2$  and the related organomagnesium reagent. This gave high chemoselectivity and excellent yields of substitution products.<sup>157</sup> However, the scope of the Kumada reaction catalyzed by manganese remained limited to the aryl compounds containing electron-withdrawing groups until 2007. During this year Rueping and coworkers developed a cross-coupling reaction of various chloro-heterocycles with aryl or alkyl magnesium halides catalyzed by  $\text{MnCl}_2$  (2-5 mol%) (Scheme 3.25, b).<sup>158</sup> Additionally a procedure for coupling of aryl Grignard reagents with nonactivated alkenyl halides by the employment of  $\text{MnCl}_2$  10 mol% was established (Scheme 3.25, c).<sup>159</sup> Alkenyl bromides and iodides were suitable substrates for this reaction while the corresponding chlorides led to poor yields. In most cases the reaction showed retention of the vinyl halide stereochemistry.



**Scheme 3.25.**  $\text{MnCl}_2$  catalyzed Kumada couplings.

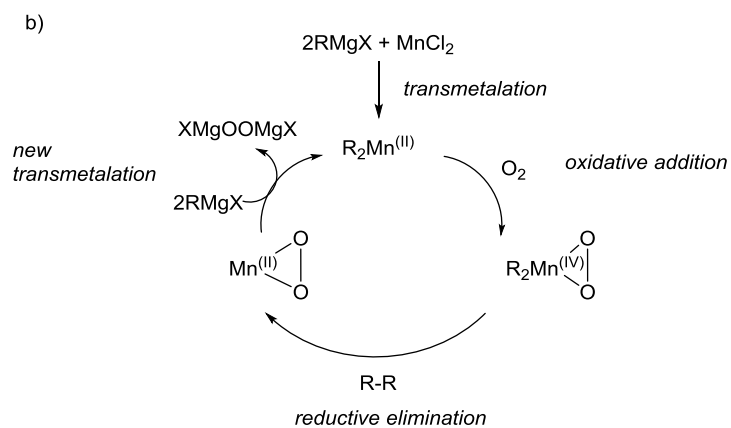
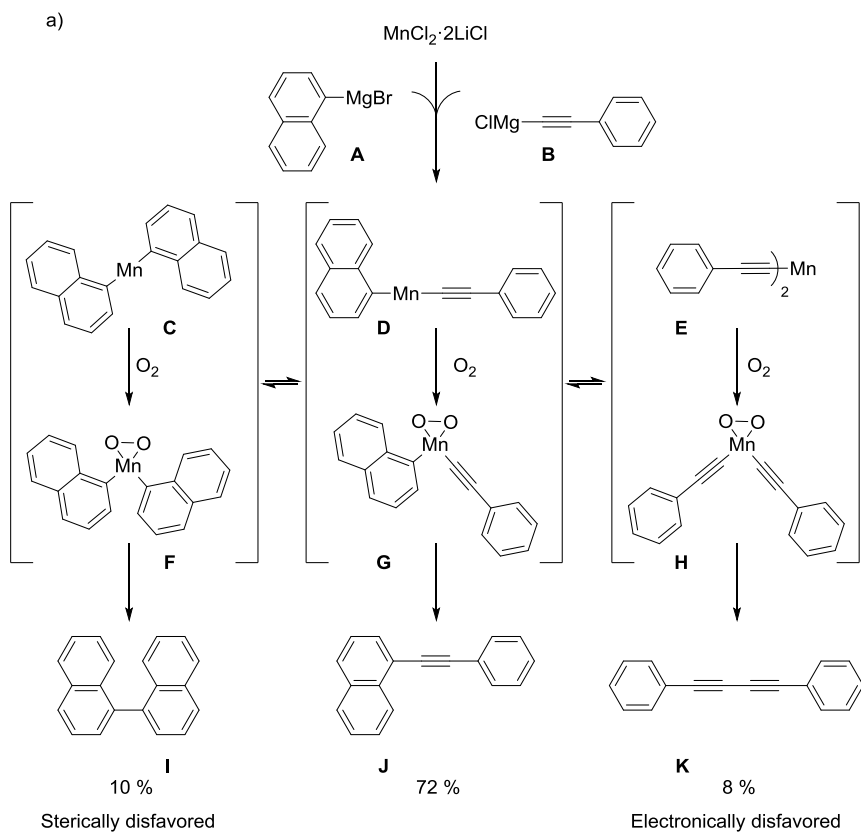
Based on success of the oxidative homocoupling of Grignard reagents catalyzed by manganese utilizing oxygen as the oxidant,<sup>160</sup> the foundations for the oxidative heterocoupling process of two organomagnesium compounds under similar conditions have been established. Thus, it is possible to couple two Grignard reagents  $R^1MgX$  and  $R^2MgX$  by taking into account the steric and electronic properties of  $R^1$  and  $R^2$ . In fact, the rate constant of the reaction is highly dependent on these two features. The procedure in which  $MnCl_2 \cdot 2LiCl$  (20 mol%) was used as catalyst,  $O_2$  as oxidant, THF as solvent and  $0^\circ C$  as temperature, has been applied for the synthesis of biaryls and aryl acetylenes in good yields (Scheme 3.26).<sup>161,162</sup>



**Scheme 3.26.** Example of heterocoupling reaction under oxidative  $MnCl_2$  catalysis.

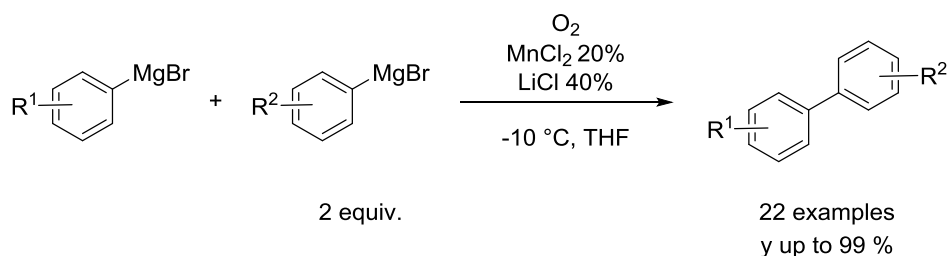
A tentative mechanism was also proposed by the authors in the paper. Reaction of two different Grignard reagent like **A** and **B** can form three different diorganomanganese species **C**, **D** and **E** which can each react with oxygen by forming the corresponding peroxomanganate complexes **F**, **G** and **H**. Subsequently, a reductive elimination affords two homocoupling products **I** and **K** which are disfavored for sterical and electronic reasons and the heterocoupling product **J** as the major product (Scheme 3.27). The mechanism for the cross-coupling reaction was examined more in detail by Cahiez and collaborators very recently by DFT calculations and a manganese(II)-manganese(IV) cycle was proposed (Scheme 3.27).<sup>161,162</sup>





**Scheme 3.27.** a) Tentative mechanism for Mn-catalyzed oxidative heterocoupling.<sup>66</sup> b) Mechanism for Mn-catalyzed oxidative heterocoupling reaction which has been recently investigated by DFT calculations.<sup>67</sup>

Very recently R. Madsen and co-workers reported an improved protocol for the  $\text{MnCl}_2$  catalyzed aerobic cross-coupling transformation between two aryl magnesium halides (Scheme 3.28).<sup>163</sup> The improvement of the reaction performance is very dependent on the temperature and the amount of time the reaction mixture is stirred after combining the reactants and before injecting dioxygen. The ratio used between the two organomagnesium compounds is 2:1 and the cross-coupling reaction gives excellent yield when the limiting Grignard reagent shows a mild propensity to undergo a competitive homocoupling process. Finally the reaction proved to be successful with *meta*- and *para*-substituted arylmagnesium halides. For the *ortho*-substituted substrates due to the influence of the steric effects lower, but still good yields were obtained.



**Scheme 3.28.**  $\text{MnCl}_2$  catalyzed aerobic cross-coupling reaction with different Grignard reagents.

### 3.3 Manganese in radical reactions

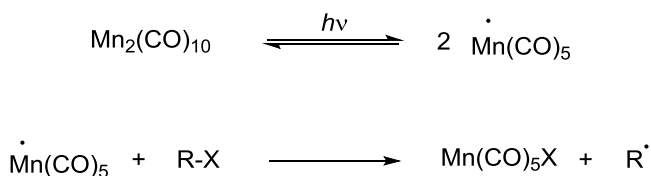
Generally two pathways can be considered for the mechanism of a reaction catalyzed by a transition metal, and they are strictly related to the electronic properties of the transition metal compounds. As already illustrated in chapter 1, one possible route normally consists of an oxidative addition at the beginning of the cycle and a reductive elimination to restore the active catalyst at the end of the cycle. These two steps are characterized by a two-electron transfer process in which the oxidation state of the metal changes by two.<sup>164</sup> The other possibility is

the radical pathway that follows an electron transfer (ET) mechanism between transition metal complexes and the organic substrates. The ability of a metal complex to undergo this ET mechanism is related to its first ionization energy. This is low for 3d metals and their complexes in general present a competition between an electron donation and a two-electron oxidative addition. On the other hand, 4d and 5d metals display high first ionization energy and typically undergo a two-electron pathway. However the nature of the ligands as well as the substrates and the reaction conditions has in general a great influence on the behavior of the metal complex.<sup>4</sup>

Manganese is a 3d transition metal belonging to group VII and its radical activity is known in the literature. In the following some examples of radical reactions in which manganese is involved as a catalyst or an initiator are reported.

### 3.3.1 Participation of Mn(0), Mn(II) and Mn(III) in radical reactions

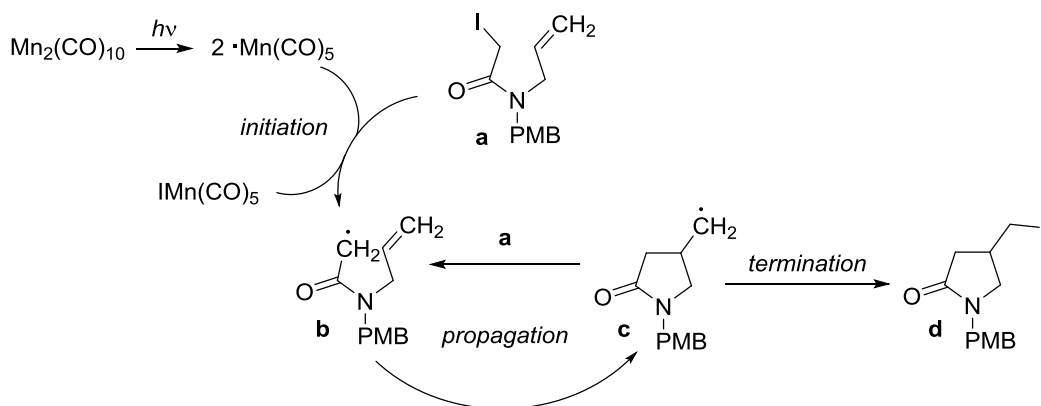
Following the order of the oxidation states, the first active manganese species in radical chemistry is the manganese(0) complex which is commercially available as manganese decacarbonyl ( $\text{Mn}_2(\text{CO})_{10}$ ). The employment of  $\text{Mn}_2(\text{CO})_{10}$  in cooperation with organohalides results in a free radical generation process (Scheme 3.29).<sup>165</sup>



R = alkyl or polymer chain  
X = Cl, Br, I

**Scheme 3.29.** Free radical  $\cdot\text{R}$  generation by  $\cdot\text{Mn}(\text{CO})_5$ .

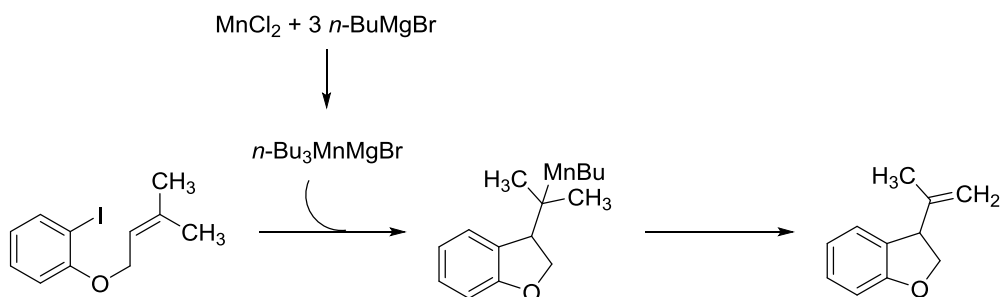
This has been widely utilized in organic and macromolecular chemistry either for the synthesis of very simple systems such as esters, amides and various heterocyclic products or for the synthesis of polymers and hyper-branched polymers. As an example Kondo and co-workers reported a photochemically induced formation of esters from alkyl iodides, where 5 mol% of  $\text{Mn}_2(\text{CO})_{10}$  is used as catalyst. As displayed in Scheme 3.29 the photolysis of  $\text{Mn}_2(\text{CO})_{10}$  results in the reactive manganese pentacarbonyl  $\cdot\text{Mn}(\text{CO})_5$ , that is the initiator of the reaction.<sup>166</sup> Ryu and coworkers recently improved the procedure by lowering the  $\text{Mn}_2(\text{CO})_{10}$  catalyst loading to 2.5-4 mol% and extending it to the formation of amides with moderate to good yields.<sup>167</sup> Parsons and coworkers observed that the use of 10 mol%  $\text{Mn}_2(\text{CO})_{10}$  at room temperature can induce a radical cyclization of *N*-allyl iodoacetamide giving 4-iodomethylpyrrolidone in 78% yield.<sup>168,169</sup> The product is unreactive towards the radical  $\cdot\text{Mn}(\text{CO})_5$  species. The mechanism of the reaction is shown in Scheme 3.30.



**Scheme 3.30.** Parsons and co-workers proposed mechanism for radical cyclization of *N*-allyl iodoacetamide initiated by  $\text{Mn}_2(\text{CO})_{10}$ .

The photolysis of  $\text{Mn}_2(\text{CO})_{10}$  gives  $\cdot\text{Mn}(\text{CO})_5$  as the initiator of the reaction and it abstracts iodine from *N*-allyl iodoacetamide **a**. The resulting radical intermediate **b** undergoes cyclization affording the radical 4-methylpyrrolidone species **c**. The following abstraction of iodine from the initial substrate provides 4-iodomethylpyrrolidone **d** as product and allows continuation of the catalytic cycle. As mentioned earlier the use of  $\text{Mn}_2(\text{CO})_{10}$  has also been successful in the field of polymers. Yagci and co-workers have extensively employed the manganese pentacarbonyl radical species for different purposes.<sup>170–174</sup> A very recent publication from his group disclosed that the use of iodo functionalized polyethylene (PE-I) combined with  $\text{Mn}_2(\text{CO})_{10}$  can initiate a controlled radical polymerization for the synthesis of block copolymers of polyolefins.<sup>175</sup>

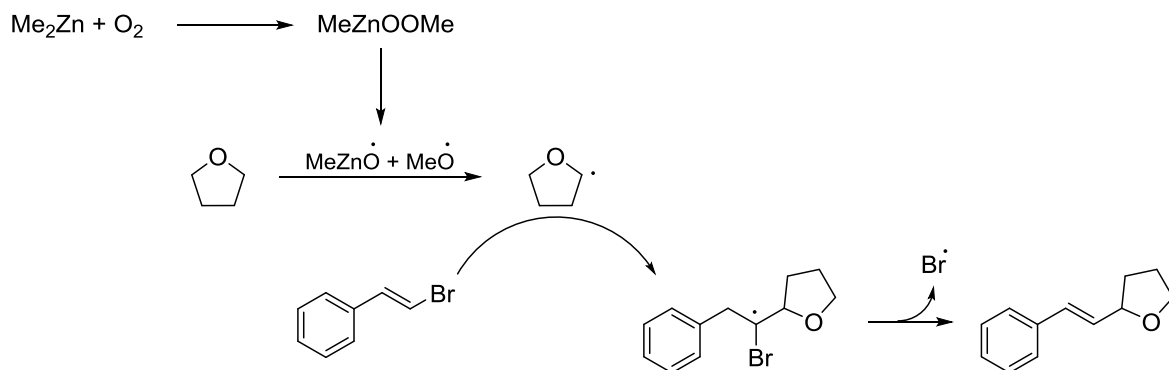
A few examples of Mn(II) used as an initiator does exist in the literature. Oshima and co-workers in 1997 reported that tributylmanganate derived from a catalytic amount of  $\text{MnCl}_2$  (20 mol%) and 3 equivalents of butylmagnesium bromide or butyllithium affords the synthesis of indoline, dihydrobenzofuran and 2-alkoxytetrahydrofuran derivatives.<sup>176</sup> The intermediary organomanganese species could be trapped by different electrophiles which prove its existence (Scheme 3.31).



**Scheme 3.31.** *In situ* formed tributylmanganate catalyzes aryl radical cyclization.

A recent work from our group<sup>177</sup> reveals a procedure for introducing a styryl group at the  $\alpha$ -position of ethers and tertiary amines. The transformation is mediated by

$\text{Me}_2\text{Zn}$  and a substoichiometric amount of  $\text{MnCl}_2$  (10 mol%). The mechanism for these couplings has not been investigated but is believed to proceed through a radical pathway. Previous studies reported that  $\text{Me}_2\text{Zn}$  reacts with dioxygen to form methylperoxide which undergoes homolysis resulting in two radical species  $\text{MeZnO}\cdot$  and  $\text{MeO}\cdot$ .<sup>178,179</sup> A proposed mechanism suggests the reaction between these two radical molecules and THF or a tertiary amine to give  $\alpha$ -alkoxy or  $\alpha$ -amino alkyl radicals. Further addition to  $\beta$ -bromostyrene provides the benzylic radical. The subsequent elimination of a bromine radical species results in the product (Scheme 3.32).



**Scheme 3.32.** Proposed mechanism for radical addition-elimination with THF.<sup>64</sup>

$\text{Mn(III)}$  is recognized to be an efficient promotor in radical reactions. In particular  $\text{Mn(OAc)}_3$  is known to be a stoichiometric one-electron oxidant and it is used to prompt radical additions and cyclizations thanks to its great ability to form radical species from carbonyls, unsaturated hydrocarbons, organophosphates, heterocycles, arylhydrazines, arylboronic acids, carbohydrates etc.<sup>180,181</sup> Among the manganese(III) compounds that have been particularly successful in organic synthesis, the Jacobsen catalyst, based on a  $\text{Mn(III)}$  salen complex, have found a widely application for the enantioselective formation of epoxides from *cis*-alkenes, the so called Jacobsen-Katsuki epoxidation.<sup>182,183</sup> Even though there have been

several debates toward the mechanism of the reaction in particular for the oxygen transfer to the double bond, one of the generally accepted pathways proceeds via radical intermediates. In general, taking into account both substrates and additives which take part into the reaction, the formation of side products with *trans* stereochemistry is explained by a radical mechanism and is applicable to conjugated alkenes, while a concerted mechanism clarified the construction of *cis*-products and is more appropriate for alkyl-substituted alkenes.<sup>184–186</sup>

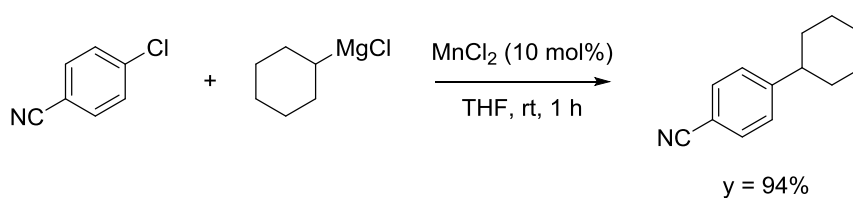
### 3.4 Conclusion

The importance of cross-coupling reactions has been highlighted in the current section, emphasizing the historical lineage and the tremendous impact it has had so far. Particular attention has been focused on the Kumada reaction since it represents the main matter of discussion in the next section. Moreover, the Kumada coupling can be carried out by catalytic amounts of sustainable and inexpensive first row transition metals such as iron and manganese. In particular, manganese salts, which widely exist in nature, have gained much attention in organic synthesis since they are inexpensive, chemical stable and display metal reactivity properties. Further investigations are still needed to understand the limits and the scope in the cross-coupling field. A further step forward would be a mechanistic study of the reactions, taking into account the propensity of manganese to undergo radical processes which would show a further diversification from the palladium or nickel catalyzed cross-coupling reactions.

## 3.5 Results and discussion

### 3.5.1 Study by another PhD student

The reaction between an aryl halide and a Grignard reagent catalyzed by  $\text{MnCl}_2$  was first explored by a PhD student in our group, which represents the starting point for the cross-coupling presented in this section.<sup>187</sup> At the beginning of the study it was found that the reaction of *p*-chlorobenzonitrile with cyclohexylmagnesium chloride in the presence of 10% of  $\text{MnCl}_2$  afforded the cross-coupling product in 94% yield (Scheme 3.33).<sup>187</sup>



**Scheme 3.33.** Coupling between cyclohexylmagnesium chloride and *p*-chlorobenzonitrile.

This result initiated a study of different *para*-substituted halobenzenes under the same conditions, but only methyl *p*-chlorobenzoate gave the expected product in 65% yield.<sup>187</sup> Interestingly when other electron withdrawing groups were involved in the reaction such as  $\text{CF}_3$  and  $\text{NO}_2$  no product formation was observed.<sup>187</sup> The reaction scope was expanded to a variety of aryl- and alkylmagnesium halides.<sup>187</sup> Both the *ortho*- and *para*-chlorobenzonitriles afforded the cross-coupling product in comparable yields when reacted with the different Grignard reagents.<sup>187</sup> In particular high yields were achieved with phenylmagnesium bromide producing the coupling product with *p*-chlorobenzonitrile or *o*-chlorobenzonitrile in 93% and 91% yield, respectively.<sup>187</sup>

The temperature seemed to be an important variable for the reaction. In fact, when *p*-chlorobenzonitrile and phenyl magnesium bromide reacted with 10% of  $\text{MnCl}_2$  at



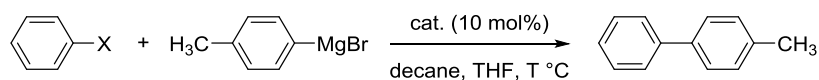
-12 °C, *p*-phenylbenzotrile was not formed, while at 0 °C about 5% of the product was generated.<sup>187</sup> Interestingly at room temperature the coupling went to completion within one minute and the solvent immediately started to reflux because of the exothermic nature of the reaction.<sup>187</sup>

Since the scope of the cross-coupling under these reaction conditions was limited to the cyano- and ester-activated substrates, the reaction was also investigated by employing bromobenzene and *p*-tolylmagnesium bromide in a 1:2 ratio with 10% MnCl<sub>2</sub>, and THF as the solvent. No cross-coupling occurred at room temperature or upon refluxing the reaction mixture.<sup>187</sup> Although these results were not encouraging, a hypothesis that the coupling process needed more energy in order to be activated led to the development of a new synthetic method using high temperatures (which is described in the next section).

### 3.5.2 Optimization of the reaction conditions

To broaden the substrate scope beyond cyano/ ester-activated substrates it was decided to conduct the experiments in a microwave oven. The reaction could then be run in a closed system with temperatures above the boiling point of the solvents. Initially bromobenzene and *p*-tolylmagnesium bromide in THF solution were chosen as the substrates in a ratio of 1:2 and 10% of the catalyst MnCl<sub>2</sub> was employed. The influence of the temperature on the reaction was investigated first by performing the experiments with temperatures between 100-200 °C (Table 3.1). As illustrated in Table 3.1 all the experiments afforded the desired heterocoupling product albeit in poor yields. When the reaction mixture was heated to 180 °C in the microwave oven, the transformation went to completion after 2 h and 40% of *p*-phenyltoluene was formed (entry 1). Interestingly, when the reaction temperature was further increased to 200 °C a reaction time of only 1 h was necessary to fully convert the bromobenzene, but the yield of the heterocoupling product dropped to 29% (entry 2). Decreasing the temperature to 160 °C and 140 °C did not improve

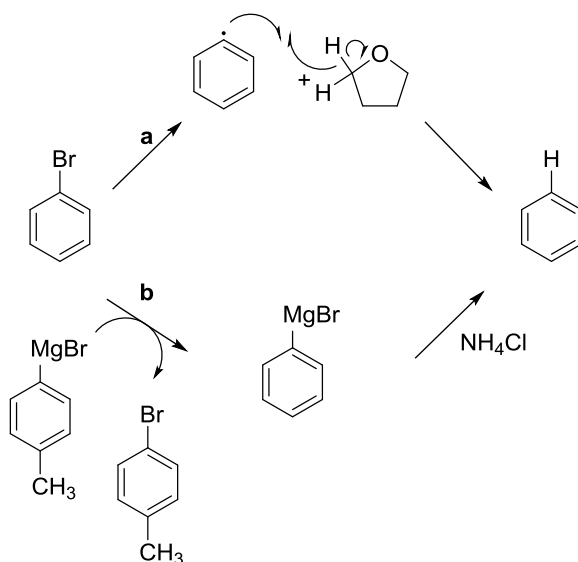
the reaction and *p*-phenyltoluene was obtained in 33% and 34% yields, respectively (entry 3-4). Conducting the experiment at 120 °C gave a slightly lower yield (21%), and the reaction time increased to 14 h to ensure the completion of the coupling process (entry 5). It was noticed that when bromobenzene reacted with *p*-tolylmagnesium bromide at 160 °C in 4 mL of THF (Grignard concentration 1 M, entry 6) the heterocoupling product was obtained in 30% yield which is comparable to the yield reported in entry 3. As it proved to be difficult to optimize the reaction through temperature and concentration, a change of catalyst was undertaken to verify whether the choice of the manganese salt can influence the reaction outcome. Exchanging MnCl<sub>2</sub> for MnF<sub>2</sub>, MnBr<sub>2</sub>, and MnI<sub>2</sub> resulted in low yields (entries 7-9). With one equivalent of MnCl<sub>2</sub> the coupling yield increased to 49% (entry 10). Attempts were also made by employing fluorobenzene, chlorobenzene, and iodobenzene as aryl halides. Fluorobenzene and chlorobenzene were not fully converted after 18 h and furnished the heterocoupling product in 4% and 20% yield, respectively (entries 11-12). On the other hand, the reaction with iodobenzene as the substrate went to completion after 2 h, although only 24% yield of *p*-methylbiphenyl was formed (entry 13).

**Table 3.1.** Optimization of cross-coupling catalyzed by MnCl<sub>2</sub>.<sup>[a]</sup>

entry	X	cat.	T [°C]	t [h]	yield [%] <sup>[b]</sup>
1	Br	MnCl <sub>2</sub>	180	2	40
2	Br	MnCl <sub>2</sub>	200	1	29
3	Br	MnCl <sub>2</sub>	160	2	33
4	Br	MnCl <sub>2</sub>	140	2	34
5	Br	MnCl <sub>2</sub>	120	14	21
6 <sup>[c]</sup>	Br	MnCl <sub>2</sub>	160	2	30
7 <sup>[c]</sup>	Br	MnF <sub>2</sub>	160	2	10
8 <sup>[c]</sup>	Br	MnBr <sub>2</sub>	160	2	29
9 <sup>[c]</sup>	Br	MnI <sub>2</sub>	160	2	28
10 <sup>[d]</sup>	Br	MnCl <sub>2</sub>	160	2	49
11	F	MnCl <sub>2</sub>	160	18	4
12	Cl	MnCl <sub>2</sub>	160	18	20
13	I	MnCl <sub>2</sub>	160	2	24

<sup>[a]</sup> Conditions: aryl halide (2 mmol), *p*-tolylmagnesium bromide (4 mmol), MnCl<sub>2</sub> (0.2 mmol), decane (1 mmol, internal standard) and solvent (8 mL, i.e. Grignard concentration 0.5 M) in a closed vial with microwave heating. <sup>[b]</sup> GC yield. <sup>[c]</sup> 4 mL solvent (Grignard concentration 1 M). <sup>[d]</sup> 1 equiv. of MnCl<sub>2</sub>.

The low yields obtained from the reactions described so far can probably be explained by the dehalogenation of bromobenzene which was found to be the major side reaction. This process can be explained in two different ways and both of them are equally valid (Scheme 3.34).



**Scheme 3.34.** Possible explanations for dehalogenation: a) involvement of a radical pathway, b) metal-halogen exchange

If the reaction between bromobenzene and *p*-tolylmagnesium bromide is assumed to proceed by a radical pathway it is possible to imagine the formation of a benzene radical (a, Scheme 3.34). This hypothesis can be validated by taking into account the bond dissociation energies (BDEs) of both benzene and THF, in fact the BDE for a benzene C-H bond<sup>188</sup> is 112 kcal/mol which is higher than the BDE for the  $\alpha$ -C-H bond of THF (89.8 kcal/mol).<sup>189</sup>

Dehalogenation can be also explained considering the metal-halogen exchange between bromobenzene and *p*-tolylmagnesium bromide under the reaction conditions. The presence of an electron-donating group in the *para* position of the Grignard reagent would allow to a transmetalation with bromobenzene, and phenyl magnesium bromide is generated from the reaction (b, Scheme 3.34).<sup>190</sup> The general work up procedure for the cross-coupling employed in this work provided the use of a saturated solution of ammonium chloride to quench the reaction mixture which eventually generates benzene.

Furthermore, traces of biphenyl were detected by GC spectra and this again could conceivably be explained by the metal halogen exchange between the aryl Grignard and the aryl bromide. Hence, it was decided to reverse the functionality for the cross-coupling. In other words it was chosen to employ *p*-bromotoluene as the aryl halide and phenyl magnesium bromide as the Grignard reagent. Interestingly, when the reaction was run with these substrates at 160 °C in THF (Grignard concentration 0.5 M), only 7% of *p*-methylbiphenyl was observed (entry 1 Table 3.2).

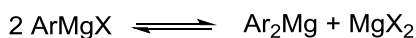
**Table 3.2.** Optimization of cross-coupling catalyzed by MnCl<sub>2</sub>.<sup>[a]</sup>



entry	X	solvent	T [°C]	t [h]	yield [%] <sup>[b]</sup>
1	Br	THF	160	2	7
2 <sup>[c]</sup>	Br	THF	160	2	15
3 <sup>[c]</sup>	Br	Et <sub>2</sub> O	160	1	23
4	Br	Et <sub>2</sub> O	160	1	60
5	Br	Et <sub>2</sub> O	140	2	57
6	Br	Et <sub>2</sub> O	120	5	70
7	Br	Et <sub>2</sub> O	100	12	69
8	Br	2-MeTHF	160	2	65
9	I	Et <sub>2</sub> O	120	5	75
10	Cl	Et <sub>2</sub> O	120	5	33

<sup>[a]</sup> Conditions: *p*-bromotoluene (2 mmol), phenylmagnesium bromide (4 mmol), MnCl<sub>2</sub> (0.2 mmol), decane (1 mmol, internal standard) and 1.3 mL solvent (Grignard concentration 3 M) in a closed vial with microwave heating. <sup>[b]</sup> GC yield. <sup>[c]</sup> 4 mL solvent (Grignard concentration 1 M).

The reaction resulted in a slightly better yield when the concentration of the Grignard reagent was increased to 1 M (entry 2) and Et<sub>2</sub>O was employed as the solvent (entry 3). A great improvement in the outcome of the coupling was achieved by further raising the Grignard reagent concentration from 1 M to 3 M, providing yields from 60 - 70% depending on the temperature and the reaction time (entries 4-7). Reaction in entry 6 was also performed by conventional heating in an oil bath overnight and *p*-methylbiphenyl was afforded with 62% yield. The importance of the concentration to suppress the dehalogenation was highlighted when *p*-bromotoluene was allowed to react with the same concentration of phenylmagnesium bromide in 2-methyltetrahydrofuran (entry 8). Here it is important to mention the Schlenk equilibrium which is represented by the equation in Scheme 3.35.



**Scheme 3.35.** Schlenk equilibrium for an arylmagnesium halide.

This equilibrium is shifted towards ArMgX in Et<sub>2</sub>O while Ar<sub>2</sub>Mg + MgX<sub>2</sub> are favored in THF.<sup>191</sup> This may offer an explanation about the improvement of the reaction by the switch in solvent from THF to Et<sub>2</sub>O. The reactions conditions were later applied to *p*-iodotoluene instead of *p*-bromotoluene, and a slightly better yield was achieved (entry 9) while replacing *p*-bromotoluene with *p*-chlorotoluene resulted in poor yield (entry 10).

A control experiment where *p*-bromotoluene was reacted with phenylmagnesium bromide in the absence of MnCl<sub>2</sub> confirmed that the reaction is assisted by MnCl<sub>2</sub>. In this case no conversion of the substrate was observed, not even formation of the dehalogenated product was detected. Furthermore no cross-coupling occurred when *p*-tolyl trifluoromethanesulfonate was treated with phenylmagnesium bromide under the reaction conditions.

Subsequent studies on the method were conducted at a temperature of 120 °C with 3 M solution of Grignard reagent in Et<sub>2</sub>O as these conditions presented a reasonable reaction time in the microwave (entry 6, Table 3.2).

## Additives

In order to examine a possible influence of additives on the reaction outcome, the cross-coupling procedure was performed in the presence of LiCl, LiBr, and MgBr<sub>2</sub> as additives. The presence of these did not improve nor considerably deteriorate the reaction rate. In fact, the conversion of *p*-bromotoluene over time showed the same progress with or without the presence of the additives (Figure 3.1).

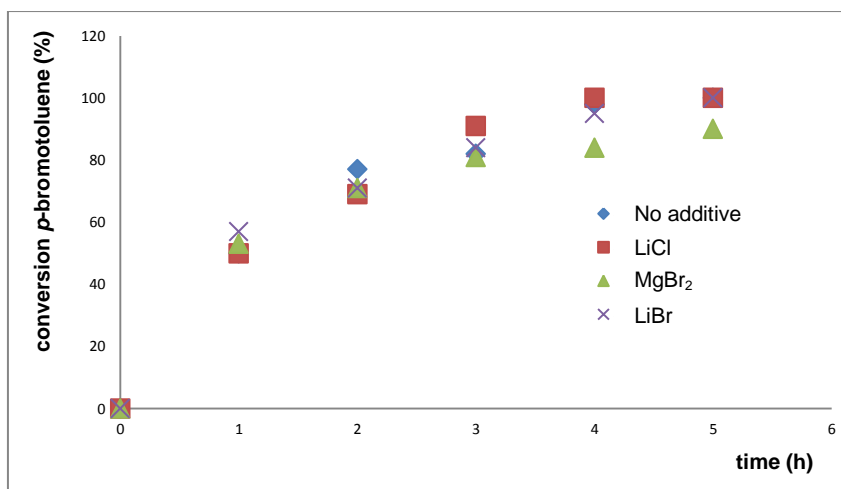


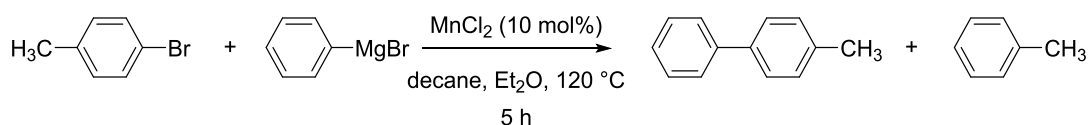
**Figure 3.1.** Conversion of *p*-bromotoluene as a function of time with and without additives.

## Reaction side products

For the results so far the dehalogenation represented the major side reaction, which consequently limited the yield of the actual cross-coupling to 70% (Table 3.3, entry 1). Since the metal halogen exchange represents one possible path

through which the dehalogenation can occur, different ratios of *p*-bromotoluene and phenylmagnesium bromide were employed under the examined reaction conditions. Table 3.3 shows that when a 1:1 ratio of the two substrates was used, the yield of the heterocoupling product dropped to 22%, and 24% of toluene was produced, while the remaining is unreacted *p*-bromotoluene (entry 2). The worst result was obtained with a 2:1 ratio of *p*-bromotoluene to phenylmagnesium bromide where only traces of *p*-methylbiphenyl and toluene were generated (entry 3). Differently, when *p*-bromotoluene and phenylmagnesium bromide were used in a 1:4 ratio, the reaction afforded *p*-methylbiphenyl and toluene in 66% and 32% yield, respectively. In this case, the ratio between the two main products is comparable to the one reported in entry 1.

**Table 3.3.** Cross-coupling reaction employing different ratio of *p*-bromotoluene and phenylmagnesium bromide.<sup>[a]</sup>



entry	n ( <i>p</i> -bromotol.)	n (phenylMgBr)	<i>p</i> -methylbiphenyl y [%] <sup>[b]</sup>	toluene y [%] <sup>[b]</sup>
1	2	4	70	26
2	2	2	22	24
3	4	2	traces	traces
4	2	8	66	32

<sup>[a]</sup> Conditions: *p*-bromotoluene (n mmol), phenylmagnesium bromide (n mmol), MnCl<sub>2</sub> (0.2 mmol), decane (1 mmol, internal standard) and 1.3 mL solvent (Grignard concentration 3 M) in a closed vial with microwave heating. <sup>[b]</sup> GC yield.

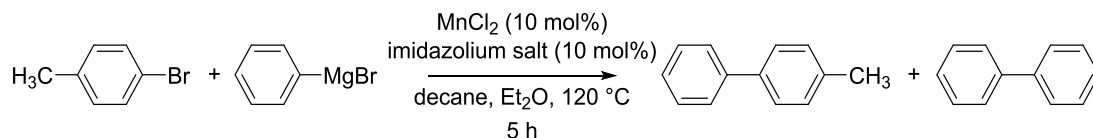
As already mentioned in the introduction section, one of the most common challenges of the aryl-aryl cross-coupling process is the competition with the homocoupling reaction. Recently, it was found that the employment of NHC



precursors plays a key role in suppressing the homocoupling product for the cross-coupling between *p*-chlorobenzene and *p*-tolylmagnesium bromide catalyzed by  $\text{FeF}_3 \cdot 3\text{H}_2\text{O}$ .<sup>192</sup>

Biphenyl is the homocoupling product for the reaction under examination deriving from phenylmagnesium bromide. This collateral reaction subtracts phenylmagnesium bromide from the cross-coupling which is one of the reasons the Grignard reagent was added in excess with respect to *p*-bromotoluene. In view of this it was decided to conduct the pilot reaction in the presence of 10% of an imidazolium salt to verify the possibility of minimizing the competing side product. As reported in Table 3.4 the use of 10% of 1,3-bis(2,6-diisopropylphenyl)imidazolium chloride resulted in 36% of the heterocoupling product and the 17% of the homocoupling indicating that no suppression of the collateral reaction was achieved and moreover the reaction generated *p*-methylbiphenyl in low yield (entry 2). When 10% of 1,3-diisopropylimidazolium chloride was employed, *p*-methylbiphenyl and biphenyl were produced instead in 63% and 29% yield, respectively. Consequently comparable ratio between the heterocoupling and the homocoupling products was observed with or without addition of imidazolium salts.

**Table 3.5.** Cross-coupling reaction between *p*-bromotoluene and phenylmagnesium bromide in the presence of imidazolium salts.<sup>[a]</sup>



entry	Imidazolium salt	<i>p</i> -methylbiphenyl y [%] <sup>[b]</sup>	biphenyl y [%] <sup>[c]</sup>
1	-	70	33
2		36	17
3		63	29

<sup>[a]</sup> Conditions: *p*-bromotoluene (2 mmol), phenylmagnesium bromide (4 mmol), MnCl<sub>2</sub> (0.2 mmol), decane (1 mmol, internal standard) and 1.3 mL solvent (Grignard concentration 3 M) in a closed vial with microwave heating. <sup>[b]</sup> GC yield. <sup>[c]</sup> GC yield based on the amount of phenylmagnesium bromide.

### 3.5.3 Substrate scope and limitations

This part of the study was conducted in collaboration with a visiting PhD student.\* The scope of the reaction was explored with the optimized procedure employing an aryl bromide or iodide (2 mmol) as well as phenylmagnesium bromide (4 mmol, Grignard concentration 3 M) in the presence of MnCl<sub>2</sub> (10 mol%) at 120 °C in the microwave oven (Table 3.6). All the reactions were purified by column chromatography and the yields reported in Table 3.6 refer to isolated products or are based on <sup>1</sup>H-NMR when the products were not completely pure. Both aryl bromides and aryl iodides can be used as substrates for the cross-coupling, but lower product yields were observed after purification when the substrates were

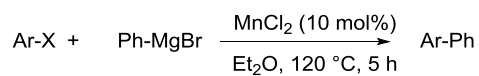
\* Somayyeh Sarvi Beigbaghlou Kharazmi University, Tehrān, August-December, 2017

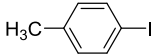
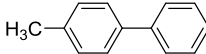
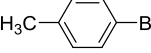
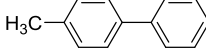
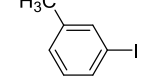
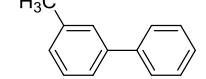
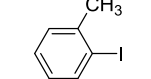
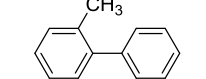
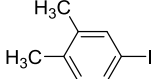
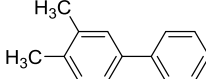
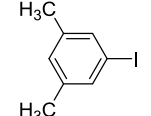
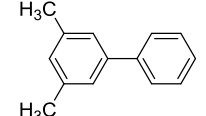
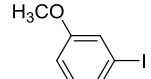
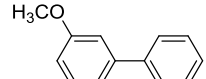
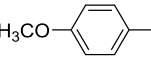
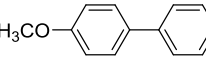
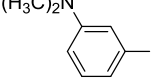
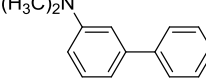
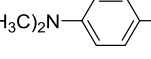
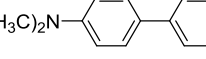
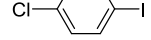
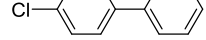
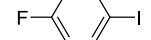
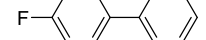
aryl bromides. The first two examples reported in Table 3.6 involved *p*-iodotoluene and *p*-bromotoluene as the substrate, and the product was afforded in 66% and 47% yields, respectively (entries 1-2). It is possible to note that a certain discrepancy between the isolated yields and the GC yields exists. This might arise from an uncertainty in the calibration curve, due to inaccuracies in measuring the internal standard which may result in a variation in the detected yield or the product loss during the workup of the reaction.

When *m*-iodotoluene was reacted with phenylmagnesium bromide under the reaction conditions, *m*-methylbiphenyl was obtained in 50% yield (entry 3). A lower yield was achieved with *m*-bromotoluene, where only 20% of the heterocoupling product was obtained from the reaction (result not shown). *o*-Iodotoluene furnished the corresponding coupling product in 34% yield (entry 4). This low result may be explained by consideration of the steric effect exercised by the neighboring methyl group on the reaction site. Interestingly, when two methyl groups were present on the aryl iodide as 1-iodo-3,4-dimethylbenzene and 1-iodo-3,5-dimethylbenzene, 77% and 62% yield of the corresponding biphenyl product was obtained (entries 5-6). The reaction was also expanded to aryl iodides bearing a methoxy group in the *para* or *meta* position, although poor yields were observed in both cases. In fact 3-methoxybiphenyl was achieved in 26% yield while *p*-methoxybiphenyl was produced in 23% yield. When a dimethylamino group was used instead, the corresponding coupling product was afforded in a slightly better yield (entries 9-10). *p*-Chloroiodo- and *p*-fluoroiodo-benzene were also subjected to the reaction conditions, but in these cases the reaction resulted in only 13% and 6% yield.

Others substrates were tested under the coupling conditions, but they did not show any reactivity or different products than the expected one was produced. This was in particular the case of the *p*-bromo(trifluoromethyl)benzene which was examined by GC and gave a substitution of the three fluorides with three phenyl groups belonging to the Grignard reagent and dehalogenation resulting in tetraphenylmethane as the only product.

**Table 3.6.** Cross-coupling with different aryl halides.<sup>[a]</sup>



entry	Ar-X	Ar-Ph	yield [%] <sup>[b]</sup>
1			66 <sup>[c]</sup>
2			47 <sup>[c]</sup>
3			50 <sup>[c]</sup>
4			34 <sup>[c]</sup>
5			77
6			62 <sup>[c]</sup>
7			26
8			23
9			33
10			28
11			13
12			6

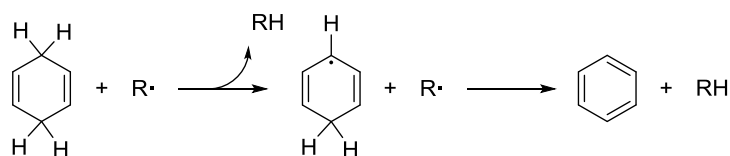
<sup>[a]</sup> Conditions: aryl bromide (2 mmol), phenylmagnesium bromide (4 mmol), MnCl<sub>2</sub> (0.2 mmol), and 1.3 mL solvent (Grignard concentration 3 M) in a closed vial with microwave heating. <sup>[b]</sup> Isolated yield. <sup>[c]</sup> Yield based on NMR since isolated product was not completely pure.

Moreover, no cross-coupling was observed when *p*-iodophenylbenzene or *m*-iodophenylbenzene was reacted with phenylmagnesium bromide.

Conclusively, the study conducted on the substrate scope of the cross-coupling clearly underlined its limit for the use on a wide array of aryl halides. However, it highlighted the possibility to obtain a decent yield with simple methyl substituted substrates.

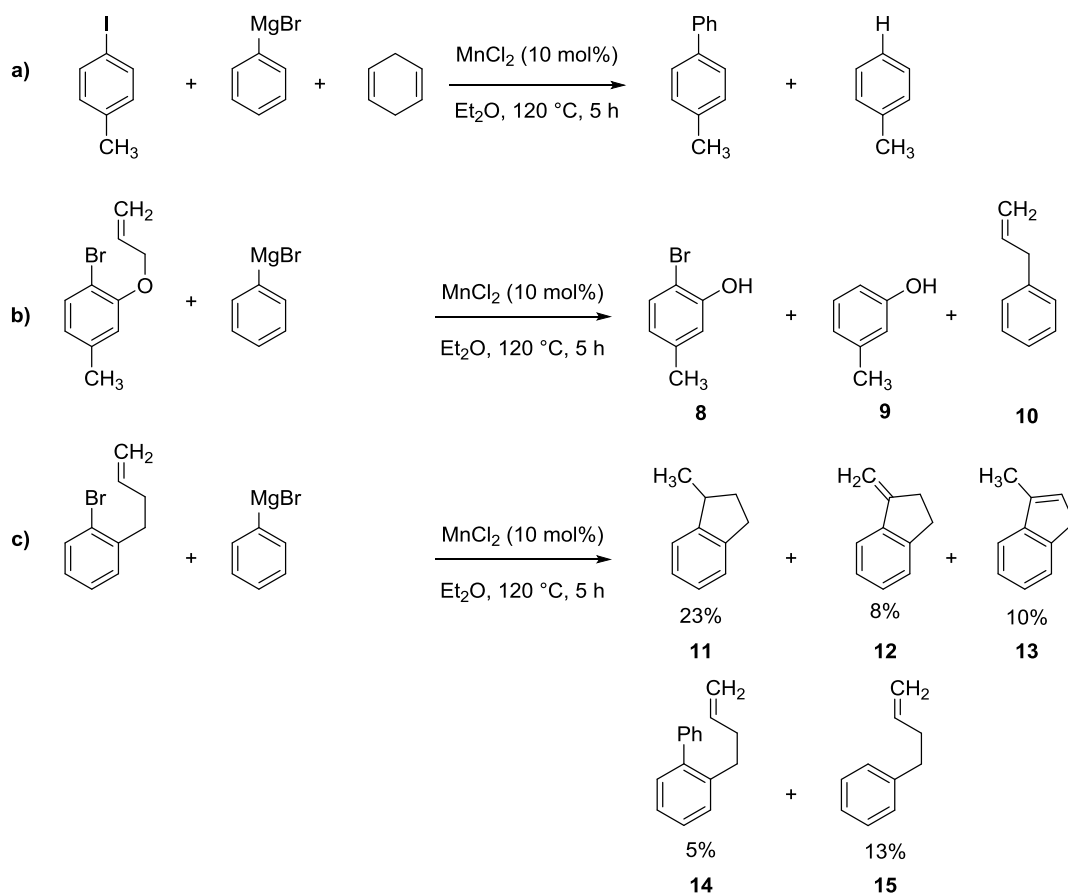
### 3.5.4 Investigation of the reaction mechanism

A further step in the study of the cross-coupling between the aryl halide and the Grignard reagent assisted by  $\text{MnCl}_2$  was a mechanistic investigation to gain insight into the reaction pathway. Previous work in our group on the coupling with chlorobenzonitriles and Grignard reagents reported that the reaction may proceed by a radical nucleophilic aromatic substitution ( $\text{S}_{\text{RN}}1$ ) mechanism.<sup>187</sup> Based on this, a similar line of study was followed to verify whether the reaction may involve a similar radical pathway. Consequently, two experiments were conducted in order to trap a possible aryl radical intermediate. A conceivable radical trapping agent which could be employed in this reaction system is 1,4-cyclohexadiene, well known as a two hydrogen atoms donor.<sup>193</sup> In fact the reaction between a radical species  $\text{R}\cdot$  and 1,4-cyclohexadiene results in benzene and the hydrogenated  $\text{RH}$  (Scheme 3.36).



**Scheme 3.36.** Schematic reaction of radical trapping by 1,4-cyclohexadiene.

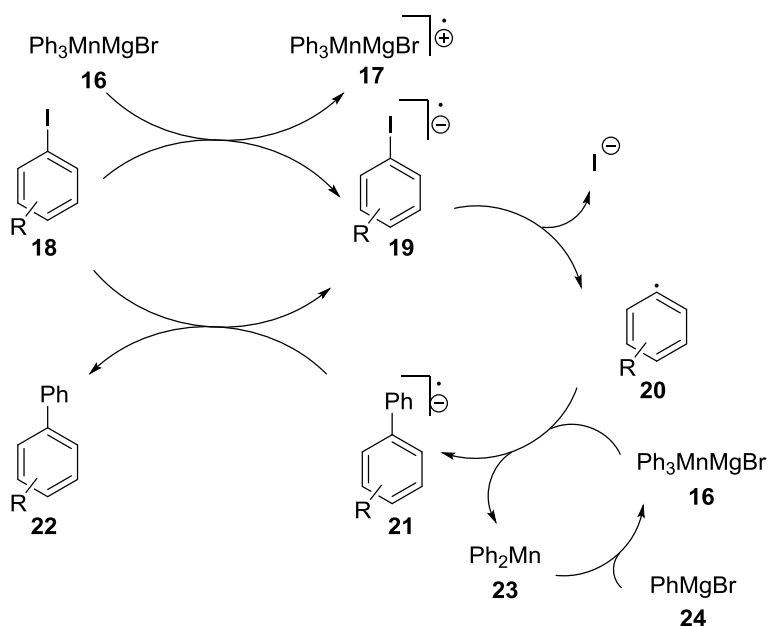
Hence *p*-iodotoluene, phenylmagnesium bromide, and ten equivalents of 1,4-cyclohexadiene were subjected to the general procedure and the progress of the reaction was monitored by GC (Scheme 3.37, a). The process afforded only 7% yield of *p*-methylbiphenyl while the dehalogenation product was obtained in 56% yield indicating the possibility of an aryl radical being involved in the reaction.



**Scheme 3.37.** Aryl radical trapping experiments with a) 1,4-cyclohexadiene, b) 2-(allyloxy)-1-bromo-4-methylbenzene, and c) 4-(2-bromophenyl)-but-1-ene.

A further useful radical trap experiment that could be conducted in this case concerned the employment of an aryl halide bearing alkenyl group or allyl ether in

the *ortho* position. This type of compounds is known to give unimolecular ring-closure mostly by *exo*-mode under radical conditions.<sup>194,195</sup> For this reason it was decided to run an experiment employing 2-(allyloxy)-1-bromo-4-methylbenzene and 4-(2-bromophenyl)-but-1-ene as the radical scavengers. In particular the result we expected in case of a radical reaction was the formation of cyclization products at the expense of the cross-coupling product. In the first case the reaction with phenylmagnesium bromide under the optimized conditions resulted in a mixture of three compounds **8-10**. These were formed by decomposition of 2-(allyloxy)-1-bromo-4-methylbenzene which were detected by GC but not quantified (Scheme 3.37, b). In the second case the reaction between 4-(2-bromophenyl)-but-1-ene and phenylmagnesium bromide furnished the cyclization product **11** in 23% yield (Scheme 3.37, c). Olefins **12** and **13** were also generated from the radical trap experiment in a 8% and 10% yield, respectively, and this can be explained by the ease with which the formed radicals are trapped by the solvent.<sup>196</sup> Moreover only 5% of the cross-coupling product **14** was obtained in addition to 13% of the dehalogenation product **15**. This result may give further confirmation of the involvement of an aryl radical in the process. Together, these outcomes suggested the same  $S_{RN}1$  mechanism as in the previously reported cross-couplings with chlorobenzonitriles (Scheme 3.38).<sup>187</sup>



**Scheme 3.38.** Proposed mechanism for cross-coupling reaction catalyzed by  $\text{MnCl}_2$ .

Triphenylmanganate complex **16** is believed to be the radical initiator for the cross-coupling reaction here reported. It is known from the literature that it mediates radical processes<sup>197</sup> and can be formed very easily from  $\text{MnCl}_2$  and phenylmagnesium bromide.<sup>149</sup> An electron transfer from complex **16** to the aryl halide **18** results in the radical anion **19**. This subsequently loses the halide generating the aryl radical **20** which undergoes a reaction with triphenylmanganate complex **16** thus producing a biphenyl radical anion **21**. Triphenylmanganate complex **16** is a softer nucleophile than a Grignard reagent<sup>149</sup> and according to the reaction mechanism previously suggested in our group,<sup>187</sup> it is most likely the only nucleophile which acts in the mechanism.

The consequent ET from the biphenyl radical anion **21** to the aryl halide affords the heterocoupling product **22** and closes the catalytic cycle.



### 3.6 Conclusion

The purpose of this work was to extend the cross-coupling reaction catalyzed by 10 mol% of  $\text{MnCl}_2$  to aryl halides other than *o*-/*p*-chlorobenzonitriles. This was achieved when the reaction was conducted with a 3 M solution of phenylmagnesium bromide in  $\text{Et}_2\text{O}$  at 120 °C in a microwave oven. The scope of the coupling was expanded to a short variety of substituted aryl halides. The corresponding heterocoupling products were obtained in low to good yields. In general, methyl substituted aryl halides gave the best yields demonstrating that the reaction remains limited to these substrates. Additional limitations of the reaction are represented by collateral processes as the dehalogenation of the aryl halide and the homocoupling of the Grignard reagent which are responsible of lowering the yield of the heterocoupling products. Moreover, the mechanistic profile of the reaction was studied. The use of trapping agents as 1,4-cyclohexadiene as well as 4-(2-bromophenyl)-but-1-ene indicated the involvement of an aryl radical during the reaction. This result suggested that the cross-coupling studied here between the aryl halide and phenylmagnesium bromide under the studied conditions possibly undergo a radical nucleophilic aromatic substitution ( $\text{S}_{\text{RN}}1$ ).

### 3.7 Experimental section

#### General methods

All the reactions were performed in Biotage microwave reactor and monitored by gas chromatography on a Shimadzu GCMS-QP2012S instrument equipped with an Equity-5, 30 × 0.25mm × 0.25µm column. Decane was used as the internal standard and GC yields were determined with the following equation i).

$$i) y(\%) = \left( \frac{A_p}{A_0} \cdot \frac{m_0}{MW_0} \cdot \frac{MW_s}{m_s} \cdot k \cdot 100 \right)$$

Where  $A_p$  = product peak's area,  $A_0$  = standard peak's area,  $m_0$  = mass (mg) of the internal standard in the reaction mixture,  $MW_0$  = molecular weight of the internal standard,  $m_s$  = mass (mg) of the initial substrate,  $MW_s$  = molecular weight of the initial substrate,  $k$  = value extrapolated by the product's calibration curve. All chemicals were purchased from Sigma-Aldrich and ABCR and used without further purifications. Thin layer chromatography (TLC) was performed on aluminum sheets precoated with silica gel (Merck 25, 20 X 20 cm, 60 F<sub>254</sub>). The plates were visualized under UV-light.

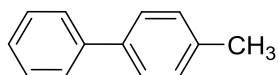
Flash column chromatography was performed on silica gel 60 (40 – 63 µm) with specified solvents given as volume ratio. NMR spectra were recorded on a Bruker Ascend 400 spectrometer. Chemical shifts were measured relative to the signals of residual  $\text{CHCl}_3$  ( $\delta_{\text{H}} = 7.26$  ppm) and  $\text{CDCl}_3$  ( $\delta_{\text{C}} = 77.16$  ppm). Multiplicity are reported as s = singlet, d = doublet, t = triplet, q = quartet, dd = double doublet, dt = double triplet, dq = double quartet, ddt = double double triplet, s = sextet, m = multiplet, br. s = broad singlet, while coupling constants are shown in Hz.

#### General procedure for cross-coupling catalyzed by $\text{MnCl}_2$

$\text{MnCl}_2$  (25 mg, 0.2 mmol) was placed in a predried microwave vial (with a liquid volume allowance between 0.5 mL and 2 mL) equipped with a magnetic stirrer and

then sealed with a rubber septum. The vial was evacuated and refilled three times with nitrogen through a syringe. The aryl halide (2 mmol) and decane (1 mmol, internal standard) were placed in the vial followed by addition of 3 M phenylmagnesium bromide (4 mmol) in diethyl ether under a flow of nitrogen. The reaction vial was sealed with a cap and placed in the microwave reactor at 120 °C for 5 h. The mixture was quenched with a saturated solution of ammonium chloride. The phases were separated and the aqueous phase extracted with diethyl ether (3 x 5 mL). The combined organic phases were dried over Na<sub>2</sub>SO<sub>4</sub>, filtered and evaporated *in vacuo* to give the crude product, which were purified by flash chromatography eluting with pentane or pentane containing 0.5 – 10% EtOAc.

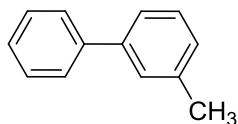
#### 4-Methyl-1,1'-biphenyl



Prepared from *p*-iodotoluene and phenylmagnesium bromide according to the general procedure. The residue was purified by flash column chromatography eluting with pentane to yield a mixture of biphenyl and 4-methyl-1,1'-biphenyl. The yield of the latter was determined by a <sup>1</sup>H-NMR.

<sup>1</sup>H NMR (400 MHz, CDCl<sub>3</sub>): δ = 7.52-7.49 (m, 2H), 7.42-7.32 (m, 4H), 7.28-7.21 (m, 1 H), 7.18-7.14 (m, 2 H), 2.31 (s, 3 H) ppm. <sup>13</sup>C NMR (100 MHz, CDCl<sub>3</sub>): δ = 141.3, 138.5, 137.1, 129.6, 128.8, 127.1, 127.1, 21.2 ppm. MS (m/z) 168.00 [M]<sup>+</sup>. The observed chemical shifts are in accordance with the literature values.<sup>198</sup>

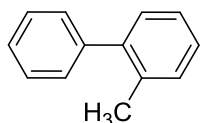
### 3-Methyl-1,1'-biphenyl



Prepared from *m*-iodotoluene and phenylmagnesium bromide according to the general procedure. The residue was purified by flash column chromatography eluting with pentane to yield a mixture of biphenyl and 3-methyl-1,1'-biphenyl. The yield of the latter was determined by a  $^1\text{H-NMR}$  spectrum.

$^1\text{H NMR}$  (400 MHz,  $\text{CDCl}_3$ ):  $\delta = 7.62\text{-}7.59$  (m, 2 H),  $7.48\text{-}7.33$  (m, 6 H),  $7.19\text{-}7.17$  (m, 1 H),  $2.44$  (s, 3 H) ppm.  $^{13}\text{C NMR}$  (100 MHz,  $\text{CDCl}_3$ ):  $\delta = 141.5, 141.4, 138.5, 128.8, 128.8, 128.1, 127.3, 124.4, 21.7$  ppm. MS ( $m/z$ )  $168.05$   $[\text{M}]^+$ . The observed chemical shifts are in accordance with the literature values.<sup>198</sup>

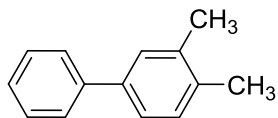
### 2-Methyl-1,1'-biphenyl



Prepared from *o*-iodotoluene and phenylmagnesium bromide according to the general procedure. The residue was purified by flash column chromatography eluting with pentane to yield a mixture of biphenyl and 2-methyl-1,1'-biphenyl. The yield of the latter was determined by a  $^1\text{H-NMR}$  spectrum.

$^1\text{H NMR}$  (400 MHz,  $\text{CDCl}_3$ ):  $\delta = 7.46\text{-}7.40$  (m, 2 H),  $7.37\text{-}7.32$  (m, 3 H),  $7.28\text{-}7.23$  (m, 4 H),  $2.28$  (s, 3 H) ppm.  $^{13}\text{C NMR}$  (100 MHz,  $\text{CDCl}_3$ ):  $\delta = 142.1, 142.1, 135.5, 130.4, 129.9, 129.3, 128.2, 127.3, 126.9, 125.9, 20.69$  ppm. MS  $m/z$   $168.05$   $[\text{M}]^+$ . The observed chemical shifts are in accordance with the literature values.<sup>199</sup>

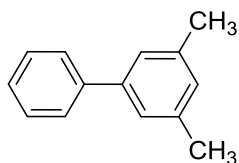
### 3,4-Dimethyl-1,1'-biphenyl



Prepared from 1-iodo-3,4-dimethylbenzene and phenylmagnesium bromide according to the general procedure. The residue was purified by flash column chromatography eluting with pentane to yield the desired product as a colorless oil (75%).

$^1\text{H}$  NMR (400 MHz,  $\text{CDCl}_3$ ):  $\delta$  = 7.60-7.58 (m, 2 H), 7.45-7.39 (m, 3 H), 7.36-7.31 (m, 2 H), 7.22 (d,  $J$  = 7.7 Hz 1H), 2.35 (s, 3 H), 2.32 (s, 3 H) ppm.  $^{13}\text{C}$  NMR (100 MHz,  $\text{CDCl}_3$ ):  $\delta$  = 141.4, 139.0, 137.0, 135.8, 130.2, 128.8, 128.6, 127.1, 127.0, 124.6, 20.1, 19.6 ppm. MS  $m/z$  182.00  $[\text{M}]^+$ . The observed chemical shifts are in accordance with the literature values.<sup>200</sup>

### 3,5-Dimethyl-1,1'-biphenyl

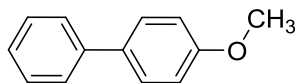


Prepared from 1-iodo-3,5-dimethylbenzene and phenylmagnesium bromide according to the general procedure. The residue was purified by flash column chromatography eluting with pentane to yield a mixture of biphenyl and 3,5-methyl-1,1'-biphenyl. The yield of the latter was determined by a  $^1\text{H}$ -NMR spectrum.

$^1\text{H}$  NMR (400 MHz,  $\text{CDCl}_3$ ):  $\delta$  = 7.63-7.59 (m, 2 H), 7.49-7.43 (m, 2 H), 7.39-7.33 (m, 2 H), 7.24 (br s, 1 H), 2.41 (s, 6 H) ppm.  $^{13}\text{C}$  NMR (100 MHz,  $\text{CDCl}_3$ ):  $\delta$  = 141.6, 141.4, 138.4, 129.0, 128.8, 127.3, 127.2, 125.2, 21.6 ppm. MS  $m/z$  182.00  $[\text{M}]^+$ .

The observed chemical shifts are in accordance with the literature values.<sup>198</sup>

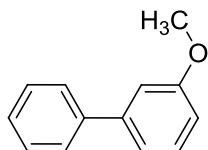
### 4-Methoxy-1,1'-biphenyl



Prepared from *p*-iodoanisole and phenylmagnesium bromide according to the general procedure. The residue was purified by flash column chromatography eluting with pentane/ ethyl acetate (10:0.05 v/v) to yield the desired product as a white solid (23%).

<sup>1</sup>H NMR (400 MHz, CDCl<sub>3</sub>):  $\delta$  = 7.57-7.52 (m, 4 H), 7.44-7.40 (m, 2 H), 7.33-7.28 (m, 1 H), 7.00-6.97 (m, 2 H), 3.86 (s, 3 H) ppm. <sup>13</sup>C NMR (100 MHz, CDCl<sub>3</sub>):  $\delta$  = 159.3, 141.0, 133.9, 128.9, 128.3, 126.9, 126.8, 114.3, 55.5 ppm. MS m/z 184.00 [M]<sup>+</sup>. The observed chemical shifts are in accordance with the literature values.<sup>198</sup>

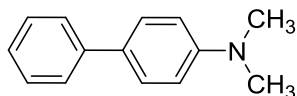
### 3-Methoxy-1,1'-biphenyl



Prepared from 3-iodoanisole and phenylmagnesium bromide according to the general procedure. The residue was purified by flash column chromatography eluting with pentane/ ethyl acetate (10:0.05 v/v) to yield the desired product as a white solid (26%).

<sup>1</sup>H NMR (400 MHz, CDCl<sub>3</sub>):  $\delta$  = 7.61-7.58 (m, 2 H), 7.46-7.42 (m, 2 H), 7.38-7.33 (m, 2 H), 7.20-7.18 (m, 1 H), 7.14-7.13 (m, 1 H), 6.92-6.89 (m, 1 H), 3.87 (s, 3 H) ppm. <sup>13</sup>C NMR (100 MHz, CDCl<sub>3</sub>):  $\delta$  = 160.1, 142.9, 141.3, 128.9, 128.9, 127.6, 127.3, 119.8, 113.0, 112.8, 55.5 ppm. MS m/z 184.00 [M]<sup>+</sup>. The observed chemical shifts are in accordance with the literature values.<sup>199</sup>

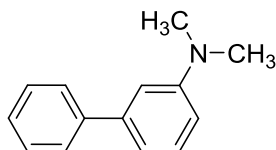
### N,N-Dimethyl[1,1'-biphenyl]-4-amine



Prepared from *p*-bromo-N,N-dimethylaniline and phenylmagnesium bromide according to the general procedure. The residue was purified by flash column chromatography eluting with pentane/ ethyl acetate (10:1 v/v) to yield the desired product as a white solid (28%).

<sup>1</sup>H NMR (400 MHz, CDCl<sub>3</sub>):  $\delta$  = 7.59-7.52 (m, 4 H), 7.43-7.39 (m, 2 H), 7.29-7.25 (m, 1 H), 6.84-6.82 (m, 2 H), 3.01 (s, 6 H) ppm. <sup>13</sup>C NMR (100 MHz, CDCl<sub>3</sub>):  $\delta$  = 150.1, 141.3, 128.8, 127.9, 126.4, 126.1, 113.0, 40.8 ppm. MS m/z 197.00 [M]<sup>+</sup>. The observed chemical shifts are in accordance with the literature values.<sup>201</sup>

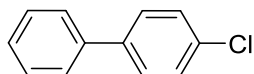
### N,N-Dimethyl[1,1'-biphenyl]-3-amine



Prepared from *m*-bromo-N,N-dimethylaniline and phenylmagnesium bromide according to the general procedure. The residue was purified by flash column chromatography eluting with pentane/ ethyl acetate (10:1 v/v) to yield the desired product as a colorless oil (33%).

<sup>1</sup>H NMR (400 MHz, CDCl<sub>3</sub>):  $\delta$  = 7.64-7.61 (m, 2 H), 7.47-7.44 (m, 2 H), 7.38-7.32 (m, 2 H), 7.00-6.97 (m, 2 H), 6.80-6.77 (m, 1 H), 3.03 (s, 6 H) ppm. <sup>13</sup>C NMR (100 MHz, CDCl<sub>3</sub>):  $\delta$  = 151.1, 142.4, 142.4, 129.5, 128.7, 127.5, 127.2, 116.1, 111.8, 111.8, 40.9. MS m/z 197.05 [M]<sup>+</sup>. The observed chemical shifts are in accordance with the literature values.<sup>202</sup>

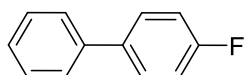
#### 4-Chloro-1,1'-biphenyl



Prepared from 1-chloro-4-iodobenzene and phenylmagnesium bromide according to the general procedure. The residue was purified by flash column chromatography eluting with pentane to yield the desired product as a white solid (13%).

$^1\text{H}$  NMR (400 MHz,  $\text{CDCl}_3$ ):  $\delta$  = 7.58-7.51 (m, 4 H), 7.48-7.36 (m, 5 H) ppm.  $^{13}\text{C}$  NMR (100 MHz,  $\text{CDCl}_3$ ):  $\delta$  = 140.1, 139.8, 133.5, 129.0, 129.0, 128.5, 127.7, 127.1 ppm. MS  $m/z$  187.90  $[\text{M}]^+$ . The observed chemical shifts are in accordance with the literature values.<sup>203</sup>

#### 4-Fluoro-1,1'-biphenyl



Prepared from *p*-fluoroiodobenzene and phenylmagnesium bromide according to the general procedure. The residue was purified by flash column chromatography, eluting with pentane to yield the desired product as a white solid (6%).

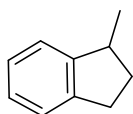
$^1\text{H}$  NMR (400 MHz,  $\text{CDCl}_3$ ):  $\delta$  = 7.58-7.54 (m, 4 H), 7.47-7.43 (m, 2 H), 7.38-7.34 (m, 1 H), 7.17-7.11 (m, 2 H) ppm.  $^{13}\text{C}$  NMR (100 MHz,  $\text{CDCl}_3$ ):  $\delta$  = 162.60 (d,  $J$  = 246.2 Hz), 140.39, 137.47 (d,  $J$  = 3.3 Hz), 128.95, 128.82 (d,  $J$  = 8.1 Hz), 127.39, 127.16, 115.85 (d,  $J$  = 21.3 Hz) ppm. MS  $m/z$  172.05  $[\text{M}]^+$ . The observed chemical shifts are in accordance with the literature values.<sup>198</sup>



### Radical clock experiment in Scheme 3.37

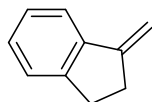
Commercially available 4-(2-bromophenyl)-but-1-ene was treated with  $\text{MnCl}_2$  and phenylmagnesium bromide as described above in the general procedure to afford an inseparable mixture of compounds **4** – **6** and **8** which were characterized by NMR and the yield determined with an internal standard. In addition, compound **7** was isolated as a mixture with biphenyl and again characterized by NMR.

#### 1-Methylindan (**4**)



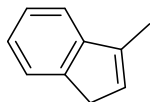
$^1\text{H}$  NMR (400 MHz,  $\text{CDCl}_3$ ):  $\delta$  = 7.53–7.12 (m, 4 H), 3.20 (sextet,  $J$  = 7.2 Hz, 1 H), 3.02–2.79 (m, 2 H), 2.36–2.28 (m, 1 H), 1.66–1.57 (m, 1 H), 1.31 (d,  $J$  = 6.9 Hz, 3 H) ppm.  $^{13}\text{C}$  NMR (100 MHz,  $\text{CDCl}_3$ ):  $\delta$  = 148.9, 144.0, 128.4, 126.2, 124.5, 123.3, 39.6, 34.9, 31.6, 20.0 ppm. MS:  $m/z$  = 132.05  $[\text{M}]^+$ . The observed chemical shifts are in accordance with the literature values.<sup>204</sup>

#### 1-Methyleneindan (**5**)



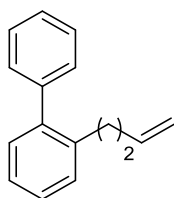
$^1\text{H}$  NMR (400 MHz,  $\text{CDCl}_3$ ):  $\delta$  = 7.53–7.12 (m, 4 H), 5.47 (t,  $J$  = 2.6 Hz, 1 H), 5.09–5.08 (m, 1 H), 3.02–2.98 (m, 2 H), 2.93–2.79 (m, 2 H) ppm.  $^{13}\text{C}$  NMR (100 MHz,  $\text{CDCl}_3$ ):  $\delta$  = 150.7, 146.9, 141.2, 128.4, 126.5, 125.5, 120.7, 102.6, 31.3, 30.2 ppm. The observed chemical shifts are in accordance with the literature values.<sup>205</sup>

### 3-Methyl-1*H*-indene (6)



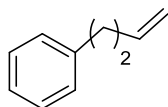
$^1\text{H}$  NMR (400 MHz,  $\text{CDCl}_3$ ):  $\delta$  = 7.53–7.12 (m, 4 H), 6.22–6.21 (m, 1 H), 3.34–3.33 (m, 2 H), 2.20–2.18 (m, 3 H) ppm.  $^{13}\text{C}$  NMR (100 MHz,  $\text{CDCl}_3$ ):  $\delta$  = 146.2, 144.5, 140.1, 128.9, 126.2, 124.6, 123.7, 119.0, 37.8, 13.2 ppm. The observed chemical shifts are in accordance with the literature values.<sup>205</sup>

### 2-(But-3-en-1-yl)-1,1'-biphenyl (7)



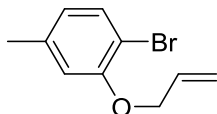
$^1\text{H}$  NMR (400 MHz,  $\text{CDCl}_3$ ):  $\delta$  = 7.63–7.24 (m, 9 H), 5.73 (ddt,  $J$  = 16.9, 10.2, 6.6 Hz, 1 H), 4.94 (q,  $J$  = 1.7 Hz, 1 H), 4.91–4.89 (m, 1 H), 2.72–2.68 (m, 2 H), 2.26–2.20 (m, 2 H) ppm.  $^{13}\text{C}$  NMR (100 MHz,  $\text{CDCl}_3$ ):  $\delta$  = 142.1, 142.0, 139.4, 138.3, 130.2, 129.3, 128.2, 127.5, 126.9, 125.9, 114.8, 35.3, 32.7 ppm. MS:  $m/z$  = 208.00  $[\text{M}]^+$ . The observed chemical shifts are in accordance with the literature values.<sup>206</sup>

### 4-Phenyl-1-butene (8)



$^1\text{H}$  NMR (400 MHz,  $\text{CDCl}_3$ ):  $\delta$  = 7.53–7.12 (m, 5 H), 5.88 (ddt,  $J$  = 16.9, 10.2, 6.6 Hz, 1 H), 5.05–5.04 (m, 1 H), 5.00 (dd,  $J$  = 10.2, 1.6 Hz, 1 H), 2.75–2.71 (m, 2 H), 2.42–2.37 (m, 2 H) ppm.  $^{13}\text{C}$  NMR (100 MHz,  $\text{CDCl}_3$ ):  $\delta$  = 142.0, 138.2, 128.6, 126.2, 125.9, 115.0, 35.7, 35.5 ppm. MS:  $m/z$  = 132.05  $[\text{M}]^+$ . The observed chemical shifts are in accordance with the literature values.<sup>207</sup>

## 2-(Allyloxy)-1-bromo-4-methylbenzene



Prepared from 2-bromo-5-methylphenol and allyl bromide, according to the procedure found in literature.<sup>8</sup> The residue was purified by flash column chromatography, eluting with hexane/ ethyl acetate (35:1 v/v) to yield the desired product as a colorless oil (71%).

<sup>1</sup>H NMR (400 MHz, CDCl<sub>3</sub>):  $\delta$  = 7.40 (d,  $J$  = 8.0 Hz, 1 H), 6.72-6.71 (m, 1 H), 6.67-6.65 (m, 1 H), 6.08 (ddt,  $J$  = 17.2, 10.3, 5.0 Hz, 1 H), 5.50 (dq,  $J$  = 17.2, 1.7 Hz, 1 H), 5.32 (dq,  $J$  = 10.6, 1.5 Hz, 1 H), 4.59 (dt,  $J$  = 5.0, 1.7 Hz, 2 H), 2.31 (s, 3 H) ppm. <sup>13</sup>C NMR (100 MHz, CDCl<sub>3</sub>):  $\delta$  = 154.7, 138.7, 133.0, 132.8, 122.9, 117.7, 114.7, 109.0, 69.7, 21.5 ppm. MS:  $m/z$  = 225.85 [M]<sup>+</sup>. HRMS calcd. for C<sub>10</sub>H<sub>12</sub>BrO [MH<sup>+</sup>]: 227.0066, found: 227.0034.

## 4 Study of the dehydrogenative synthesis of imines from primary alcohols and amines catalyzed by manganese complexes

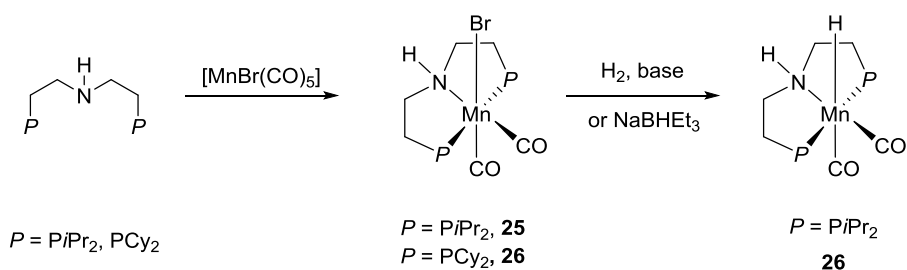
---

The present chapter describes the dehydrogenative formation of imines catalyzed by manganese. This project was done during the last month of my PhD, and it is a middle ground between the two works previously reported in chapter 2 and 3. In fact, the importance of the acceptorless dehydrogenation reaction to generate oxidized species and dihydrogen is now combined with the potentials of manganese as a catalyst in order to make catalysis in this field more sustainable. In the following, a brief introduction is presented to illustrate the very recent developments in the dehydrogenation reactions catalyzed by manganese, as well as a preliminary study of the reaction I conducted which is currently under further investigation in our research group.

### 4.1 Introduction

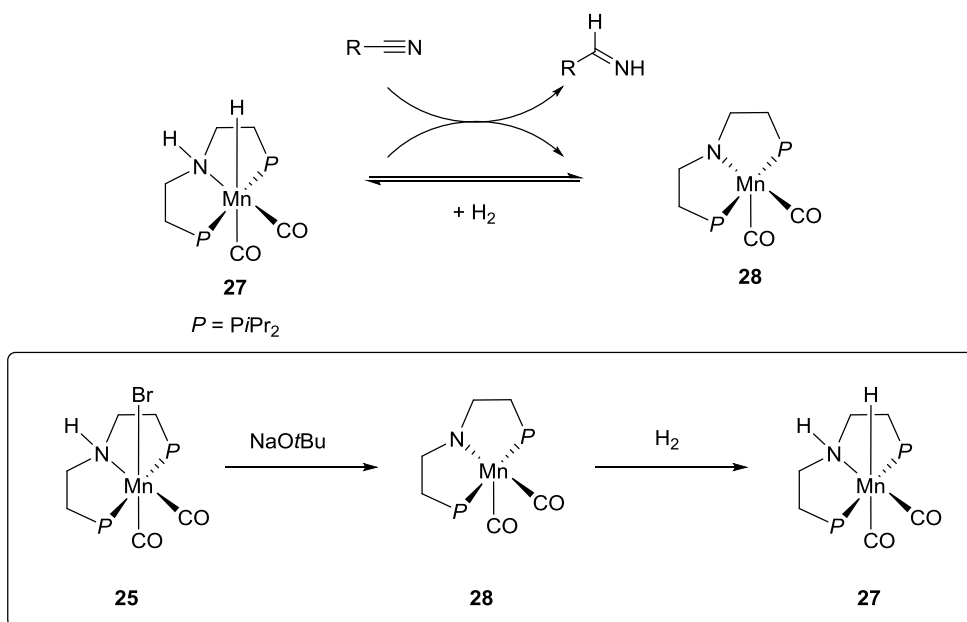
As previously mentioned, lately research in catalysis has been focusing the attention on exploring new eco-friendly metal catalysts to replace the expensive and toxic metal complexes based on palladium, platinum, and rhodium. Manganese has gained particular consideration during this period as it is the third most abundant transition metal in the Earth's crust only surpassed by iron and titanium. Very recently a number of low valent manganese pincer complexes have been applied to hydrogenation, dehydrogenation and borrowing-hydrogen reactions.<sup>208</sup> Scheme 4.1 reports the relatively easy synthesis of PNP manganese complexes **25**, **26** and **27** which have found applications in the hydrogenation of

nitriles, aldehydes and ketones.<sup>209</sup> Complexes **25** and **26** are synthesized by the reaction between the manganese carbonyl precursor  $\text{MnBr}(\text{CO})_5$  with the PNP ligand in toluene at 100 °C, while complex **27** is generated by treatment of complex **25** with sodium triethylborohydride or by treatment with a base and hydrogen.



**Scheme 4.1.** Synthesis of manganese pincer complexes **25-27**.

Typically, the reactions between complex **25** and nitriles, aldehydes, or ketones are conducted in the presence of  $\text{NaOtBu}$  or  $\text{KOtBu}$  under a hydrogen atmosphere giving rise to amines, primary alcohols, and secondary alcohols respectively in good to high yields.<sup>209</sup> Moreover, the presence of the base guarantees the formation of the deprotonated complex **28** which reversibly generates the hydride complex **27** in the presence of hydrogen (Scheme 4.2). Mechanistic investigations of the reaction with nitrile substrates suggested complex **27** and complex **28** as the catalytically active species. In fact **27** and **28** are believed to be involved in an outer-sphere mechanism where the hydride from the manganese center and the proton from the ligand nitrogen are simultaneously transferred to the nitrile. This results in the imine as the intermediate which is subsequently reduced to the amine in a second catalytic cycle.<sup>209</sup>

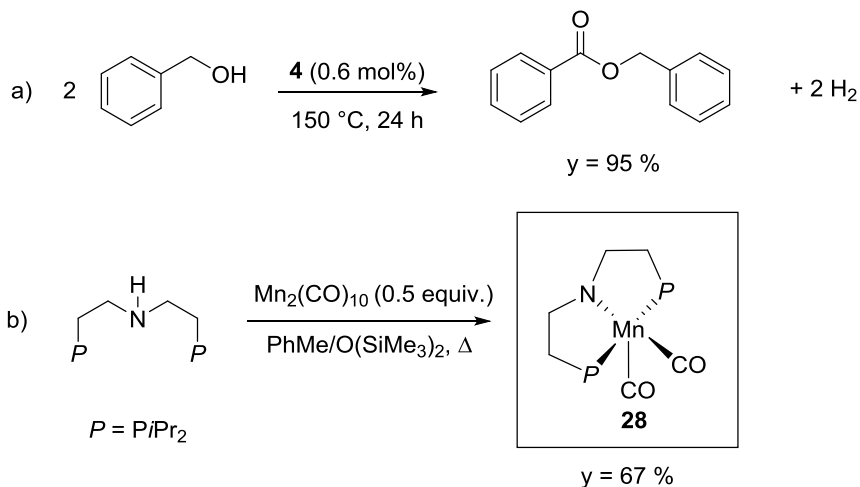


**Scheme 4.2.** Proposed outer-sphere mechanism for hydrogenative synthesis of amines from nitriles.

#### 4.1.1 Manganese-catalyzed dehydrogenation reactions of primary alcohols

Recently several interesting works have reported the dehydrogenative coupling reactions of alcohols involving different manganese complexes. In all these reactions the catalyst design plays an important role. Without questions it seems that pincer ligands are essential to ensure a high catalytic efficiency under relatively mild conditions. As an example, Gauvin and co-workers described the acceptorless dehydrogenative coupling (ADC) of a large number of primary alcohols to form the corresponding esters catalyzed by 0.6% of the PNP manganese complex **28** in good to high yields (Scheme 4.3, a).<sup>210</sup> This complex could be isolated from the reaction between  $Mn_2(CO)_{10}$  and the aliphatic  $iPr_2PNP$  ligand (Scheme 4.3, b). However, it is evident from the supporting information reported by the authors that the reaction is air sensitive since a glove box filled with argon is necessary for the addition to the primary alcohol. The

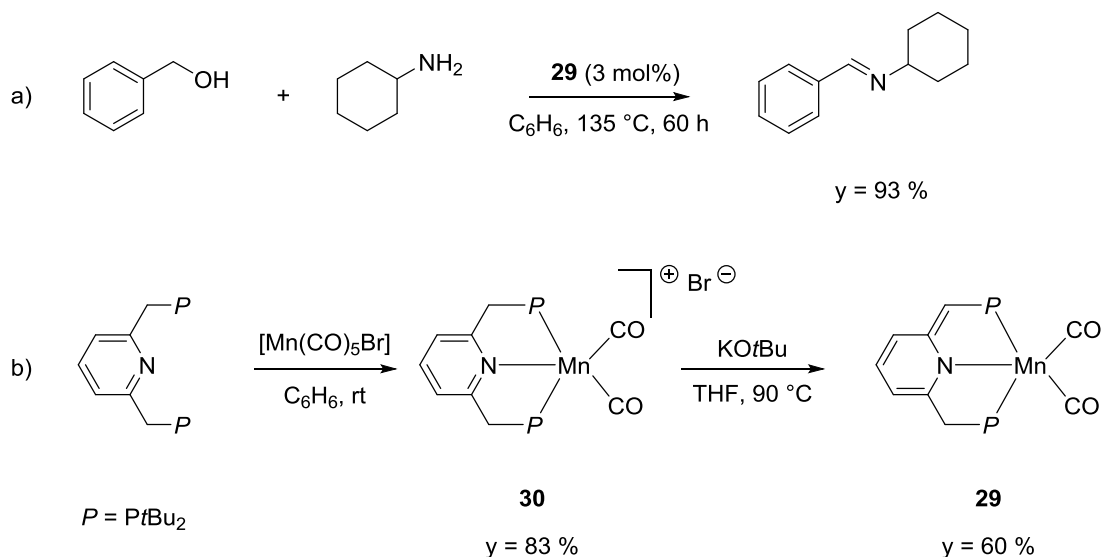
dehydrogenative synthesis of esters catalyzed by this aliphatic PNP pincer complex demonstrated sensitivity to steric properties of the alcohols, and in fact neopentyl alcohol did not show any reactivity.<sup>210</sup>



**Scheme 4.3.** a) Dehydrogenative coupling of benzyl alcohol to form benzyl benzoate; b) synthesis of complex **28**.

The possibility of synthesizing imines by dehydrogenation of primary alcohols catalyzed by a ruthenium-based complex has been already discussed in this thesis in chapter 2. This process proceeds by the formation of the aldehyde and the hemiaminal as the intermediates, leading to the formation of dihydrogen and water as the only by-products.

In 2016 Milstein and co-workers reported the catalytic activity of a PNP manganese complex towards the dehydrogenative coupling of amines and primary alcohols.<sup>211</sup> The ADC between the primary alcohols and amines reported by Milstein occurred with 3% of complex **29** at 135 °C in dry benzene over 60 h and afforded the corresponding imines in high yields (Scheme 4.4, a). The complex again can be prepared from  $[Mn(CO)_5Br]$  and the pincer ligand resulting in the cationic complex **30** which subsequently underwent treatment with  $KOtBu$  to form the actual dearomatized catalyst **29** (Scheme 4.4, b).



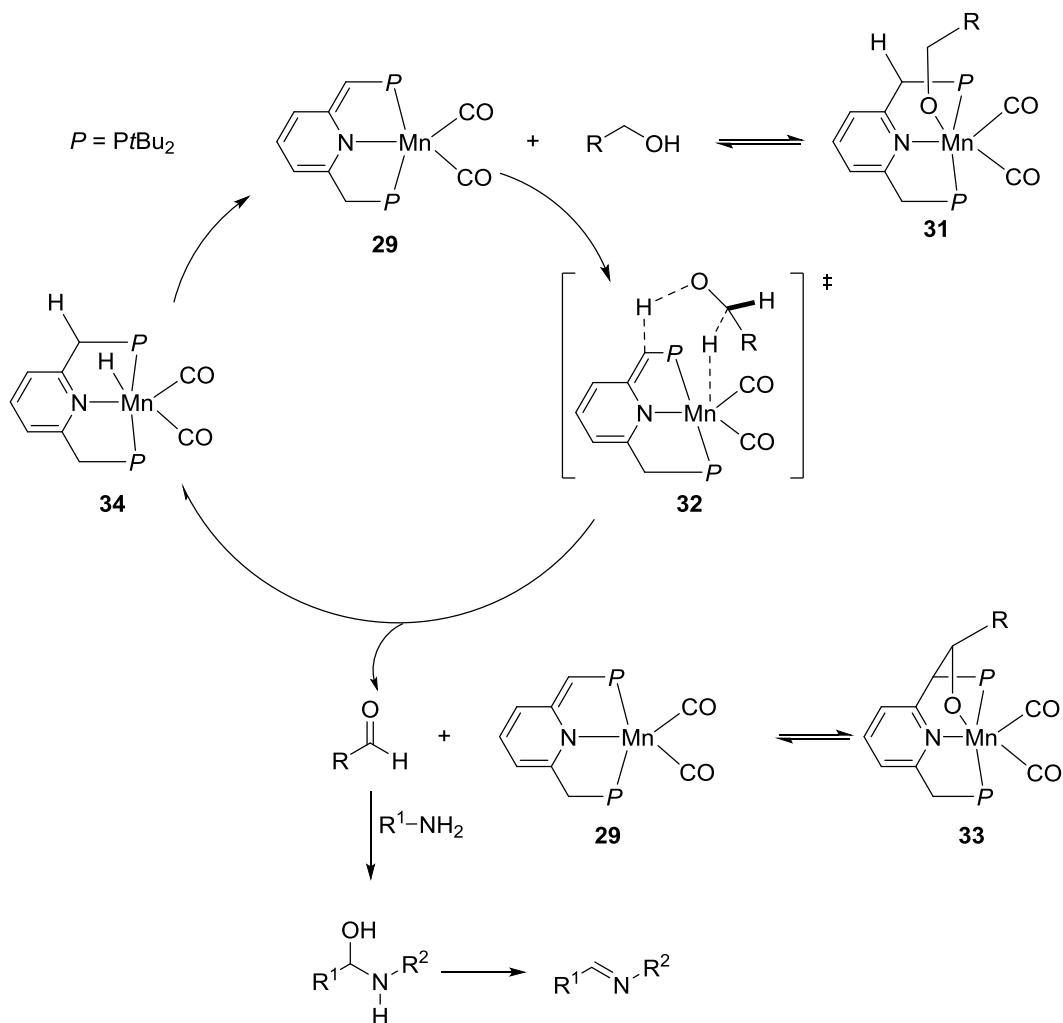
**Scheme 4.4.** a) Dehydrogenative synthesis of imines catalyzed by complex **29**; b) synthesis of the manganese PNP pincer complex **29**.

Mechanistic insights were also reported and the proposed mechanism is illustrated in Scheme 4.5.<sup>211</sup> Here the metal-ligand cooperation through dearomatization and aromatization of the ligand plays a key role in the catalytic cycle. The reaction intermediates were intercepted by proton-decoupled <sup>31</sup>P NMR spectroscopy, and this gives evidence that the primary alcohol coordinates to complex **29** affording the Mn alkoxo complex **31**. Moreover, the dehydrogenation of the alcohol which is presumed to be concerted, proceeds through a bifunctional proton and hydride transfer explained by transition state **32**. Furthermore, the dehydrogenation of the alcohol affords the aldehyde which subsequently performs an electrophilic attack on the dearomatized ligand giving rise to complex **33**. This can also be prepared independently by the reaction between complex **29** and 20 equivalents of the aldehyde.<sup>211</sup>

The aldehyde so produced is released and undergoes a reaction with the amine generating the unstable hemiaminal. This eventually loses a molecule of water to



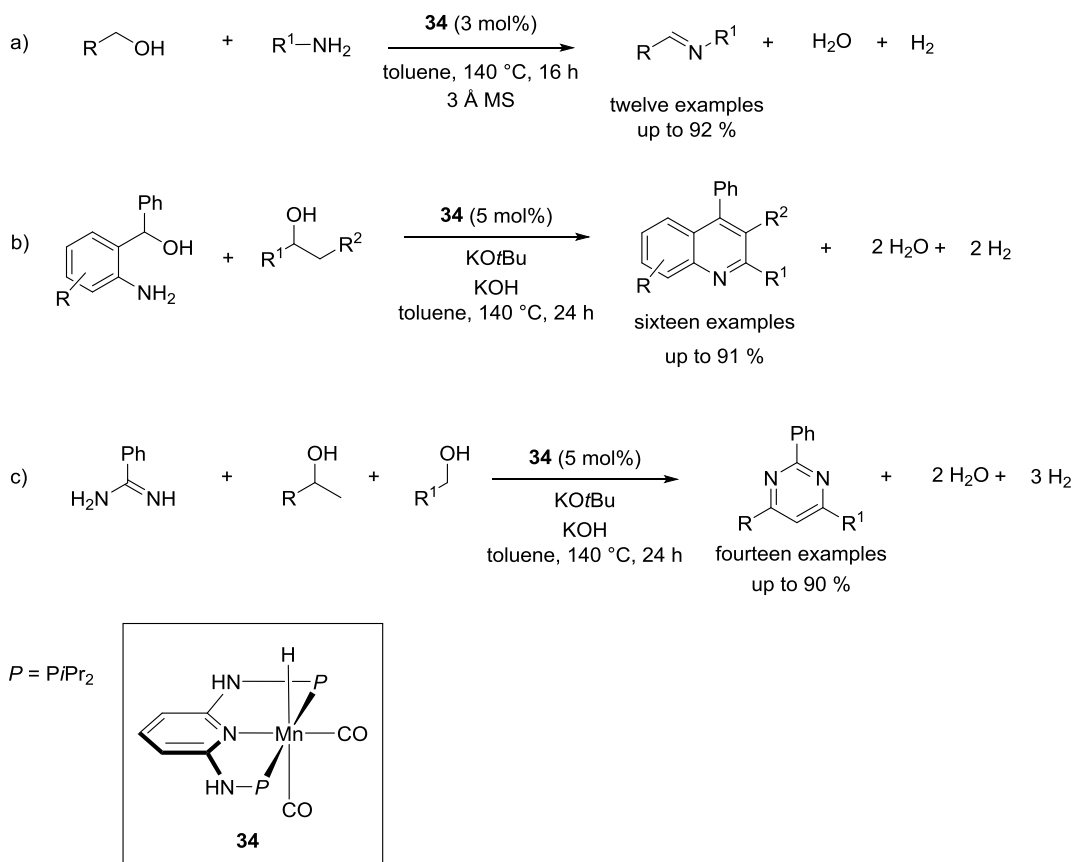
form the imine product, while the active complex **29** is restored by the dihydrogen liberation from complex **34** which is then ready to reenter a new catalytic cycle.<sup>211</sup>



**Scheme 4.5.** Proposed mechanism for imine formation.

During the same year Kirchner and co-workers described the dehydrogenative condensation of primary alcohols and amines catalyzed by 3% of a hydride manganese PNP complex, **34**.<sup>212</sup> In this case, the reaction was conducted in a closed vial in toluene at 140 °C with 3 Å molecular sieves for 16 h, affording the

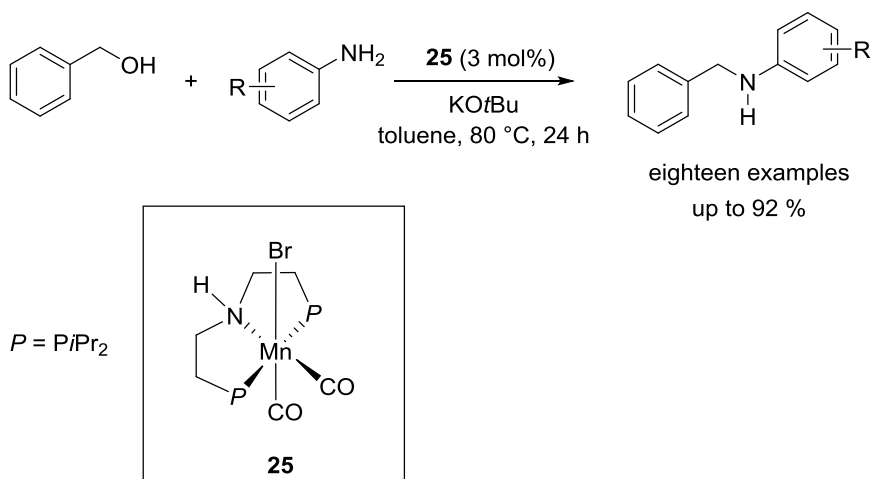
imine products in good to high yield (Scheme 4.6, a). The same manganese complex was able to couple 2-amino benzyl alcohols and secondary alcohols to form quinolines or to perform a three-component pyrimidine synthesis by coupling benzamidine with primary and secondary alcohols (Scheme 4.6, b, c).<sup>213</sup>



**Scheme 4.6.** Synthesis of a) imines, b) quinolines, c) pyrimidines as reported by Kirchner.

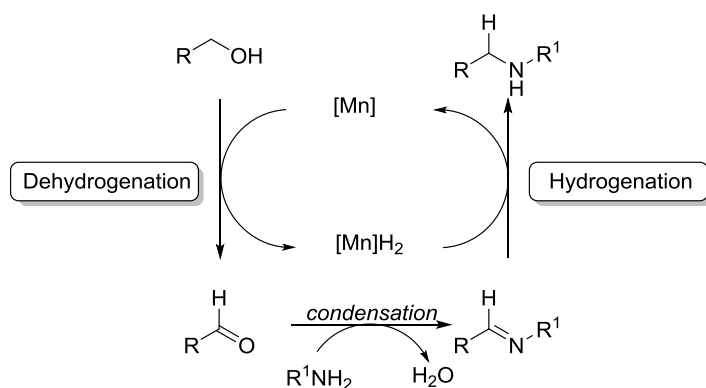
As mentioned in chapter 2 the hydrogen liberated from the dehydrogenation reactions can be used for direct hydrogenation of an unsaturated molecule in the reaction mixture. A useful application of a dehydrogenation-hydrogenation cascade can be found for example in the formation of C-N bonds. In 2016 Beller and his group reported the alkylation of an amine with several primary alcohols

catalyzed by the manganese PNP complex **25** through a hydrogen auto-transfer methodology (Scheme 4.7).<sup>214</sup>



**Scheme 4.7.** *N*-Alkylation of various amines with benzyl alcohol reported by Beller and co-workers.

The reaction proceeds through an initial dehydrogenation of the primary alcohol to the aldehyde intermediate, which undergoes a condensation with the amine resulting in the imine. The latter is hydrogenated by the manganese catalyst using the borrowed hydrogen thus generating the final amine (Scheme 4.8).<sup>214</sup>



**Scheme 4.8.** General scheme of dehydrogenation-hydrogenation for the *N*-alkylation of amines catalyzed by manganese.

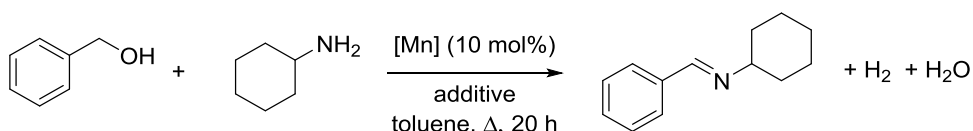
## 4.2 Conclusion

This brief introduction aimed to present the recent developments in manganese catalysis for the dehydrogenation reaction. All the low valent manganese PNP complexes presented here can be synthesized from the simplest commercially available complexes  $[\text{Mn}(\text{CO})_5\text{Br}]$  and  $\text{Mn}_2(\text{CO})_{10}$ . Consequently, it would be interesting to examine whether commercially available and simple low valent manganese complexes can exhibit catalytic activity in these transformations.

## 4.3 Results and discussion

### 4.3.1 Preliminary study

The commercially available complexes  $\text{CpMn}(\text{CO})_3$ ,  $\text{Mn}(\text{CO})_5\text{Br}$ , and  $\text{Mn}_2(\text{CO})_{10}$  were screened in order to study their reactivity towards the dehydrogenative synthesis of imines from primary alcohols and amines. Temperature, solvent and equipment were selected taking into account the previously reported work.<sup>212</sup> Thus for the initial study benzyl alcohol and cyclohexylamine were reacted with 10% of the manganese complex in degassed toluene as the solvent at 140 °C in a closed vial for 20 h, and the reaction was monitored by GC. It was ascertained that under these initial conditions  $\text{CpMn}(\text{CO})_3$  was not active and no coupling occurred between benzyl alcohol and cyclohexylamine. Interestingly, when  $\text{Mn}(\text{CO})_5\text{Br}$  and  $\text{Mn}_2(\text{CO})_{10}$  were employed, 10% and 30% of the imine product was obtained, respectively. Although the yields obtained were very low, these results encouraged further analysis of the dehydrogenation. The reaction conditions used so far were not optimal from an operative point of view, and the coupling between benzyl alcohol and cyclohexylamine was therefore attempted in a Schlenk tube to verify whether it was possible to observe the conversion of the substrates at low temperature under atmospheric pressure (Table 4.1).

**Table 4.1.** Imination reaction with  $\text{CpMn}(\text{CO})_3$ ,  $\text{Mn}(\text{CO})_5\text{Br}$ , and  $\text{Mn}_2(\text{CO})_{10}$  complexes.<sup>[a]</sup>

entry	[Mn]	additive	y [%] <sup>[b]</sup>
1	$\text{CpMn}(\text{CO})_3$	-	-
2	$\text{Mn}(\text{CO})_5\text{Br}$	-	-
3	$\text{Mn}_2(\text{CO})_{10}$	-	6
4	$\text{CpMn}(\text{CO})_3$	4Å MS	-
5	$\text{Mn}(\text{CO})_5\text{Br}$	4Å MS	6
6	$\text{Mn}_2(\text{CO})_{10}$	4Å MS	10

<sup>[a]</sup> Benzyl alcohol (1 mmol), cyclohexylamine (1 mmol), [Mn] (0.1 mmol), decane (0.5 mmol, internal standard) in 4 mL of toluene. <sup>[b]</sup> GC yield.

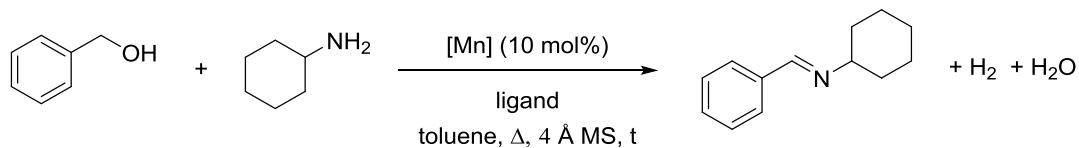
Under these conditions  $\text{CpMn}(\text{CO})_3$  and  $\text{Mn}(\text{CO})_5\text{Br}$  did not show any reactivity and benzyl alcohol and cyclohexylamine were not converted to the coupling product (entries 1-2). However, using  $\text{Mn}_2(\text{CO})_{10}$  as the catalyst afforded 6% of the desired imine (entry 3). The addition of molecular sieves to the reaction system to secure removal of water during the reaction gave a very minor improvement. In fact in this case the employment of  $\text{Mn}(\text{CO})_5\text{Br}$  and  $\text{Mn}_2(\text{CO})_{10}$  gave rise to 6% and 10% of the product, respectively (entries 5-6). Based on these outcomes  $\text{Mn}_2(\text{CO})_{10}$  and  $\text{Mn}(\text{CO})_5\text{Br}$  were further investigated along with influence of different ligands. Monodentate and bidentate phosphine ligands, as well as amine and NHC ligands were tested in different loadings (Table 4.2). The reaction was carried out first using  $\text{Mn}_2(\text{CO})_{10}$  with 20% of  $\text{PCy}_3$  and  $\text{PPh}_3$  as the ligands for 48 h (entries 1-2). Only 7% of the imine was observed in the first case, while the use of  $\text{PPh}_3$  resulted in no conversion of benzyl alcohol and the amine. The use of the bidentate phosphine ligand dppe under the reaction conditions did not improve the

imine yield considerably (entry 3). When DABCO and DMAP were tested with either  $\text{Mn}_2(\text{CO})_{10}$  and  $\text{Mn}(\text{CO})_5\text{Br}$  no conversion of the substrates was observed (entries 4-7). No conversion was also observed with the bidentate amine 2,2'-bipyridine (entries 8,9). The influence of a carbene ligand was also investigated with  $\text{Mn}_2(\text{CO})_{10}$ , but when 1,3-bis(2,6-diisopropylphenyl)imidazolium chloride was added to the reaction mixture along with  $\text{KO}^t\text{Bu}$ , no product was detected (entry 10). As shown in entry 11 and 12, pyridine and phenanthroline in combination with  $\text{Mn}(\text{CO})_5\text{Br}$  gave rise to the imine in very poor yield, 3% and 4% respectively. For  $\text{Mn}(\text{CO})_5\text{Br}$  the best result was achieved with 2-pyridinemethanol, and in this case 23% yield of the imine was observed (entry 13). Interestingly, when the coupling between benzyl alcohol and cyclohexylamine was performed in the presence of *N,N*-bis(salicylidene)ethylenediamine, also known as salen, and  $\text{Mn}_2(\text{CO})_{10}$ , the yield of the reaction increased to 38% after 48 h (entry 14). However, the same ligand combined with  $\text{Mn}(\text{CO})_5\text{Br}$  showed only 15% of the imine after 68 h (entry 15).

The low yields reported in table 4.2 are attributed to the poor conversion of the substrates. No side products nor amine formation were observed during the reaction.

From Table 4.2 it is evident that the best outcome of the reaction was obtained with salen as the ligand and  $\text{Mn}_2(\text{CO})_{10}$  as the manganese complex. This result inspired an attempt to perform the dehydrogenative coupling between benzyl alcohol and cyclohexylamine with the Jacobsen complex. This is commercially available and a cheap manganese(III) complex bearing salen as the ligand.

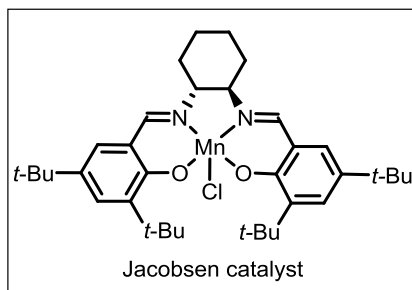
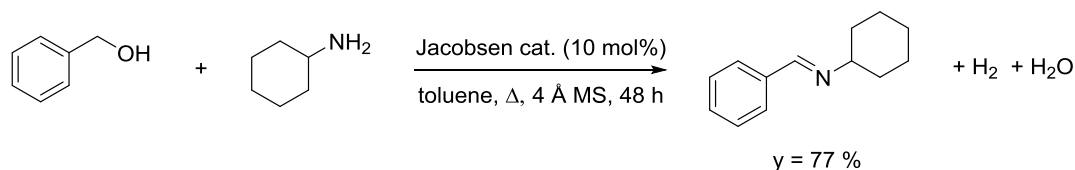
**Table 4.2.** Employment of  $\text{Mn}_2(\text{CO})_{10}$  and  $\text{Mn}(\text{CO})_5\text{Br}$  in the presence of different ligands for the imination reaction.



entry	ligand	Ligand [mol %]	[Mn]	t [h]	y [%] <sup>[b]</sup>
1	PCy <sub>3</sub>	20	$\text{Mn}_2(\text{CO})_{10}$	48	4
2	PPh <sub>3</sub>	20	$\text{Mn}_2(\text{CO})_{10}$	48	-
3	dppe	10	$\text{Mn}_2(\text{CO})_{10}$	48	7
4	DABCO	20	$\text{Mn}_2(\text{CO})_{10}$	48	-
5	DABCO	20	$\text{Mn}(\text{CO})_5\text{Br}$	68	-
6	DMAP	20	$\text{Mn}_2(\text{CO})_{10}$	48	-
7	DMAP	20	$\text{Mn}(\text{CO})_5\text{Br}$	68	-
8	2,2'-bipyridine	10	$\text{Mn}_2(\text{CO})_{10}$	48	-
9	2,2'-bipyridine	10	$\text{Mn}(\text{CO})_5\text{Br}$	68	3
10 <sup>[c]</sup>	SIPr-HCl	20	$\text{Mn}_2(\text{CO})_{10}$	48	-
11	pyridine	20	$\text{Mn}(\text{CO})_5\text{Br}$	68	3
12	phenanthroline	10	$\text{Mn}(\text{CO})_5\text{Br}$	68	4
13	2-pyridinemethanol	10	$\text{Mn}(\text{CO})_5\text{Br}$	68	23
14	<i>N,N'</i> -bis(salicylidene)ethylenediamine	10	$\text{Mn}_2(\text{CO})_{10}$	48	38
15	<i>N,N'</i> -bis(salicylidene)ethylenediamine	10	$\text{Mn}(\text{CO})_5\text{Br}$	68	15

<sup>[a]</sup> Benzyl alcohol (1 mmol), cyclohexylamine (1 mmol), [Mn] (0.1 mmol), decane (0.5 mmol, internal standard) in 4 mL of degassed toluene. <sup>[b]</sup> GC yield. <sup>[c]</sup> KO<sup>t</sup>Bu (20 mol%).

Unexpectedly when benzyl alcohol was reacted with cyclohexylamine in the presence of 10% of Jacobsen's catalyst in refluxing toluene, 77% of the imine product was afforded after 48 h (Scheme 4.9). Moreover, the reaction gave full conversion of the substrates and no side products were observed by GC.



**Scheme 4.9.** Coupling between benzyl alcohol and cyclohexylamine with Jacobsen catalyst.

A natural question which arose after this surprising result was whether the reaction proceeded through liberation of hydrogen gas. Hence, the hydrogen evolution was measured by conducting the reaction under the established conditions in a Schlenk tube connected to a burette filled with water. A total gas volume of 17.2 mL was collected corresponding to approximately 0.7 mmol which is comparable to what would be expected if the reaction is dehydrogenative, and this is therefore believed to be the case.

#### 4.4 Conclusion

A preliminary study of the dehydrogenative synthesis of an imine from a primary alcohol and an amine catalyzed by low valent manganese complexes was carried out. The results observed clearly show a low or even absent reactivity of CpMn(CO)<sub>3</sub>, Mn(CO)<sub>5</sub>Br, and Mn<sub>2</sub>(CO)<sub>10</sub> towards this reaction. The addition of ligands to the reaction mixture did not improve the outcome of the reaction, but it prompted the study of the process under the employment of the Jacobsen complex which resulted in the desired imine in 77% yield. Gas evolution confirmed that the reaction occurred through dihydrogen evolution.



The dehydrogenative synthesis of the imines catalyzed by this manganese-salen complex is under current examination by another PhD student of our research group.

## **4.5 Experimental section**

### **4.5.1 General methods**

All chemicals were obtained from Sigma-Aldrich and used without further purification. All the reactions were performed in dry and freshly degassed toluene and monitored by gas chromatography on a Shimadzu GCMS-QP2010S instrument fitted with an Equity 5, 30 m × 0.25 mm × 0.25 μm column.

### **4.5.2 General procedure for the dehydrogenative imine synthesis catalyzed by Jacobsen complex**

Jacobsen's complex (0.1 mmol) and 4 Å molecular sieves (150 mg) were placed in an oven dried Schlenk tube equipped with a cold finger. The tube was then evacuated and refilled three times with argon and charged with benzyl alcohol (1 mmol), cyclohexylamine (1 mmol), decane (0.5 mmol) as the internal standard, freshly degassed dry toluene (4 mL) and a stir bar. The reaction mixture was then refluxed for 48 h. After cooling the reaction mixture to room temperature a sample of 50 μL was withdrawn, transferred to a GC vial, diluted with 1 mL of CH<sub>2</sub>Cl<sub>2</sub> and subjected to GC-MS analysis.

### **4.5.3 Gas development**

Following the general procedure for the imination reaction, benzyl alcohol (1 mmol), cyclohexylamine (1 mmol), decane (0.5 mmol) were added to a Schlenk

tube. The tube was connected to a burette filled with water and stirred at 110 °C. The bottom of the burette was further connected to a water reservoir with a large surface area. At the end of the reaction, 17.2 mL was collected corresponding to 0.7 mmol of molecular hydrogen according to the ideal gas law.

# Publications

---

## **Dehydrogenative Synthesis of Carboxylic Acids from Primary Alcohols and Hydroxide Catalyzed by a Ruthenium N-Heterocyclic Carbene Complex.**

Carola Santilli, Ilya S.Makarov, Peter Fristrup and Robert Madsen,

*J. Org. Chem.* **2016**, *81*,9931-9938.

## **The Manganese-Catalyzed Cross-Coupling Reaction and the Influence of Trace Metals.**

Carola Santilli, Somayyeh Sarvi Beigbaghlou, Andreas Ahlburg, Giuseppe Antonacci, Peter Fristrup, Per-Ola Norrby, and Robert Madsen,

Submitted for publication in *Eur. J. Org. Chem.*

# Bibliography

---

- (1) Hartwig J. F. *Organotransition Metal Chemistry. From Bonding to Catalysis*; 2010.
- (2) Crabtree, R. H. *The organometallic chemistry of the transition metals*; Wiley, 2009.
- (3) Kurosawa, H.; Yamamoto, A. *Fundamentals of molecular catalysis*; Elsevier, 2003.
- (4) Jahn, U. *Top. Curr. Chem.*; 2011; 320, 121–189.
- (5) Parsons, A. F. *An introduction to free-radical chemistry*; Blackwell Science, 2000.
- (6) Studer, A.; Curran, D. P. *Angew. Chem. Int. Ed.* **2016**, 55 (1), 58–102.
- (7) Venning, A. R. O.; Bohan, P. T.; Alexanian, E. J. *J. Am. Chem. Soc.* **2015**, 137 (11), 3731–3734.
- (8) Pintauer, T.; Matyjaszewski, K. *Chem. Soc. Rev.* **2008**, 37 (6), 1087-1097.
- (9) Eckenhoff, W. T.; Garrity, S. T.; Pintauer, T. *Eur. J. Inorg. Chem.* **2008**, (4), 563–571.
- (10) Cheung, H.; Tanke, R. S.; Torrence, G. P. In *Ullmann's Encyclopedia of Industrial Chemistry*; Wiley-VCH Verlag GmbH & Co. KGaA: Weinheim, Germany, 2000.
- (11) Sunley, G. J.; Watson, D. J. *Catal. Today* **2000**, 58 (4), 293–307.
- (12) Tojo, G.; Fernández, M. *Oxidation of Primary Alcohols to Carboxylic Acids A Guide to Current Common Practice*; 2007.
- (13) Heyns, K. *Liebigs Ann. Chem.* **1947**, 558, 177-187.
- (14) Maurer, P. J.; Takahata, H.; Rapoport, H. *J. Am. Chem. Soc.* **1984**, 106 (4), 1095–1098.
- (15) Venema, F. R.; Peters, J. A.; van Bekkum, H. *J. Mol. Catal.* **1992**, 77 (1), 75–85.

- (16) Heyns, K.; Paulsen, H. *Chem. Ber.* **1953**, *86* (7), 833–840.
- (17) Heyns, K.; Paulsen, H. *Angew. Chemie* **1957**, *69* (18–19), 600–608.
- (18) Heyns, K.; Paulsen, H. *Chem. Ber.* **1956**, *89* (5), 1152–1160.
- (19) Heyns, K.; Blazejowicz, L. *Tetrahedron* **1960**, *9* (1–2), 67–75.
- (20) Heyns, K.; Lenz, J.; Paulsen, H. *Chem. Ber.* **1962**, *95* (12), 2964–2975.
- (21) Roberts, B. W.; Poonian, M. S.; Welch, S. C. *J. Am. Chem. Soc.* **1969**, *91* (12), 3400–3401.
- (22) Mühlman, A.; Classon, B.; Hallberg, A.; Samuelsson, B. *J. Med. Chem.* **2001**, *44* (21), 3402–3406.
- (23) Mawson, S. D.; Weavers, R. T. *Tetrahedron* **1995**, *51* (41), 11257–11270.
- (24) Nunez, M. T.; Martin, V. S. *J. Org. Chem.* **1990**, *55* (6), 1928–1932.
- (25) Chong, J. M.; Sharpless, K. B. *J. Org. Chem.* **1985**, *50* (9), 1560–1563.
- (26) Hourii, A. F.; Xu, Z.; Cogan, D. A.; Hoveyda, A. H. *J. Am. Chem. Soc.* **1995**, *117* (10), 2943–2944.
- (27) Hu, T.; Panek, J. S. *J. Am. Chem. Soc.* **2002**, *124* (38), 11368–11378.
- (28) Greenfield, A. A.; Butera, J. A.; Caufield, C. E. *Tetrahedron Lett.* **2003**, *44* (13), 2729–2732.
- (29) Lucio Anelli, P.; Biffi, C.; Montanari, F.; Quici, S. *J. Org. Chem.* **1987**, *52* (12), 2559–2562.
- (30) Zhao, M.; Li, J.; Mano, E.; Song, Z.; Tschaen, D. M.; Grabowski, E. J. J.; Reider, P. J. *J. Org. Chem.* **1999**, *64* (7), 2564–2566.
- (31) Lindgren, B. O.; Nilsson, T. *Acta Chem. Scand.* **1973**, *27*, 888–890.
- (32) Epp, J. B.; Widlanski, T. S. *J. Org. Chem.* **1999**, *64* (1), 293–295.
- (33) Gunanathan, C.; Milstein, D. *Science* **2013**, *341* (6143), 1229712.
- (34) Crabtree, R. H. *Chem. Rev.* **2017**, *117* (13), 9228–9246.
- (35) Fujita, K.; Yoshida, T.; Imori, Y.; Yamaguchi, R. *Org. Lett.* **2011**, *13* (9), 2278–2281.
- (36) Kawahara, R.; Fujita, K.-I.; Yamaguchi, R. *J. Am. Chem. Soc.* **2012**, *134* (8), 3643–3646.

- (37) Zweifel, T.; Naubron, J.-V.; Grützmacher, H. *Angew. Chem. Int. Ed.* **2009**, *48* (3), 559–563.
- (38) Cheng, J.; Zhu, M.; Wang, C.; Li, J.; Jiang, X.; Wei, Y.; Tang, W.; Xue, D.; Xiao, J. *Chem. Sci.* **2016**, *7* (7), 4428–4434.
- (39) Blum, Y.; Shvo, Y. *J. Organomet. Chem.* **1984**, *263* (1), 93–107.
- (40) Blum, Y.; Reshef, D.; Shvo, Y. *Tetrahedron Lett.* **1981**, *22* (16), 1541–1544.
- (41) Blum, Y.; Shvo, Y. *J. Organomet. Chem.* **1985**, *282* (1), C7–C10.
- (42) Conley, B. L.; Pennington-Boggio, M. K.; Boz, E.; Williams, T. J. *Chem. Rev.* **2010**, *110* (4), 2294–2312.
- (43) Comas-Vives, A.; Ujaque, G.; Lledós, A. *Organometallics* **2007**, *26* (17), 4135–4144.
- (44) Zhang, J.; Balaraman, E.; Leitius, G.; Milstein, D. *Organometallics* **2011**, *30* (21), 5716–5724.
- (45) Srimani, D.; Balaraman, E.; Gnanaprakasam, B.; Ben-David, Y.; Milstein, D. *Adv. Synth. Catal.* **2012**, *354* (13), 2403–2406.
- (46) Zhang, J.; Leitius, G.; Ben-David, Y.; Milstein, D. *J. Am. Chem. Soc.* **2005**, *127* (31), 10840–10841.
- (47) Zeng, H.; Guan, Z. *J. Am. Chem. Soc.* **2011**, *133* (5), 1159–1161.
- (48) Gnanaprakasam, B.; Balaraman, E.; Ben-David, Y.; Milstein, D. *Angew. Chem. Int. Ed.* **2011**, *50* (51), 12240–12244.
- (49) Gnanaprakasam, B.; Milstein, D. *J. Am. Chem. Soc.* **2011**, *133* (6), 1682–1685.
- (50) Gunanathan, C.; Ben-David, Y.; Milstein, D. *Science* **2007**, *317* (5839), 790–792.
- (51) Li, H.; Wang, X.; Wen, M.; Wang, Z.-X. *Eur. J. Inorg. Chem.* **2012**, (31), 5011–5020.
- (52) Gnanaprakasam, B.; Zhang, J.; Milstein, D. *Angew. Chem. Int. Ed.* **2010**, *49* (8), 1468–1471.
- (53) Kossoy, E.; Diskin-Posner, Y.; Leitius, G.; Milstein, D. *Adv. Synth. Catal.*

- 2012**, 354 (2–3), 497–504.
- (54) Gunanathan, C.; Gnanaprakasam, B.; Iron, M. A.; Shimon, L. J. W.; Milstein, D. *J. Am. Chem. Soc.* **2010**, 132 (42), 14763–14765.
- (55) Gunanathan, C.; Shimon, L. J. W.; Milstein, D. *J. Am. Chem. Soc.* **2009**, 131 (9), 3146–3147.
- (56) Gunanathan, C.; Milstein, D. *Top. Organomet. Chem.* **2011**, 37, 55–84.
- (57) Gunanathan, C.; Milstein, D. *Acc. Chem. Res.* **2011**, 44 (8), 588–602.
- (58) Balaraman, E.; Khaskin, E.; Leitius, G.; Milstein, D. *Nat. Chem.* **2013**, 5 (2), 122–125.
- (59) Li, H.; Hall, M. B. *J. Am. Chem. Soc.* **2014**, 136 (1), 383–395.
- (60) Dove, A. P.; Pratt, R. C.; Lohmeijer, B. G. G.; Li, H.; Hagberg, E. C.; Waymouth, R. M.; Hedrick, J. L. In *N-Heterocyclic Carbenes in Synthesis*; Wiley-VCH Verlag GmbH & Co. KGaA: Weinheim, Germany, 2006; pp 275–296.
- (61) Vougioukalakis, G. C.; Grubbs, R. H. *Chem. Rev.* **2010**, 110 (3), 1746–1787.
- (62) Enthaler, S.; Jackstell, R.; Hagemann, B.; Junge, K.; Erre, G.; Beller, M. *J. Organomet. Chem.* **2006**, 691 (22), 4652–4659.
- (63) Ortega, N.; Urban, S.; Beiring, B.; Glorius, F. *Angew. Chem. Int. Ed.* **2012**, 51 (7), 1710–1713.
- (64) Lund, C. L.; Sgro, M. J.; Cariou, R.; Stephan, D. W. *Organometallics* **2012**, 31 (3), 802–805.
- (65) Lee, J. P.; Ke, Z.; Ramirez, M. A.; Gunnoe, T. B.; Cundari, T. R.; Boyle, P. D.; Petersen, J. L. *Organometallics* **2009**, 28 (6), 1758–1775.
- (66) O, W. W. N.; Lough, A. J.; Morris, R. H. *Organometallics* **2011**, 30 (5), 1236–1252.
- (67) Burling, S.; Paine, B. M.; Nama, D.; Brown, V. S.; Mahon, M. F.; Prior, T. J.; Pregosin, P. S.; Whittlesey, M. K.; Williams, J. M. J. *J. Am. Chem. Soc.* **2007**, 129 (7), 1987–1995.

- (68) Fernandez, F. E.; Puerta, M. C.; Valerga, P. *Organometallics* **2012**, *31* (19), 6868–6879.
- (69) Maggi, A.; Madsen, R. *Organometallics* **2012**, *31* (1), 451–455.
- (70) Nordstrøm, L. U.; Vogt, H.; Madsen, R. *J. Am. Chem. Soc.* **2008**, *130* (52), 17672–17673.
- (71) Dam, J. H.; Osztrovszky, G.; Nordstrøm, L. U.; Madsen, R. *Chem. Eur. J.* **2010**, *16* (23), 6820–6827.
- (72) Makarov, I. S.; Fristrup, P.; Madsen, R. *Chem. Eur. J.* **2012**, *18* (49), 15683–15692.
- (73) Sølvhøj, A.; Madsen, R. *Organometallics* **2011**, *30* (21), 6044–6048.
- (74) Makarov, I. S.; Madsen, R. *J. Org. Chem.* **2013**, *78* (13), 6593–6598.
- (75) Santilli, C.; Makarov, I. S.; Fristrup, P.; Madsen, R. *J. Org. Chem.* **2016**, *81* (20), 9931–9938.
- (76) Mazziotta, A.; Makarov, I. S.; Fristrup, P.; Madsen, R. *J. Org. Chem.* **2017**, *82* (11), 5890–5897.
- (77) Netherton, M. R.; Fu, G. C. *Org. Lett.* **2001**, *3* (26), 4295–4298.
- An intramolecular Cannizzaro reaction has previously been proposed in the conversion of glycerol and trioses to lactate: (78) Pescarmona, P. P.; Janssen, K. P. F. *Green Chem.* **2010**, *12* (6), 1083. (79) Sharninghausen, L. S.; Campos, J.; Manas, M. G.; Crabtree, R. H. *Nat. Commun.* **2014**, *5*, 5084.
- (80) Walters, E. A.; Long, F. A. *J. Phys. Chem.* **1972**, *76* (3), 362–365.
- (81) Bryantsev, V. S.; Diallo, M. S.; van Duin, A. C. T.; Goddard, W. A. *J. Chem. Theory Comput.* **2009**, *5* (4), 1016–1026.
- (82) Solari, E.; Gauthier, S.; Scopelliti, R.; Severin, K. *Organometallics* **2009**, *28* (15), 4519–4526.
- (83) Dam, J. H.; Osztrovszky, G.; Nordstrøm, L. U.; Madsen, R. *Chem. Eur. J.* **2010**, *16* (23), 6820–6827.
- (84) Yuan, H.; Yoo, W.-J.; Miyamura, H.; Kobayashi, S. *J. Am. Chem. Soc.*



- 2012**, 134 (34), 13970–13973.
- (85) Kobayashi, K.; Kondo, Y. *Org. Lett.* **2009**, 11 (9), 2035–2037.
- (86) Zweifel, T.; Naubron, J.-V.; Grützmacher, H. *Angew. Chem. Int. Ed.* **2009**, 48 (3), 559–563.
- (87) Du, Z.; Zhou, W.; Wang, F.; Wang, J.-X. *Tetrahedron* **2011**, 67 (26), 4914–4918.
- (88) Berger, P.; Bessmerykh, A.; Caille, J.-C.; Mignonac, S. *Synthesis* **2006**, (18), 3106–3110.
- (89) Zimmermann, F.; Meux, E.; Mieloszynski, J.-L.; Lecuire, J.-M.; Oget, N. *Tetrahedron Lett.* **2005**, 46 (18), 3201–3203.
- (90) Saisaha, P.; Buettner, L.; van der Meer, M.; Hage, R.; Feringa, B. L.; Browne, W. R.; de Boer, J. W. *Adv. Synth. Catal.* **2013**, 355 (13), 2591–2603.
- (91) Yabuuchi, T.; Kusumi, T. *J. Org. Chem.* **2000**, 65 (2), 397–404.
- (92) Lafrance, D.; Bowles, P.; Leeman, K.; Rafka, R. *Org. Lett.* **2011**, 13 (9), 2322–2325.
- (93) Zhao, J.; Mück-Lichtenfeld, C.; Studer, A. *Adv. Synth. Catal.* **2013**, 355 (6), 1098–1106.
- (94) Ray, W. J.; Katon, J. E.; Krause, P. F. *Appl. Spectrosc.* **1979**, 33, 492–495.
- (95) Barrelle, M.; Béguin, C.; Tessier, S. *Org. Magn. Reson.* **1982**, 19, 102–104.
- (96) Kawashima, M.; Sato, T.; Fujisawa, T. *Tetrahedron* **1989**, 45 (2), 403–412.
- (97) Johansson Seechurn, C. C. C.; Kitching, M. O.; Colacot, T. J.; Snieckus, V. *Angew. Chem. Int. Ed.* **2012**, 51 (21), 5062–5085.
- (98) Glaser, C. *Ber. Dtsch. Chem. Ges.* **1869**, 2 (1), 422–424.
- (99) Siemsen, P.; Livingston, R. C.; Diederich, F. *Angew. Chem. Int. Ed.* **2000**, 39 (15), 2632–2657.
- (100) Ullmann, F.; Bielecki, J. *Ber. Dtsch. Chem. Ges.* **1901**, 34 (2), 2174–2185.
- (101) Bennett, G. M.; Turner, E. E. *J. Chem. Soc., Trans.* **1914**, 105 (0), 1057–1062.

- (102) Krizewsky, J.; Turner, E. E. *J. Chem. Soc., Trans.* **1919**, 115 (0), 559–561.
- (103) Kharasch, M. S.; Fields, E. K. *J. Am. Chem. Soc.* **1941**, 63 (9), 2316–2320.
- (104) Kharasch, M. S.; Fuchs, C. F. *J. Am. Chem. Soc.* **1943**, 65 (4), 504–507.
- (105) Chodkiewicz, W.; Cadiot, P. *C. R. Hebd. Seances Acad. Sci.* **1955**, 241, 1055–1057.
- (106) Chodkiewicz, W. *Ann. Chim. Paris* **1957**, 2, 819–869.
- (107) Naemura, K.; Hokura, Y.; Nakazaki, M. *Tetrahedron* **1986**, 42 (6), 1763–1768.
- (108) Shi Shun, A. L. K.; Tykwinski, R. R. *Angew. Chem. Int. Ed.* **2006**, 45 (7), 1034–1057.
- (109) Gung, B. W.; Kumi, G. *J. Org. Chem.* **2004**, 69 (10), 3488–3492.
- (110) Biajoli, A. F. P.; Schwalm, C. S.; Limberger, J.; Claudino, T. S.; Monteiro, A. L. *J. Braz. Chem. Soc.* **2014**, 25 (12), 2186–2214.
- (111) Corriu, R. J. P.; Masse, J. P. *J. Chem. Soc. Chem. Commun.* **1972**, (3), 144a.
- (112) Tamao, K.; Sumitani, K.; Kumada, M. *J. Am. Chem. Soc.* **1972**, 94 (12), 4374–4376.
- (113) Tamao, K.; Sumitani, K.; Kiso, Y.; Zembayashi, M.; Fujioka, A.; Kodama, S.; Nakajima, I.; Minato, A.; Kumada, M. *Bull. Chem. Soc. Jpn.* **1976**, 49 (7), 1958–1969.
- (114) Murahashi, S.; Yamamura, M.; Yanagisawa, K.; Mita, N.; Kondo, K. *J. Org. Chem.* **1979**, 44 (14), 2408–2417.
- (115) Tamura, M.; Kochi, J. *Synthesis* **1971**, 6, 303–305.
- (116) Tamura, M.; Kochi, J. K. *J. Am. Chem. Soc.* **1971**, 93 (6), 1487–1489.
- (117) Neumann, S. M.; Kochi, J. K. *J. Org. Chem.* **1975**, 40 (5), 599–606.
- (118) Sherry, B. D.; Fürstner, A. *Acc. Chem. Res.* **2008**, 41 (11), 1500–1511.
- (119) Martin, R.; Buchwald, S. L. *J. Am. Chem. Soc.* **2007**, 129 (13), 3844–3845.
- (120) Manolikakes, G.; Knochel, P. *Angew. Chem. Int. Ed.* **2009**, 48 (1), 205–209.
- (121) Krasovskiy, A. L.; Haley, S.; Voigtritter, K.; Lipshutz, B. H. *Org. Lett.* **2014**,

- 16 (16), 4066–4069.
- (122) Yoshikai, N.; Mashima, H.; Nakamura, E. *J. Am. Chem. Soc.* **2005**, *127* (51), 17978–17979.
- (123) Guo, W.-J.; Wang, Z.-X. *J. Org. Chem.* **2013**, *78* (3), 1054–1061.
- (124) Gosmini, C.; Bégouin, J.-M.; Moncomble, A. *Chem. Commun.* **2008**, *0* (28), 3221–3223.
- (125) Beletskaya, I. P.; Cheprakov, A. V. *Coord. Chem. Rev.* **2004**, *248* (21), 2337–2364.
- (126) Tsuji, T.; Yorimitsu, H.; Oshima, K. *Angew. Chem. Int. Ed.* **2002**, *41* (21), 4137–4139.
- (127) Mao, J.; Liu, F.; Wang, M.; Wu, L.; Zheng, B.; Liu, S.; Zhong, J.; Bian, Q.; Walsh, P. J. *J. Am. Chem. Soc.* **2014**, *136* (50), 17662–17668.
- (128) Fürstner, A.; Leitner, A. *Angew. Chem. Int. Ed.* **2002**, *41* (4), 609–612.
- (129) Scheiper, B.; Bonnekessel, M.; Krause, H.; Fürstner, A. *J. Org. Chem.* **2004**, *69* (11), 3943–3949.
- (130) Scheiper, B.; Glorius, F.; Leitner, A.; Fürstner, A. *Proc. Natl. Acad. Sci. U. S. A.* **2004**, *101* (33), 11960–11965.
- (131) Fürstner, A.; Leitner, A. *Angew. Chem. Int. Ed.* **2003**, *42* (3), 308–311.
- (132) Fürstner, A.; Leitner, A.; Méndez, M.; Krause, H. *J. Am. Chem. Soc.* **2002**, *124* (46), 13856–13863.
- (133) Hatakeyama, T.; Nakamura, M. *J. Am. Chem. Soc.* **2007**, *129* (32), 9844–9845.
- (134) Terao, J.; Todo, H.; Begum, S. A.; Kuniyasu, H.; Kambe, N. *Angew. Chem. Int. Ed.* **2007**, *46* (12), 2086–2089.
- (135) Maaliki, C.; Thiery, E.; Thibonnet, J. *Eur. J. Org. Chem.* **2017**, (2), 209–228.
- (136) Saito, B.; Fu, G. C. *J. Am. Chem. Soc.* **2007**, *129* (31), 9602–9603.
- (137) Saito, B.; Fu, G. C. *J. Am. Chem. Soc.* **2008**, *130* (21), 6694–6695.
- (138) Zultanski, S. L.; Fu, G. C. *J. Am. Chem. Soc.* **2011**, *133* (39), 15362–15364.
- (139) Wilsily, A.; Tramutola, F.; Owston, N. A.; Fu, G. C. *J. Am. Chem. Soc.* **2012**,

- 134 (13), 5794–5797.
- (140) Hintermann, L.; Xiao, L.; Labonne, A. *Angew. Chem. Int. Ed.* **2008**, *47* (43), 8246–8250.
- (141) Han, C.; Buchwald, S. L. *J. Am. Chem. Soc.* **2009**, *131* (22), 7532–7533.
- (142) Joshi-Pangu, A.; Wang, C.-Y.; Biscoe, M. R. *J. Am. Chem. Soc.* **2011**, *133* (22), 8478–8481.
- (143) Lohre, C.; Dröge, T.; Wang, C.; Glorius, F. *Chem. Eur. J.* **2011**, *17* (22), 6052–6055.
- (144) Ren, P.; Stern, L.-A.; Hu, X. *Angew. Chem. Int. Ed.* **2012**, *51* (36), 9110–9113.
- (145) Emsley, J. *Nature's building blocks: an A-Z guide to the elements*; Oxford University Press, 2001.
- (146) Santamaria, A. B.; Sulsky, S. I. *J. Toxicol. Environ. Heal. Part A* **2010**, *73* (2–3), 128–155.
- (147) Avila, D. S.; Puntel, R. L.; Aschner, M. *Manganese in Health and Disease*; Springer Netherlands, 2013.
- (148) Carney, J. R.; Dillon, B. R.; Thomas, S. P. *Eur. J. Org. Chem.* **2016**, (23), 3912–3929.
- (149) Cahiez, G.; Duplais, C.; Buendia, J. *Chem. Rev.* **2009**, *109* (3), 1434–1476.
- (150) Cahiez, G.; Figadere, B. *Tetrahedron Lett.* **1986**, *27* (37), 4445–4448.
- (151) Kang, S.-K.; Kim, J.-S.; Choi, S.-C. *J. Org. Chem.* **1997**, *62* (13), 4208–4209.
- (152) Jiangbin, Q.; Wenfang, Z.; Guanglan, Z.; Hao, Z.; Xuanzhen, J. *Chinese J. Catal.* **2008**, *29* (293), 209–211.
- (153) Zong, Z.; Wang, W.; Bai, X.; Xi, H.; Li, Z. *Asian J. Org. Chem.* **2015**, *4* (7), 622–625.
- (154) Qi, X.; Jiang, L.-B.; Wu, X.-F. *Tetrahedron Lett.* **2016**, *57* (15), 1706–1710.
- (155) Cossy, J. *Grignard reagents and transition metal catalysts: formation of C-C bond by cross-coupling*; 2016.

- (156) Cahiez, G.; Lepifre, F.; Ramiandrasoa, P. *Synthesis* **1999**, (12), 2138–2144.
- (157) Cahiez, G.; Luart, D.; Lecomte, F. *Org. Lett.* **2004**, 6 (24), 4395–4398.
- (158) Rueping, M.; leawsuwan, W. *Synlett* **2007**, (2), 0247–0250.
- (159) Cahiez, G.; Gager, O.; Lecomte, F. *Org. Lett.* **2008**, 10 (22), 5255–5256.
- (160) Cahiez, G.; Moyeux, A.; Buendia, J.; Duplais, C. *J. Am. Chem. Soc.* **2007**, 129 (45), 13788–13789.
- (161) Bottoni, A.; Cahiez, G.; Calvaresi, M.; Moyeux, A.; Giacinto, P.; Miscione, G. Pietro. *J. Organomet. Chem.* **2016**, 814, 25–34.
- (162) Cahiez, G.; Duplais, C.; Buendia, J. *Angew. Chem. Int. Ed.* **2009**, 48 (36), 6731–6734.
- (163) Ghaleshahi, H. G.; Antonacci, G.; Madsen, R. *Eur. J. Org. Chem.* **2017**, (10), 1331–1336.
- (164) Jahn, U. *Top. Curr. Chem.* **2011**, 320, 121–189.
- (165) Asandei, A. D.; Adebolu, O. I.; Simpson, C. P. *J. Am. Chem. Soc.* **2012**, 134 (14), 6080–6083.
- (166) Kondo, T.; Sone, Y.; Tsuji, Y.; Watanabe, Y. *J. Organomet. Chem.* **1994**, 473 (1–2), 163–173.
- (167) Fukuyama, T.; Nishitani, S.; Inouye, T.; Morimoto, K.; Ryu, I. *Org. Lett.* **2006**, 8, 1383–1386.
- (168) Gilbert, B. C.; Kalz, W.; Lindsay, C. I.; McGrail, P. T.; Parsons, A. F.; Whittaker, D. T. E.; Trach, F. *J. Chem. Soc. Perkin Trans. 1* **2000**, 39 (8), 1187–1194.
- (169) Gilbert, B. C.; Kalz, W.; Lindsay, C. I.; McGrail, P. T.; Parsons, A. F.; Whittaker, D. T. E. *Tetrahedron Lett.* **1999**, 40 (33), 6095–6098.
- (170) Bektas, S.; Ciftci, M.; Yagci, Y. *Macromolecules* **2013**, 46 (17), 6751–6757.
- (171) Iskin, B.; Yilmaz, G.; Yagci, Y. *Macromol. Chem. Phys.* **2013**, 214 (1), 94–98.
- (172) Ciftci, M.; Batat, P.; Demirel, A. L.; Xu, G.; Buchmeiser, M.; Yagci, Y. *Macromolecules* **2013**, 46 (16), 6395–6401.

- (173) Kahveci, M. U.; Acik, G.; Yagci, Y. *Macromol. Rapid Commun.* **2012**, *33* (4), 309–313.
- (174) Yagci, Y.; Hepuzer, Y. *Macromolecules* **1999**, *32* (19), 6367–6370.
- (175) Ciftci, M.; Norsic, S.; Boisson, C.; D'Agosto, F.; Yagci, Y. *Macromol. Chem. Phys.* **2015**, *216* (9), 958–963.
- (176) Nakao, J.; Inoue, R.; Shinokubo, H.; Oshima, K. *J. Org. Chem.* **1997**, *62* (7), 1910–1911.
- (177) Sølvhøj, A.; Ahlburg, A.; Madsen, R. *Chem. Eur. J.* **2015**, *21* (45), 16272–16279.
- (178) Lewiński, J.; Suwała, K.; Kubisiak, M.; Ochal, Z.; Justyniak, I.; Lipkowski, J. *Angew. Chem. Int. Ed.* **2008**, *47* (41), 7888–7891.
- (179) Kubisiak, M.; Zelga, K.; Bury, W.; Justyniak, I.; Budny-Godlewski, K.; Ochal, Z.; Lewiński, J.; Incarvito, C. D.; Zuberbühler, A. D.; Rheingold, A. L.; Karlin, K. D. *Chem. Sci.* **2015**, *6* (5), 3102–3108.
- (180) Mondal, M.; Bora, U. *RSC Adv.* **2013**, *3* (41), 18716–18754.
- (181) Snider, B. B. *Chem. Rev.* **1996**, *96* (1), 339–364.
- (182) Linker, T. *E. Chem. Int. Ed. En.* **1997**, *36* (19), 2060–2062.
- (183) Norrby, P.-O.; Linde, C.; Aakermark, B. *J. Am. Chem. Soc.* **1995**, *117* (44), 11035–11036.
- (184) Irie, R.; Noda, K.; Ito, Y.; Matsumoto, N.; Katsuki, T. *Tetrahedron: Asymmetry* **1991**, *2* (7), 481–494.
- (185) Jacobsen, E. N.; Zhang, W.; Muci, A. R.; Ecker, J. R.; Deng, L. *J. Am. Chem. Soc.* **1991**, *113* (18), 7063–7064.
- (186) Zhang, W.; Loebach, J. L.; Wilson, S. R.; Jacobsen, E. N. *J. Am. Chem. Soc.* **1990**, *112* (7), 2801–2803.
- (187) Antonacci, G.; Ahlburg, A.; Fristrup, P.; Norrby, P.-O.; Madsen, R. *Eur. J. Org. Chem.* **2017**.
- (188) Davico, G. E.; Bierbaum, V. M.; DePuy, C. H.; Ellison, G. B.; Squires, R. R. *J. Am. Chem. Soc.* **1995**, *117* (9), 2590–2599.

- (189) Shtarev, A. B.; Tian, F.; Dolbier, W. R.; Smart, B. E. *J. Am. Chem. Soc.* **1999**, *121* (32), 7335–7341.
- (190) Poirier, M.; Chen, F.; Bernard, C.; Wong, Y.-S.; Wu, G. G. *Org. Lett.* **2001**, *3* (23), 3795–3798.
- (191) Tammiku-Taul, J.; Burk, P.; Tuulmets, A. *J. Phys. Chem. A* **2004**, *108* (1), 133–139.
- (192) Hatakeyama, T.; Nakamura, M. *J. Am. Chem. Soc.* **2007**, *129* (32), 9844–9845.
- (193) Ashby, E. C.; Argyropoulos, J. N. *J. Org. Chem.* **1985**, *50* (18), 3274–3283.
- (194) Abeywickrema, A. N.; Beckwith, A. L. *J. Chem. Soc., Chem. Commun.* **1986**, (6), 464–465.
- (195) Beckwith, A. L. J.; Schiesser, C. H. *Tetrahedron* **1985**, *41* (19), 3925–3941.
- (196) Ha, C.; Homer, J. H.; Newcomb, M.; Varick, T. R.; Arnold, B. R.; Luszyk, J. *J. Org. Chem.* **1993**, *58*, 1194–1198.
- (197) Nakao, J.; Inoue, R.; Shinokubo, H.; Oshima, K. *J. Org. Chem.* **1997**, *62* (7), 1910–1911.
- (198) Yang, H.; Zhang, L.; Jiao, L. *Chem. Eur. J.* **2017**, *23* (1), 65–69.
- (199) Liu, Q.-X.; Cai, K.-Q.; Zhao, Z.-X. *RSC Adv.* **2015**, *5* (104), 85568–85578.
- (200) Gavina, F.; Costero, A. M.; Gonzalez, A. M. *J. Org. Chem.* **1990**, *55* (7), 2060–2063.
- (201) Ohtsuki, A.; Yanagisawa, K.; Furukawa, T.; Tobisu, M.; Chatani, N. *J. Org. Chem.* **2016**, *81* (19), 9409–9414.
- (202) Heijnen, D.; Gualtierotti, J.-B.; Hornillos, V.; Feringa, B. L. *Chem. Eur. J.* **2016**, *22* (12), 3991–3995.
- (203) Thapa, S.; Basnet, P.; Gurung, S. K.; Giri, R. *Chem. Commun.* **2015**, *51* (19), 4009–4012.
- (204) Bailey, W. F.; Mealy, M. J. *J. Am. Chem. Soc.* **2000**, *122* (28), 6787–6788.
- (205) Friedfeld, M. R.; Shevlin, M.; Margulieux, G. W.; Campeau, L.-C.; Chirik, P. *J. Am. Chem. Soc.* **2016**, *138* (10), 3314–3324.

- (206) Uchiyama, N.; Shirakawa, E.; Hayashi, T. *Chem. Commun.* **2013**, 49 (4), 364–366.
- (207) Chatterjee, A.; Hopen Eliasson, S. H.; Törnroos, K. W.; Jensen, V. R. *ACS Catal.* **2016**, 6 (11), 7784–7789.
- (208) MaJi, B.; Barman, M. K. *Synthesis* **2017**, 49, 3377–3393.
- (209) Elangovan, S.; Topf, C.; Fischer, S.; Jiao, H.; Spannenberg, A.; Baumann, W.; Ludwig, R.; Junge, K.; Beller, M. *J. Am. Chem. Soc.* **2016**, 138 (28), 8809–8814.
- (210) Nguyen, D. H.; Trivelli, X.; Capet, F.; Paul, J.-F.; Dumeignil, F.; Gauvin, R. M. *ACS Catal.* **2017**, 7 (3), 2022–2032.
- (211) Mukherjee, A.; Nerush, A.; Leitus, G.; Shimon, L. J. W.; Ben David, Y.; Espinosa Jalapa, N. A.; Milstein, D. *J. Am. Chem. Soc.* **2016**, 138 (13), 4298–4301.
- (212) Mastalir, M.; Glatz, M.; Gorgas, N.; Stöger, B.; Pittenauer, E.; Allmaier, G.; Veiros, L. F.; Kirchner, K. *Chem. Eur. J.* **2016**, 22 (35), 12316–12320.
- (213) Mastalir, M.; Glatz, M.; Pittenauer, E.; Allmaier, G.; Kirchner, K. *J. Am. Chem. Soc.* **2016**, 138 (48), 15543–15546.
- (214) Elangovan, S.; Neumann, J.; Sortais, J.-B.; Junge, K.; Darcel, C.; Beller, M. *Nat. Commun.* **2016**, 7, 12641.